https://doi.org/10.15388/vu.thesis.82
https://orcid.org/0000-0002-9452-3392

VILNIUS UNIVERSITY

Benjaminas
VALIAUGA

Studies of reduction mechanisms of quinones and nitroaromatic compounds by flavoenzymes dehydrogenases-transhydrogenases

DOCTORAL DISSERTATION

Natural Sciences,
Biochemistry N004

_____

VILNIUS 2020

This dissertation was written between 2015 and 2019 in Vilnius University, Life Sciences Center, Institute of Biochemistry

Academic supervisor - habil. dr. Narimantas Čėnas (Vilnius University, Natural sciences, Biochemistry, N004)

https://doi.org/10.15388/vu.thesis.82
https://orcid.org/0000-0002-9452-3392

VILNIAUS UNIVERSITETAS

Benjaminas
VALIAUGA

Chinonų ir nitroaromatinių junginių redukcijos flavininėmis dehidrogenazėmis-transhidrogenazėmis mechanizmų tyrimai

DAKTARO DISERTACIJA

Gamtos mokslai,
Biochemija N004

_____

VILNIUS 2020

Disertacija buvo rengta 2015-2019 metais Vilniaus universiteto Gyvybės mokslų centre, Biochemijos institute

Mokslinis vadovas - habil. dr. Narimantas Čėnas (Vilniaus universitetas, gamtos mokslai, biochemija, N004)

Contents

ABBREVIATION LIST

APAD(P)H - 3-acetylpyridine adenine dinucleotide (phosphate)

$ArNO_2$ – nitroaromatic compound

CB-1954 - 5-(1-aziridinyl)-2,4-dinitrobenzamide

DTNB - 5,5'-dithiobis-(2-nitrobenzoic acid)

EDTA – ethylenediaminetetraacetic acid

FAD – flavin adenine dinucleotide

FMN – flavin mononucleotide

FRase I - *Vibrio fischeri* NAD(P)H:FMN reductase

Frp - *Vibrio harveyi* NADPH:flavin oxidoreductase

GDEPT – gene-directed enzyme prodrug therapy

GR – glutathione reductase

Grx – glutaredoxin

GSH – glutathione

GSSG - glutathione disulfide

IC_{50} - half maximal inhibitory concentration

k_{cat} – apparent catalytic constant

k_{cat}/K_m – the bimolecular rate constant

KIE - kinetic isotope effect

NfsA – *Escherichia coli* nitroreductase A

NfsB - *Escherichia coli* nitroreductase B

NQO1 - NAD(P)H:quinone oxidoreductase

NR – nitroreductase

P-450R - NADPH:cytochrome P-450 reductase

p-NBA - *p*-nitrobenzoic acid

Prx–NR - *Thermotoga maritima* peroxiredoxin-nitroreductase hybrid enzyme

Q – quinone

RH1 - 2,5-diaziridinyl-3-(hydroxymethyl)-6-methyl-1,4-benzoquinone

SOD – superoxide dismutase

SoxRS – superoxide response regulon

TmTR – *Thermotoga maritima* thioredoxin reductase

TNT – 2,4,6-trinitrotoluene

TR – thioredoxin reductase

Trx – thioredoxin

TryR - trypanothione reductase

1. INTRODUCTION

Flavoenzymes contain flavin mononucleotide (FMN) or flavin adenine dinucleotide (FAD) in their active sites, which in most cases are strongly noncovalently bound to apoenzyme (K_d = 10^{-10} –10^{-8} M). Flavoenzymes, constituting about 2% of all enzymes, are widespread in nature and participate in numerous metabolic and bioenergetic processes. The wast majority of flavoenzymes, 90%, are oxidoreductases. Their reactions include electron transfer, dehydrogenation, oxidation and hydroxylation. In most cases, the flavoenzyme catalytic cycle is characterized by separate half-reactions of flavin reduction and reoxidation. Flavoenzymes are divided into 5 classes (Hemmerich and Massey, 1979) dehydrogenases-transhydrogenases, oxidases, oxygenases, dehydrogenases-electrontransferases, and electrontransferases. This classification is based on their different ability to perform single- and two-electron transfer, and different properties of flavin semiquinones (free radicals).

Flavoenzymes play important roles in biomedicine and ecotoxicology, acting as the targets of drugs and xenobiotics, and participating in the biodegradation of environmental pollutants. In this context, the flavoenzyme-catalyzed reduction of quinones (Q) and nitroaromatic compounds ($ArNO_2$) (Fig. 1) is of particular importance.

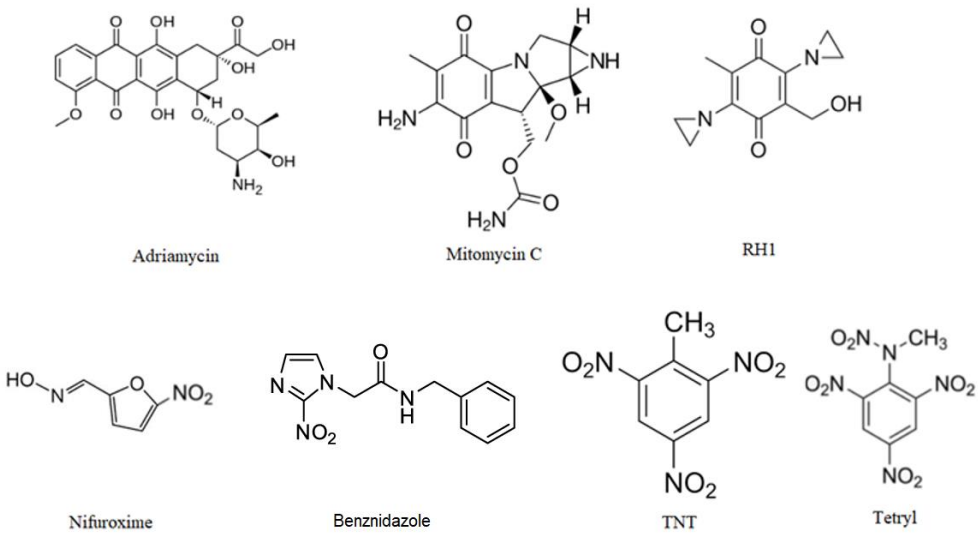

Fig. 1. Quinones and nitroaromatic compounds. Adriamycin, mitomycin C and RH1 are anticancer agents. Nifuroxime and benzinidazole are antiparasitic reagents, whereas TNT and tetryl are explosives and environmental pollutants.

Anthracyclines, mitomycines, aziridinyl-substituted benzoquinones, nitrofurans and nitroimidazoles (Fig. 1) are used or examined as antitumour, antiparasitic and antibacterial agents (McKeown *et al.*, 2007). In turn, policyclic quinones and nitroaromatic compounds are toxic atmosphere pollutants, whereas other polinitroaromatics are the components of industrial waste, pesticides, or, in the case of 2,4,6-trinitrotoluene (TNT) and tetryl (Fig. 1), toxic residues of explosives in environment. The toxic or in some cases therapeutic action of Q and $ArNO_2$ is frequently attributed to their single-electron reduction into free radicals, which are reoxidized by O_2 with the formation of superoxide ($O_2^{-\bullet}$), and, subsequently, H_2O_2 and hydroxyl radical ($OH^{\bullet}$). The latter damages DNA and proteins, thus being responsible for the "oxidative stress"-type cytotoxicity. In most cases, the single-electron reduction of Q and $ArNO_2$ is performed by flavoenzymes dehydrogenases-electrontransferases, which are characterized by high stability of neutral

flavin semiquinone, and presence of single-electron physiological oxidants, *e.g.,* heme- or FeS-proteins. Their best described representatives are mammalian NADPH:cytochrome P-450 reductase, NADH:cytochrome b_5 reductase, NADH: ubiquinone reductase (complex I), NO-synthase, plant, algal or bacterial ferredoxin:$NADP^+$ reductase, and bacterial oxygen-sensitive nitroreductases (NRs) (Peterson *et al.,* 1979; Holtzman *et al.,* 1981; Iyanagi *et al.,* 1984; Orna and Mason, 1989; Bironaitė *et al.,* 1991; Čėnas *et al.,* 1994; Anusevičius *et al.,* 1999; Kumagai *et al.,* 1998; Yamamoto *et al.,* 2005).

Two-electron reduction of Q and $ArNO_2$ plays a dual role in their action. The reduction of Q into hydroquinones contributes to their detoxification due to subsequent conjugation (Lind *et al.,* 1990), however, the reduction of aziridinyl-substituted quinones (Fig. 1) enhances the DNA alkylation by aziridine groups (Hargreaves *et al.,* 2000**)**. A net four-electron reduction of $ArNO_2$ in two two-electron steps yields toxic DNA-alkylating hydroxylamines (Williams *et al.,* 2015). On the other hand, this reaction is the first step of biodegradation of polinitroaromatic environmental pollutants (Spain, 1995). In these processes, the most relevant flavoenzymes are mammalian DT-diaphorase (NAD(P)H:quinone acceptor reductase) and bacterial oxygen-insensitive nitroreductases. They catalyze two-electron (hydride) transfer between the reducing and oxidizing substrates and possess unstable anionic flavin semiquinone state, therefore, belong to a class of dehydrogenases-transhydrogenases.

The studies of bacterial oxygen-insensitive NRs are permanently important because of the problems with $ArNO_2$ biodegradation (their estimated production may reach 10^8 tons/year). In addition to a widespread use of $ArNO_2$ against bacteria and parasites, the development of gene-directed prodrug therapy based on bacterial NRs (Williams *et al.,*

2015) fosters the use of $ArNO_2$ in cancer treatment. Thus, the main object of this work was a relatively scarsely studied oxygen-insensitive NR, *E. coli* nitroreductase-A (NfsA). For a better characterizarion of NfsA in the context of other dehydrogenases-transhydrogenases, we also studied quinone- and nitroreductase reactions of NADH:thioredoxin reductase of thermophilic microorganism *Thermotoga maritima* (TmTR). In addition to being the object of mechanistic studies, TmTR and its analogues may be regarded as potentially ecotoxicologically important targets of quinones and nitroaromatic compounds. These features may be even more important for TmTR in view of the recently emerging interest in the use of hyperthermophilic microorganisms in metabolic engineering platforms for production of fuels and industrial chemicals (Zeldes *et al.*, 2015).

GOALS AND TASKS OF THE THESIS

The goal of the thesis is to characterize the reduction of nonphysiological oxidants (quinones and nitroaromatic compounds) by dehydrogenases-transhydrogenases, belonging to two different groups, (*Escherichia coli* nitroreductase A (NfsA) and *Thermotoga maritima* thioredoxin reductase (TmTR)) and to evaluate structural parameters, which determine $1e^-$ or $2e^-$ reduction nature of these enzymes.

The tasks to achieve this goal are as following:

1. To determine and compare the reduction mechanisms of quinones and nitroaromatic compounds by NfsA and TmTR.
2. To investigate the mechanism of a net four-electron reduction of $ArNO_2$ by nitroreductases with elucidation of the role of enzymatic and chemical steps.

3. To determine the redox potential of flavin cofactors in both TmTR and NfsA.

4. To characterize a possible relationship between the single- or two-electron reduction of quinones and nitroaromatics and flavin cofactor semiquinone stability of NfsA and TmTR.

IMPORTANCE AND SCIENTIFIC NOVELTY

1. For the first time, mechanism and substrate specificity of quinone- and nitroreductase-activity of group A nitroreductase NfsA was characterized. These properties are similar to those of group B nitroreductase *Enterobacter cloacae*. Also, for the first time it was determined that nonenzymatic reduction by NADPH and not the enzymatic reduction of intermediate nitroso compound is predominant in NfsA-catalyzed 4e^- reduction of nitroaromatic compounds. These data may be important in the case of GDEPT and problems related to the biodegradation of environmental pollutants.

2. Thermodynamic properties of NfsA FMN cofactor (standard redox potential value, unstable state of semiquinone) and most credible single step hydride transfer mechanism were disclosed in this work. These properties are similar to *E. cloacae* NR. These data complement the scarce information in this area and allow to conclude that eventhough there are considerable differences in the sequences of group A and B nitroreductases, they have similar catalytic characteristics, which are determined by FAD thermodynamic properties.

3. It was determined that TmTR-catalyzed reduction mechanism, substrate specificity of quinones and nitroaromatic compounds and FAD redox potential is similar to previously characterized low molecular mass thioredoxin reductases from *A. thaliana* and *E. coli*. The data allow to conclude that these enzymes can efficiently participate in the reduction of redox active xenobiotics and environmental pollutants. These reactions may be an important factor in the biodegradation of these pollutants or action of redox active antibacterial agents.

4. Formation of intermediate FAD semiquinone in TmTR-catalyzed reduction of quinones was observed for the first time in the reactions catalyzed by low molecular mass thioredoxin reductases. It explains mixed $1e^-$ and $2e^-$ reduction of quinones and nitroaromatic compounds by TmTR.

5. Different reaction mechanisms of NfsA- and TmTR-catalyzed reduction of quinones and nitroaromatic compounds extend the data about the variety of reactions of flavoenzymes dehydrogenases-transhydrogenases. Although these enzymes are characterized by $2e^-$ reduction of the physiological oxidators, however they can catalyze $1e^-$ and $2e^-$ reduction of nonphysiological electron acceptors. It is possible that these different mechanisms are determined by different semiquinone stability of the flavin cofactor.

STATEMENTS

1. *E. coli* NfsA follows “ping-pong” mechanism in the reduction of quinones and nitroaromatic compounds. The reactivity of nitroaromatics is systematically higher than that of quinones with the same single-electron accepting potency. The reduction of quinones is mostly consistent with a single-step (H^-) hydride transfer mechanism. Oxidative half-reaction is the limiting step in the catalytic cycle of the enzyme.
2. Direct reduction of nitroso intermediate by NADPH rather than enzymatic reduction is the predominant mechanism during nitroaromatic reduction by NfsA.
3. TmTR catalyzes mixed one- and two-electron reduction of quinones and nitroaromatic compounds. The reactivity of quinones with TmTR increases with their E^1_7, and the reactivity of nitroaromatics is systematically lower than that of quinones with the same E^1_7.
4. The transient accumulation of FAD semiquinone during the enzymatic reduction of duroquinone by *T. maritima* TR shows that the limiting step of reaction is the oxidation of semiquinone.
5. The redox potentials of flavin cofactors in both TmTR and NfsA are close to those of *E. coli* TR and *Enterobacter cloacae* NR.

2. THE LITERATURE REVIEW

2.1. Redox properties and classification of flavoenzymes

The action of most flavoenzymes is characterized by oxidative and reductive half-reactions in an enzymatic cycle, which are accompanied by the cofactor absorbance changes. Oxidized isoalloxazine cofactor possesses absorbance maximum (λ_{max}) at ~ 360 nm and at ~460 nm. The reduction of enzyme by substrate is accompanied by the drop in absorbance at 460 nm, and partly at 360 nm. In the second half-reaction, the oxidants reoxidize reduced flavin.

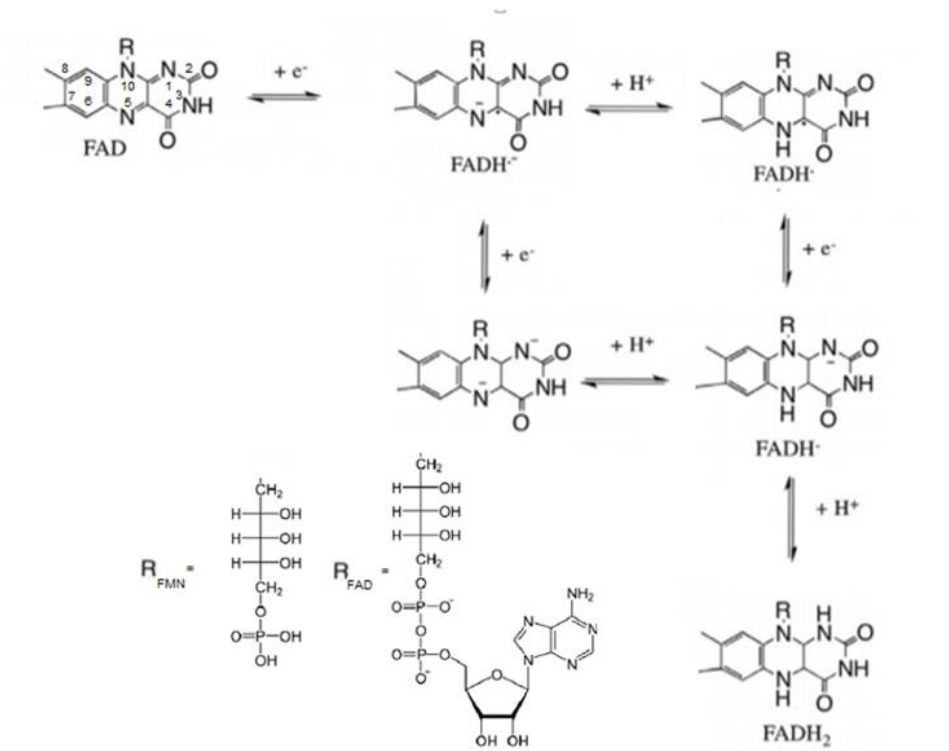

Fig. 2. The structure of FMN and FAD and their various redox states.

It is important to note that flavoenzymes are capable to perform two-electron and/or single-electron transfer, or to transform $2e^-$ transfer into

single-electron one. The later phenomenon most frequently takes place during the oxidative half-reaction. The single-electron reduced state of flavin, *i.e.* anionic (red) semiquinone ($FMN^{-\bullet}$ or $FAD^{-\bullet}$) (Fig. 2) is characterized by λ_{max} ~ 380 nm, whereas the neutral (blue) semiquinone (5-$FMNH^{\bullet}$ or 5-$FADH^{\bullet}$) possesses λ_{max} ~ 560 nm. 1 e^- reduction potential of free (unbound) FMN at pH 7.0 (E^1_7, or potential of flavin/semiquinone redox couple potential) is equal to -0.31 V **(**Anderson, 1983**),** while the potential of the transfer of the second electron (E^2_7, or potential of semiquinone/dihidroflavin redox couple) is equal to -0.172 V (Hemmerich and Massey, 1977). Free 5-$FMNH^{\bullet}$ deprotonization is characterized by pK_a = 8.5, whereas dihidroflavin (1,5-$FMNH_2$) is deprotonized with pK_a = 6.5 (Hemmerich and Massey, 1977). Binding to the apoenzyme has large influence on pK_a of flavin semiquinone or its reduced form, their single-electron potentials, and the nature of catalyzed reactions.The standard (two-electron reduction, flavin/dihydroflavin pair) redox potential of flavoenzymes at pH 7.0 (E^0_7) varies from -0.35 V to 0.1 V. Its value detpends on the nature of amino acids at the vicinity of isoalloxazine ring. In general, positively charged residues increase, and negatively charged residues decrease the redox potential.

In 1979, classification of flavin enzymes was proposed (Hemmerich and Massey, 1979), which is used up until present. According to this classification, flavoenzymes are grouped in these 5 classes:

1. Dehydrogenases-transhydrogenases catalyze two-electron (hydride) transfer in physiological reactions. Formation of flavin semiquinone during the reaction is not typical for these enzymes, unstable anionic semiquinone may be observed during redox titration.

a) C-C transhydrogenases catalyze hydride transfer from $NADP^+$ to NADH, *e.g., Azotobacter vinelandii* pyridine nucleotide transhydrogenase;
b) C-S transhydrogenases catalyze hydride transfer from NAD(P)H to disulfide oxidants, lipoamide, glutathione, thioredoxin, etc.;
c) C-N transhydrogenases catalyze hydride transfer from C-H group of substrate to N5 position of isoalloxazine of other flavoprotein, *e.g.,* electron-transferring flavoprotein (ETF) and *Peptostreptococcus elsdenii D*-lactate dehydrogenase;
d) N-N transhydrogenases transfer 2 electrons between two flavoenzymes, *i.e.,* their 5N-positions, *e.g., Megasphaera elsdenii* electron transferring flavoprotein.

NAD(P)H:quinone oxidoreductase (DT-diaphorase) and oxygen-insensitive bacterial nitroreductases should comprise the group of C-O transhydrogenases, which was unlisted at that time. They catalyze two-electron reduction of quinones into hydroquinones (Lind *et al.,* 1990), and reduction of nitroaromatic compounds into hydroxylamines (Spain *et al.,* 1995);

2. Dehydrogenases-oxidases catalyze two-electron reduction of O_2 into hydrogen peroxide (H_2O_2), *e.g.,* glucose oxidase and amino acid oxidases. Intermediate semiquinone compounds were not detected during the reaction. However, neutral or anionic flavin semiquinone may be observed during redox titration.
3. Dehydrogenases-oxygenases catalyze insertion of -OH group into substrate, consuming 4 redox equivalents – 2 from NAD(P)H and 2 from substrate, which reacts with 4a-hydroperoxyflavin, formed from reduced flavin and O_2. Flavin semiquinones are not detected during the reaction.

4. Dehydrogenases-electrontransferases transform two electron transfer into a single-electron one, for instance, $2e^-$ donor, NAD(P)H reduces $1e^-$ oxidant (cytochromes *c* and P-450, FeS protein.) The most known examples of these enzymes are NADPH:cytochrome P-450 reductase and ferredoxin:$NADP^+$ reductase. These enzymes possess highly stabilized neutral flavin semiquinones.
5. Electrontransferases (flavodoxins) transfer single electron between other flavoenzymes or FeS protein and cytochromes. They do not catalyze enzymatic reactions. These proteins possess highly stabilized neutral FMN semiquinones.

2.2. Redox properties of quinones and aromatic nitrocompounds.

Quinones and nitroaromatic compounds may be reduced in multiple ways. First, let us discuss the reduction of quinones. The net reduction of quinones proceeds with a transfer of two electrons and two protons, and is reversible:

$$Q + 2e^- + 2H^+ \rightleftharpoons QH_2 \qquad (1)$$

Typically, the E^0_7 values for Q/QH_2 couple vary from -0.30 V to 0.28 V (Čėnas *et al.*, 2004 and references therein). The introduction of electron donating substituents or addition of aromatic rings increases the E^0_7 of quinones. In fact, the reduction of quinones proceeds in two steps:

$$Q + e^- \rightleftharpoons Q^{-\cdot} + e^- + 2H^+ \rightleftharpoons QH_2 \qquad (2)$$

However, due to a low stability of semiquinone (E^1_7, or $E_7(Q/Q^{-\cdot}) < E^2_7$, or E_7 ($Q^{-\bullet}/QH_2$)), the cyclic voltammograms of quinones in aqueous medium possess single reduction and reoxidation peaks corresponding to two-electron transfer. The E^1_7 values are usually acquired in pulse-radiolysis experiments, as their radicals rapidly dismutate ($2k_d = 10^6$-10^8

$M^{-1}s^{-1}$) (Neta *et al.*, 1976), E^1_7 of quinones vary from 0.36 V (tetrachloro-1,4-benzoquinone) to -0.41 V (2-hydroxy-1,4-naphthoquinone). Like in the case of E^0_7, the E^1_7 values decrease with an increase in quinone aromatic system (1,4-benzoquinone, 0.09 V, 1,4-naphthoquinone, -0.15 V (Wardman, 1989)), and with an introduction of electron-donating substituents (2-methyl-1,4-benzoquinone, 0.01 V, tetramethyl-1,4-benzoquinone, -0,26 V (Wardman, 1989)). Quinone radicals at pH 7.0 are anionic, their pK_a (pK_a($QH^\bullet$)) are increased by electron-donating substituents (1,4-benzoquinone, pK_a($QH^\cdot$) = 4.1, tetramethyl-1,4-benzoquinone, pK_a($QH^\bullet$) = 5.1 (Swallow *et al.*, 1982)). Formation of intramolecular H-bonds also decreases semiquinone pK_a, *e.g.*, 1,4-naphthoquinone, pK_a($QH^\bullet$) = 4.1, 5,8-dihydroxy-1,4-naphthoquinone, pK_a($QH^\cdot$) = 2.80.

Flavoenzymes can reduce quinones in single-electron, mixed (single- and two-electron) and two-electron way (Iyanagi and Yamazaki, 1969,1970). Single-electron reduction is typically performed by dehydrogenases-transhydrogenases, *e.g.*, NADPH:cytochrome P-450 reductase (P-450R, EC 1.6.2.4) (Holtzman *et al.*, 1981; Orna and Mason, 1989; Čėnas *et al.*, 1994), NO-synthase (NOS, EC 1.14.13.39) (Kumagai *et al.*, 1998; Yamamoto *et al.*, 2005), ferredoxin:$NADP^+$ reductase (FNR, EC 1.18.1.2) (Orna and Mason, 1989; Anusevičius *et al.*, 1997), NADH:ubiquinone oxidoreductase (EC 1.6.99.3) (Bironaitė *et al.*, 1991), NADH:cytochrome b_5 reductase (EC 1.6.2.2) (Iyanagi *et al.*, 1984), and bacterial oxygen-sensitive nitroreductases (Peterson *et al.*, 1979). These enzymes have single-electron physiological acceptors (cytochromes, ferredoxins). Their flavin cofactor semiquinones are neutral (blue) and stabilized at equilibrium, *e.g.*, 48% $FADH^\bullet$ in *Anabaena* FNR (Faro *et al.*, 2002) and 95% $FMNH^\bullet$ in P-450R (Vermillion *et al.*, 1981, Matsuda *et al.*, 2000). After a reduction by two-electron (hydride) donor, NADPH,

these enzymes reduce two molecules of quinone in two succesive single-electron transfers. These reactions are responsible for the aerobic "oxidative stress"-type cytotoxicity of quinones. Following the formation of radicals, they are reoxidized with O_2 with the formation of superoxide ($O_2^{-\bullet}$ and hydrogen peroxide:

$$Q^{-\cdot} + O_2 \longrightarrow Q + O_2^{-\cdot} \qquad (3)$$

$$2Q^{-\cdot} + 2H^+ \longrightarrow H_2O_2 + O_2 \qquad (4)$$

Subsequently, the cytotoxic DNA-damaging hydroxyl radical ($OH^{\bullet}$) is formed in Fenton reaction:

$$Q_2^{-\cdot} + Fe^{3+} \longrightarrow O_2 + Fe^{2+} \qquad (5)$$

$$Fe^{2+} + H_2O_2 \longrightarrow Fe^{3+} + OH^- + OH\cdot \qquad (6)$$

Quinone reduction with flavoenzymes dehydrogenases-electrontransferases usually folows „outer sphere" electron transfer model (Marcus and Sutin, 1985). This model describes electron transfer when there are weak eletron interaction between reagents. Acoording to this mechanism, $1e^-$ transfer rate constant (k_{12}) depends on self-exchange constants of the substrates (k_{11} and k_{22}), and equilibrium constant (K) ($\log K = \Delta E_1$ (V)/0.059, where E_1 is $1e^-$-transfer potential):

$$k_1 = k_{11} \times k_{12} \times K_{12} \times f_{12})^{1/2} \qquad (7)$$

$$\ln f_{12} = \ln(K_{12})^2/4\ln(k_{11} \times k_{22}/Z^2) \qquad (8)$$

where Z – frequency factor (10^{11} $M^{-1}s^{-1}$). This indicates that for a series of homologous compounds (k_{22} = constant), log k_{12} is characterized by parabolic dependence on ΔE_1 with a slope of $\Delta \log k/\Delta E_1 = 8.45$ V^{-1} at $\Delta E_1 = \pm 0.15$V. This type of dependences has been observed in reactions of quinones with P-450R, ferredoxin-NADP(+) reductase and NO

synthase (Nemeikaitė-Čėnienė *et al.*, 2003; Anusevičius *et al.*, 2005; Anusevičius *et al.*, 2013).

The mechanism of two-electron reduction of quinones (Eq. 1) by flavoenzymes is less understood, and is deduced mainly from the studies of nonenzymatic oxidation of NADH and its analogues with quinones:

$$NADH + Q + H^+ \longrightarrow NAD^+ + OH_2 \qquad (9)$$

This reaction was characterized by a linear log k dependence on E^0_7 of quinones (Carlson and Miller, 1985). Kinetic isotope effect (KIE) was observed using 4-deuterated NADH. However, the use of E^0_7 as the correlation parameter does not explain the pH-independent reaction rate, because according to the Nernst equation, the difference between E^0 values of Q/QH_2 and $NAD^+/NADH$ couples and reaction rate should increase with a pH decrease. It was suggested that the limiting step for the reaction should be H^- transfer, and after that very rapid protonization follows:

$$NADH + Q \longrightarrow NAD^+ + QH^- \xrightarrow{+H^+} NAD^+ + QH_2 \quad (10)$$

In this case, the hydride-transfer potential, or potential of quinone/hidroquinone anion redox pair potential, $E_7(Q/QH^-)$ was proposed as a correlation parameter (Carlson and Miller, 1985). It is obtained from Eq. (11):

$$E_7(Q/OH^-) = E^0_7 - (pK_a(QH_2) - 7.0) \times 0.029 \text{ V} \qquad (11)$$

If $pK_a(QH_2) \leq 7.0$, then $E_7(Q/OH^-) = E^0_7$.

On the other hand, the parallel studies of reactions in nonaqueous media enabled to propose a three-step (e^-, H^+, e^-) hydride transfer mechanism (Fukuzumi *et al.*, 1989; 2000):

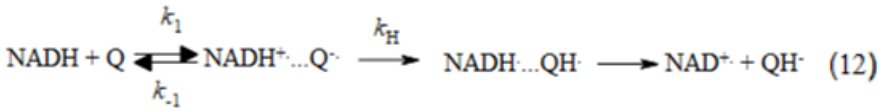

This mechanism was substantiated by the detection of reaction intermediates, charge transfer complexes, with λ_{max} = 600-800 nm (Fukuzumi *et al.,* 1989; 2000). According to this model, the transfer of first electron (k_1) and proton (k_H) are partly limiting reaction steps. The transfer of first electron is thermodinamically unfavourable, because E^1_7 of $NADH^{+\cdot}$/NADH couple is 0.93-1.05 V (Carlson *et al.,* 1984) which is much higher as compared with the potential of $Q/Q^{-\bullet}$. However, the endothermicity of this step may be decreased by the stabilization energy of ion-radical pair $NADH^{+\cdot}...Q^{-\bullet}$ (Fukuzumi *et al*., 1989; 2000). Besides, the reaction is driven forward by the exothermic proton transfer, because the pK_a of $NADH^{+\cdot}$ is equal to -3.5±0.5 (Carlson *et al.,* 1984), which is much lower than pK_a of semiquinones. The reaction rate constant increases, and KIE decreases with an increase in E^1_7.

Following the Eq. 10,12, the single-step and tree-step hydride transfer mechanisms for two-electron reduction of quinones were proposed (Nivinskas *et al*., 2002):

and

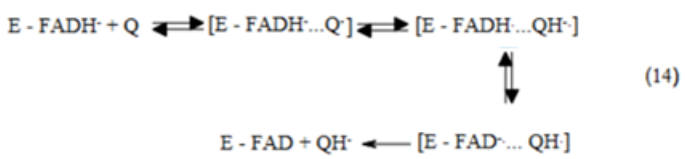

According to this scheme, the first electron transfer is thermodinamically favourable, because E^1_7 of flavin semiquinone/hydroquinone pair is much lower than that of $Q/Q^{-\bullet}$. The

stabilization energy of E-FADH$^{\bullet}$...$Q^{-\bullet}$ can be low, but the additional stabilization may be provided by the enzyme active site. Proton transfer in E-FADH$^{\bullet}$...$Q^{-\bullet}$ ion-radical pair also can take place, because the enzymes which catalyze $2e^-$ quinone reduction have unstable red (anionic) semiquinone (Tedeschi *et al.*, 1995; Haynes *et al.*, 2002). Therefore, second electron transfer can be rapid and not rate-limiting. Linear or parabolic dependence of log *k* on quinone E^1_7 can be expected.

The molecule of $ArNO_2$ can accept 6 electrons with the formation of amine ($ArNH_2$) as the final reduction product. The reaction sequence may be described as follows:

$$ArNO_2 \xrightarrow{e^-} ArNO^{\cdot-} \xrightarrow[-H_2O]{e^-,\,2H^+} ArNO \xrightarrow{2e^-,\,2H^+} ArNHOH \xrightarrow[-H_2O]{2e^-,\,2H^+} ArNH_2 \qquad (15)$$

The electrochemistry of $ArNO_2$ in aqueous media is characterized by irreversibility, *i.e.*, $ArNO_2$ is reduced to ArNHOH (see below), thus, the values of E^1_7 for $ArNO_2$ (redox pair $ArNO_2/ArNO_2^{-\bullet}$) may be obtained by pulse-radiolysis. For nitrobenzenes, they vary from -0.253 V (2,4,6-trinitrotoluene, TNT) to -0.485 V (nitrobenzene) (Wardman, 1989; Riefler and Smets, 2000). The E^1_7 values of nitrofurans are in the range of -0.28 V - -0.22 V, and those of nitroimidazoles from -0.30 V to -0.55 V (Wardman, 1989). The E^1_7 of $ArNO_2$ increase with the increasing electron-accepting properties of substituents, and depend on their *o*-, *m*-, or *p*- position with respect to nitrogroup. Besides, the decrease of coplanarity of $–NO_2$ group with aromatic system decreases the E^1_7 of nitroaromatics (Wardman and Clark, 1976). The pK_a values of $ArNO_2^{-\bullet}$ are in the range of 2.0-3.0 (Neta *et al.*, 1976).

The single-electron reduction of $ArNO_2$ by flavoenzymes dehydrogenases-electrontransferases and subsequent “oxidative stress” events are as described by Eq. 3-8. In these reactions, nitroaromatics are

typically less reactive than quinones by one order of magnitude (Čėnas *et al*., 1994; Anusevičius *et al.*, 1997), because their k_{22} values, $10^5 \div 10^6$ $M^{-1}s^{-1}$ (Meotner and Neta, 1986), are much lower than those of quinones, 10^8 $M^{-1}s^{-1}$ (Gramp and Jaenicke, 1987).

Two-electron reduction of $ArNO_2$ into ArNO proceeds with the formation of *N*,*N*-dyhydroxylamine ($ArN(OH)_2$) intermediate (Darchen and Moinet, 1977), which involves initial $2e^-$ (hydride) transfer and subsequent protonization:

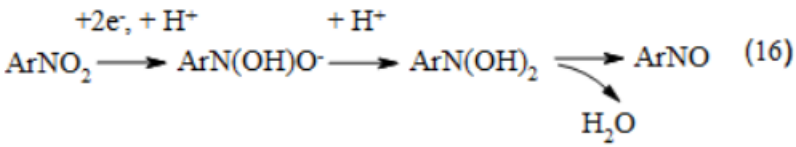

(16)

However, two-electron chemical or electrochemical reduction of $ArNO_2$ can be considered as four-electron reduction, because after the first two-electron transfer, ArNO are rapidly reduced into hydroxylamines. The electrochemical studies show that ArNO are better oxidants than $ArNO_2$, their potentials of irreversible reduction being by 0.5-1.0 V higher (Kovacic *et al*., 1990). Because of this, nitrosobenzenes can be rapidly reduced nonenzymatically, *e.g.* with NAD(P)H, GSH, or ascorbate (Uršič *et al.*, 1998).

According to the best of our knowledge, the sequence of electron and proton transfer during the reduction of $ArNO_2^{-\bullet}$ into ArNO, its reduction into ArNHOH, and the reduction of the latter into $ArNH_2$ in aqueous media is not established experimentally. However, ArNO may be formed in $ArNO_2^{-\bullet}$ dismutation ($2k_d = 10^{-7}$ $M^{-1}s^{-1}$ (Neta *et al.*, 1976)):

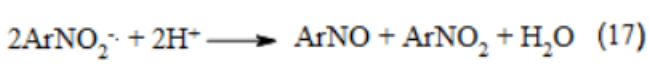

(17)

Besides, ArNHOH may undergo disproportionation with the formation of amines:

$$2ArNHOH \longrightarrow ArNO + ArNH_2 + H_2O \quad (18)$$

This explains the formation of amines as the reduction products of nitroaromatics under aerobic and partly anaerobic conditions in the organism, although this process is strongly thermodynamically unfavourable.

The mechanisms and structure-activity relationships of two-electron reduction of quinones and nitroaromatics by flavoenzymes dehydrogenases-electrontransferases are more thoroughly presented in subsequent sections.

2.3. Reduction of quinones and nitroaromatic compounds with C-O dehydrogenases-transhydrogenases

2.3.1. Reduction of quinones and nitroaromatic compounds with mammalian DT-diaphorase (NAD(P)H:quinone acceptor oxidoreductase, NQO1)

Mammalian NAD(P)H:quinone oxidoreductase (NQO1, DT-diaphorase) is a dimeric flavoenzyme containing one molecule of FAD per 30 kD subunit. It catalyzes two-electron reduction of quinones and aromatic nitrocompounds. The physiological functions of NQO1 are incompletely understood. It is supposed that it maintains vitamins K1, K2 and K3 in reduced state (Fasco and Principe, 1982), and participates in the stabilization of transcripton factor p53 (Danson *et al.,* 2004).

According to the crystal structure of DT-diaphorase (Skelly *et al.*, 1999), residues Leu104, Gln104, Trp105 and Phe106 form a pocket around the isoalloxazine moiety. The oxidant duroquinone stacks paralelly to isoalloxazine ring at 3.5 Å distance, forming hydrogen bonds with Tyr126`, Tyr128`, and His161 (Faig *et al.,* 2000). The most

occupied conformer of Tyr128` is one in which the side chain is close to Phe232 and His161 of the other monomer, shielding the region from solvent and from possible reaction with O_2 (Faig *et al.,* 2000). The binding site for $NADP^+$ involves both residues of the same subunit that binds FAD and residues from the other subunit of the dimer. The carbonyl group of the nicotinamide (07N) makes two hydrogen bonds: one with the OH of Tyr126 and the other with the OH of Tyr128` of the second monomer (Li *et al.,* 1995). The nicotinamide of $NADP^+$ and ring C of the isoalloxazine are stacked, at a distance between the planes of the two rings of about 3.4 Å. The crystal structure of NQO1 with a competitive to NAD(P)H inhibitor, dicoumarol, shows that it ccupies nicotinamide binding place (Asher *et al.,* 2006). It interacts with Tyr128`, Phe232, His161 and Gly150. Cibacron blue fully overlaps the position occupied by the rest of the $NADP^+$ but does not interfere with quinone binding. Cibacron blue and the AMP moiety of $NADP^+$ interact very similarly with the enzyme, as expected since the dye binds to proteins with nucleotide binding sites.

E^0_7 of NQO1 is equal to -159±3 mV at 25 ^oC, pH 7.0 (Tedeschi *et al.*, 1995). The maximum percent of red semiquinone was calculated to be 10 % at pH 7.0, 25 ^oC. The maximal rate of FAD reduction by NAD(P)H exceeds the limits of stopped-flow (Tedeschi *et al.,* 1995). During the reoxidation of reduced NQO1 by single-electron acceptor ferricyanide, the transient semiquinone formation was not observed. It means that the rate-limiting step of reoxidation is the the oxidation of two-electron reduced FAD (Tedeschi *et al.,* 1995).

In steady-state assays, the k_{cat} of alkyl-, hydroxy-, or aziridinyl-substituted benzo- and naphthoquinones are much higher than the k_{cat} of anthraquinones, riboflavin, mitomycin C, and glutathionyl-substituted naphthoquinones with similar E^1_7 values (Anusevičius *et al.,* 2002). In

addition to these compounds, 9,10-phenanthrene quinone, AZQ, and adriamycin may be unequivocally characterized as slow substrates of NQO1 as well (Anusevičius *et al.,* 2002). The bimolecular rate constants (k_{cat}/K_m) for NADPH oxidation and menadione reduction in 0.1 M K-phosphate buffer (pH 7.0) were equal to 1.8±0.1 x 10^7 and 6.8±0.5 x 10^8 M^{-1} s^{-1}, respectively (Anusevičius *et al.,* 2002). In the absence of activators, k_{cat} and k_{cat}/K_m for menadione reduction decreased to 380±40 s^{-1} and 8.4±0.7 x 10^7 $M^{-1}s^{-1}$, respectively, whereas k_{cat}/K_m for NADPH oxidation almost did not change, being equal to 1.7±0.1 x 10^7 M^{-1} s^{-1} (Anusevičius *et al.,* 2002).

The entropies of activation ($\Delta S^{\neq}$) in the reduction of „fast" oxidants were equal to -84 ÷ -76 J mol^{-1} K^{-1}, whereas in the reduction of „slow" oxidants $\Delta S^{\neq}$ were equal -36 ÷ -11 J mol^{-1} K^{-1} (Anusevičius *et al.,* 2002). The large negative $\Delta S^{\neq}$ points to the strong electronic coupling between the molecules of reactants (Hubig *et al.,* 1999) and/or to the formation of a charge-transfer complex as the reaction intermediate (Fukuzumi *et al.,* 2000).

$ArNO_2$ were less active NQO1 oxidants as compared to quinones (Misevičienė *et al.,* 2006). This may be explained by the fact that they have lower $\Delta S^{\neq}$ = -13 ÷ -8 J mol^{-1} K^{-1}, than compared with some of the quinones because of a less efficient electronic coupling of nitroaromatics with reduced isoalloxazine (Misevičienė *et al.,* 2006). Dicoumarol acts as an incomplete inhibitor towards an analogue of CB-1954, 5-(aziridin-1-yl)-2,4-dinitrobenzoic acid ethyl ester, and tetryl (Misevičienė *et al.,* 2006). This means that these compounds and dicoumarol bind at separate or weakly overlapping sites at the reduced form of NQO1.

In general, the log k_{cat}/K_m of nitroaromatic compounds tends to increase with an increase in their E^1_7. However, the relationship is poorly expressed (r^2 = 0.622) (Anusevičius *et al.,* 2002). It seems that the

increased affinity of nitroaromatics for NQO1, *i.e.,* their lower K_i with respect to NADPH in quinone reductase reaction, may enhance their reactivity. Another factor enhancing their reactivity is an increased nitrogroup torsion angle. Two available computer modeling studies (Chen *et al.,* 1999; Skelly *et al.,* 1999) propose that CB-1954 should form a π-π complex with the isoalloxazine ring of FAD by displacement of Tyr128', and interact with Tyr126', His161, and Phe106. In this case, CB-1954 should occupy the binding site of quinones and dicoumarol (Chen *et al.,* 1999; Bianchet *et al.,* 2004). However, the data of parallel kinetic studies (Anusevičius *et al.,* 2002; Misevičienė *et al.,* 2006) do not agree with the suggestion derived from computer modelling.

An important feature of NQO1 is that it reduces tetryl in a mixed, predominantly single-electron way (Anusevičius *et al.,* 1998). The reaction is accompanied with free radical formation, formation of nitrite and formation of N-methylpicramide as the main reduction product (Scheme 1). One may note that in this sheme the sequence of a second electron transfer and $NO2^-$ formation is not clearly established. Taken together, these data show that the most credible mechanism of reduction of quinones and nitroaromatics by NQO1 is a three-step (e^-, H^+, e^-) hydride transfer (Anusevičius *et al.,* 2002; Misevičienė *et al.,* 2006).

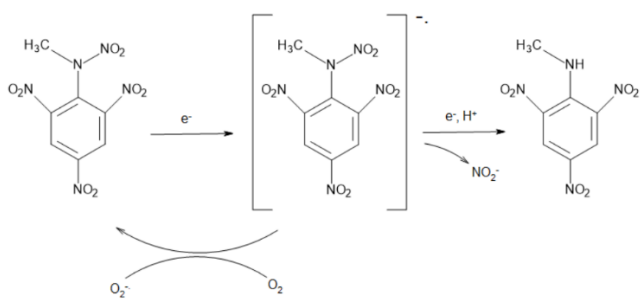

Scheme 1. Mechanism of the reduction of tetryl into *N*-methylpicramide.

The activity of NQO1 is frequently elevated in various tumors (Ross *et al.*, 2000). This provides the opportunity for designing quinoidal compounds, *e.g.*, RH1 (2,5-diaziridinyl-3-(hydroxymethyl)-6-methyl-1,4-benzoquinone), whose antitumor activity stems from their reduction by NQO1 to alkylating aziridinylhydroquinone products (Wardman, 2001).

Nitroaromatic compounds such as CB-1954 (5-(1-aziridinyl)-2,4-dinitrobenzamide) and its analogues were also intensively studied as substrates of NQO1 and potential antitumour agents (Sunters *et al.*, 1991; Knox *et al.*, 2003). However, their action is manifested only in tumours with exceptionally high NQO1 content, *e.g.* the Walker carcinoma.

2.3.2. Reduction of quinones and nitroaromatic compounds with oxygen-insensitive bacterial nitroreductases.

2.3.2.1. Classification and functions of nitroreductases

Bacterial nitroreductases are divided into oxygen-insensitive (type I) and oxygen-sensitive (type II) enzymes, which reduce nitroaromatic compounds in a two- or one-electron way, respectively. Oxygen-sensitive or type II nitroreductases catalyse $1e^-$ $ArNO_2$ reduction, forming nitroanion radicals which are rapidly reoxidized with oxygen. These enzymes were discovered in *E. coli* (Peterson *et al.*, 1979) and several *Clostridium* species (Angermaier and Simon, 1983), however they are not properly characterized. Oxygen-insensitive or type I nitroreductases catalyze NAD(P)H-dependent $ArNO_2$ $2e^-$ reduction, forming nitroso, hydroxylamine and amino products (Peterson *et al.*, 1979). Compared to type II nitroreductases, these enzymes are much more thoroughly characterized. Referring to *E. coli* nitroreductases and their homologues, these proteins are classified into groups A, B and C according to their

amino acid sequence (Table 1). Group C nitroreductases are poorly characterized (Bryant *et al.,* 1981).

Table 1. Oxygen-insensitive bacterial nitroreductases (Roldan *et al.,* 2008).

Nitroreductase	Monomer m.w. and electron donor	Oxidizing substrates
Escherichia coli NfsA (Group A)	27 kD, NADPH	Nitrofurazone and other nitrocompounds, chromate.
Escherichia coli NfsB (Group B)	24 kD, NAD(P)H	Nitrofurazone and other nitrocompounds (including CB-1954), chromate.
Salmonella enterica Cnr (Group B)	24 kD, NAD(P)H	Various aromatic nitrocompounds.
Salmonella enterica SnrA (Group A)	28 kD, NADPH	Various aromatic nitrocompounds and nitroheterocyclic compounds.
Enterobacter cloacae NR (Group B)	27 kD, NAD(P)H	Nitrofuranes, nitrobenzenes, quinones, nitroimidazoles, TNT.
Klebsiella sp. NTR I (Group B)	27 kD, NAD(P)H	TNT, 2,4-dinitrotoluene.
Pseudomonas pseudoalcaligenes NbzA (Group B)	30 kD, NADPH	Nitrobenzene, TNT, 4-nitrobiphenyl ether.
Pseudomonas putida PnrA (Group A)	28 kD, NADPH	TNT, 2,4-dinitrotoluene, 4-nitrotoluene, 4-nitrobenzoate, 3,5-dinitroaniline.
Vibrio fischeri FRase I (Group B)	25 kD, NAD(P)H	FMN, quinones, various nitrocompounds.
Vibrio harveyi Frp (Group A)	26 kD, NADPH	FMN, various nitrocompounds, chromate.
Synechocystis sp. DrgA (Group B)	26 kD, NAD(P)H	Flavins, quinones, nitrofurazone, dinoseb.

Rhodobacter capsulatus NprA (Group B)	27 kD, NAD(P)H	2,4-dinitrophenol and various nitroaromatic and nitroheterocyclic compounds.
Bacillus subtilis YwrO (Group B)	22 kD, NAD(P)H	CB-1954.
Bacillus subtilis NfrA1 (YwcG) (Group A)	29 kD, NADPH	Flavins, nitrofurazone, nitrofurantoin.
Staphylococcus aureus NfrA (Group A)	29 kD, NADPH	Flavins, nitrofurazone, nitrofurantoin.
Clostridium acetobutylicum NitA	31 kD, NADPH	TNT, 2,4-dinitrotoluene.
Clostridium acetobutylicum NitB	23 kD, NADPH	TNT, 2,4-dinitrotoluene.

To the best of our knowledge, the physiological functions and physiological electron acceptors for bacterial type I nitroreductases are not characterized. It is suggested that they plain certain role in the antioxidant defence of microorganism with participation of soxRS regulon. This regulon includes at least 15 genes that are upregulated in response to superoxide formed by redox-cycling compounds (Paterson *et al.,* 2001). A member of the soxRS regulon, *nfsA*, encodes the major oxygen-insensitive nitroreductase in *E. coli.* The activity of the promoter associated with this transcription start site was shown to be inducible by redox cycling paraquat (Paterson *et al.,* 2001). Nitroquinoline-*N*-oxide also induces the soxRS regulon (Nunoshiba and Demple, 1993). Concerning the protective effects, the overexpression of nitroreductase A protected *E. coli* against quinone adriamycin (Chatterjee *et al.,* 1995) possibly by catalyzing its divalent reduction. Also, it was determined that Frm1p and Hbn1p nitroreductases influence the response to oxidative stress in *S. cerevisae* yeast by modulating the GSH contents and

antioxidant enzymatic activities, such as superoxide dismutase, catalase and glutathione peroxidase (Oliveira *et al.*, 2009).

On the other hand, oxygen-insensitive nitroreductases may play a considerable role in the initial stages of the bioreductive degradation of polynitroaromatic explosives like 2,4,6-trinitrotoluene (TNT), and they are potential candidates for antibody- or gene-directed cancer therapies. In these cases, tumor-delivered NRs reduce the nitroaromatic prodrugs such as CB-1954 ((5-aziridin-1-yl)-2,4-dinitrobenzamide) into DNA-crosslinking hydroxylamine products (Prosser *et al.*, 2010) (Fig. 3). This enables to overcome low cancer cell sensitivity to these groups of nitroaromatics arising from low nitroreductase activity of NQO1.

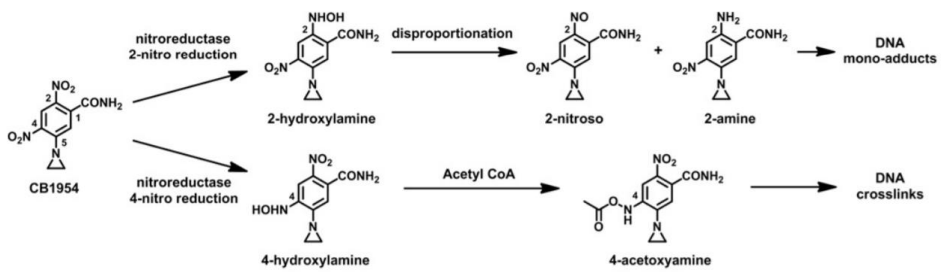

Fig. 3. Mechanism of activation and genotoxicity of metabolites of CB-1954 (Williams *et al.*, 2015).

2.3.2.2. Reduction of quinones and nitroaromatic compounds with group B nitroreductases.

Most thoroughly characterized members of group B nitroreductases are *E. coli* nitroreductase B (NfsB), *Enterobacter cloacae* nitroreductase (NR), and *Vibrio fischeri* NAD(P)H:FMN reductase (FRase I).

E. coli NfsB is FMN containing 2x24 kD homodimer, each monomer made of 5 β sheets, surrounded by α helices (Fig. 4). Enzyme

uses both NADH and NADPH as reducing substrates (Lovering *et al.*, 2001). Enzyme reduces nitroaromatic compounds via "ping-pong" mechanism. At pH 7.0 and 25 ^{o}C, maximal reduction rate of FMN exceeds 500 s^{-1}, *i.e.,* it is approaching stopped-flow limits (Race *et al.*, 2005). Maximal rate of nitrofurazone reduction, acquired by extrapolating to infinite NADH concentration, is equal to 255 s^{-1} (Race *et al.*, 2005). This indicates that reaction is limited by the oxidative half-reaction. This is also confirmed by the fact that using fixed NADH concentration, one obtains different V_{max} of reduction of different electron acceptors (Zenno *et al.*, 1996a). The studies of nitrobenzene and nitrosobenzene reduction by *E. coli* NfsB show that the latter one is reduced by 10^4 times faster than nitrobenzene (Race *et al.*, 2005). Therefore, this reaction should proceed spontaneously and the limiting step should be $ArNO_2$ reduction to ArNO. NfsB reduces a wide variety of substrates – ferricyanide, 1,4-benzoquinone and menadione with highest, rapidly, nitrofurans with slower, and flavin derivatives with slowest rates (Zenno *et al.*, 1996a). However, structure-activity and redox potential-activity relationships are not determined in NfsB reactions, as well as standard redox potential of this enzyme.

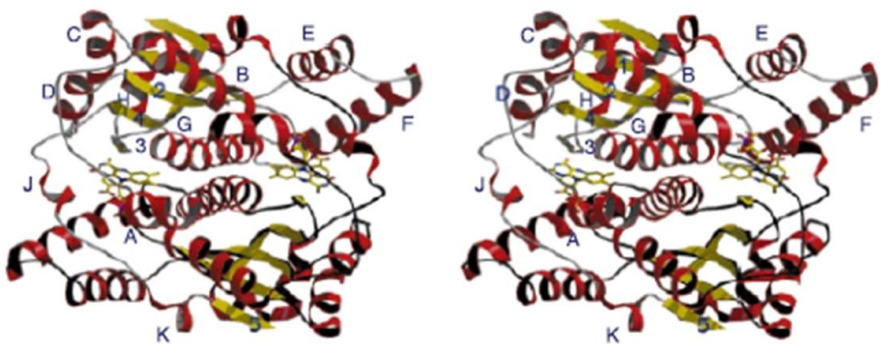

Fig. 4. Spatial structure of *E. coli* NfsB (Lovering *et al.*, 2001).

The crystal structure of *E. coli* NfsB was obtained in several studies (Parkinson *et al.,* 2000; Johansson *et al.,* 2003; Race *et al.,* 2005). According to them, FMN isoalloxazine ring is localized in intersubunit domain, its *re*-plane is solvent accesible. Nicotinamide ring of bound NAD(P)H is stacked between Phe124‘ from another subunit and isoalloxazine. Another important amino acid, which interacts with nicotinamide and isoalloxazine rings, is Ser39(40) (Johansson *et al.,* 2003).

The available crystallographic data of enzyme complexes with the oxidizing substrates demonstrate the different modes of their binding and interaction with isoalloxazine ring. Two binding sites of CB-1954 were found in different subunits of *E. coli* NfsB, Lys14, Lys74, Ser12 (A), and Phe124, Asn71, Gly166 (B). The parallel computer modelling data indicate that site B can provide more efficent π-π interaction of CB-1954 with isoalloxazine ring, evidently, due its stacking with Phe124 (Parkinson *et al.,* 2000). On the other hand, nitrufurazone binds identically in both subunits of NfsB, however, its conformation may be nonproductive, because only amide group and not nitrofuran ring interacts with isoalloxazine (Race *et al.*, 2005). Its binding causes the conformational changes of Glu165 and Phe70, and not of Phe124. Possibly, this points to the flexibility of the active site of NfsB and to considerable conformational changes occurring during oxidative half-reaction.

It appears that Phe124 which shields isoalloxazine from solvent, retards the reduction of bulky oxidants such as riboflavin, because Phe124Ser substitution in NfsB significantly increases riboflavin reduction rate, whereas the rates of reduction of quinones and nitroaromatics are affected insignificantly (Zenno *et al.*, 1996a). As with NQO1, dicoumarol efficiently inhibits NfsB, acting as a competetive

inhibitor to NADH (K_i = 2 µM (0.1 M phosphate, pH 7.0 (Anlezark *et al.*, 1992) or 10 µM (0.01 M Tris-HCl, pH 7.0 (Race *et al.*, 2005)) and as uncompetitive inhibitor to nitrofurazone or menadione. This indicates that dicoumarol binds more effectively to an oxidized NfsB. Acetate and acetamide also act as competitive inhibitors to NADH and uncompetitive inhibitors to nitrofurazon (Race *et al.*, 2005).

Various data indicate that *E. coli* NfsB reduces $ArNO_2$ with 100-1000 times faster rate than rat NQO1 (Anlezark *et al.*, 1992; Knox *et al.*, 1992). In the case of CB-1954 NQO1 produces only 4-hydroxylamine, whereas *E. coli* NfsB generates equal amounts of 2- and 4-hydroxylamine, however it cannot catalyze the reduction of both nitrogroups (Knox *et al.*, 1992; Race *et al.*, 2007).

For this reason, CB-1954/NfsB system was selected as a potential candidate for gene-directed enzyme prodrug therapy (GDEPT). Even though it has been known for more than 20 years, GDEPT is still in phases of clinical trials. GDEPT consists out of three components: non-active drug (prodrug), gene, which codes prodrug-activating enzyme and a carrier. One of the advantages of this method is that since toxic compound is only synthesized in transfected cells, toxicity for other tissues is much lower. The difference of NR/CB-1954 combination in GEDPT is that it kills both dividing as well as matured cancer cells, which have resistance towards other chemotherapeutic agents like cisplatin (Dachs *et al.*, 2009).

GDEPT can also act as a sensitive, non-invasive imaging method, which can show biodistribution, therapeutic effect of the drug and diagnostic results. One example of this are fluorescent probes – nitroheterocyclic fluorescent compounds, which are activated in hypoxic cells and form adducts with macromolecules (Olive and Durand, 1983). FSL-76 can be extremely useful in visualizing NRs, because its nitro

form is non fluorescent, but the reduced compounds has a green fluorescence (Fig. 5) (Copp *et al.*, 2017).

In order to optmize GDEPT methodology, NR/ARNO$_2$ prodrug system is getting improved by searching better enzyme mutants (Grove *et al.*, 2003, Jarrom *et al.*, 2009) and also perfecting new chemotherapeutic agents, *e.g.*, hybrid nitrogen mustard gas derivative PR-104A (Hu *et al.*, 2003; Mowday *et al.*, 2016). PR-104A (Fig. 5) is 20-fold better tolerated by humans than CB-1954 on a molar basis (Jameson *et al.*, 2010; Williams *et al.*, 2015).

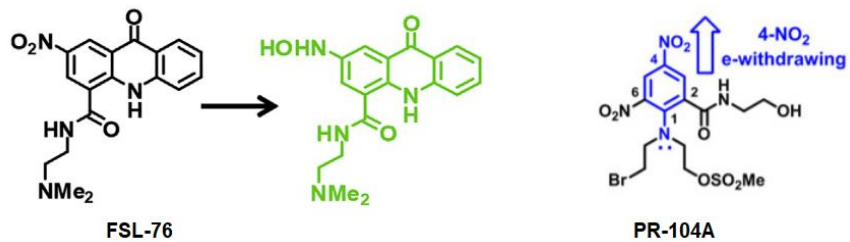

FSL-76 PR-104A

Fig. 5. The structures of FSL-76 and its reduced product, as well as the structure of potential GDEPT agent PR-104A (Copp *et al.*, 2017; Williams *et al.*, 2015).

Another well characterized group B enzyme is 2x27 kD *Enterobacter cloacae* NR, showing their typical properties. *E. coli* NfsB and *E. cloacae* NR sequence allignment (Fig. 6) shows that they are very similar (88 % homology). There is a great number of conserved amino acids in both active centres, including Phe124, Ser40, Asn71, and Gly166.

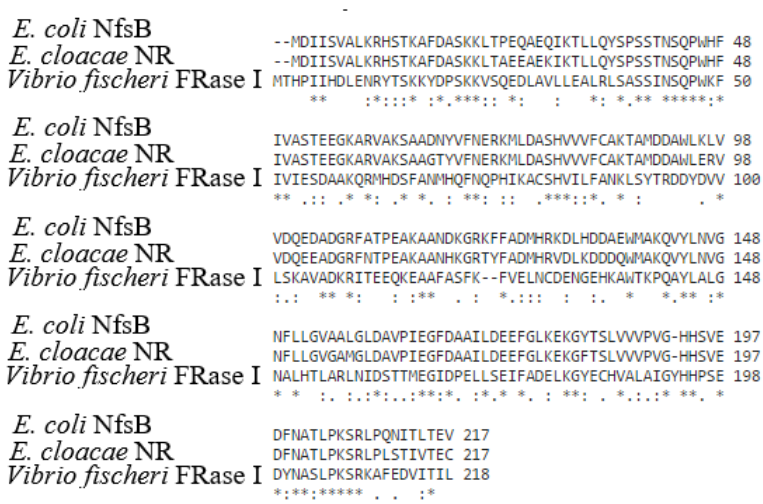

Fig. 6. *E. coli* NfsB, *E. cloacae* NR and *Vibrio fischeri* FRase I sequence allignment with Clustal.

Like NfsB, *E. cloacae* NR uses NADPH and NADH as an electron donor, but also in addition NMNH, which is by 10 times less efficient substrate as compared with NADH (Koder and Miller, 1998). Therefore it is thought that *E. cloacae* NR weakly interacts with NAD(P)H adenine group. This is also confirmed by insensitivity for inhibition with ADP-ribose. This nitroreductase is R-specific towards NADH. *E. cloacae* NR also has a wide spectra of substrates, including nitroaromatic compounds and quinones. It has been determined that: a) enzyme reduces TNT to its dihydroxylamine derivative; b) reduction of nitroaromatic compounds is non-specific, *i.e.*, their log k_{cat}/K_m increases with an increase in their single-electron reduction potential (E^1_7) or with the calculated heats of formation of their free radicals or hydride adducts ($ArN(OH)O^-$); c) reactivity of quinones (except for 2-hydroxy-1,4-naphthoquinone derivatives) is lower than that of nitroaromatic compounds with the same E^1_7 values (Nivinskas *et al.*, 2001a, 2002). Enzyme follows "ping-pong" kinetics, with k_{cat} under infinite NADPH concentrations exceeding 1000

s^{-1} in separate cases (Nivinskas *et al.,* 2002). Because this exceeds the limits of „stopped flow“ technique, it is impossible to determine the catalysis rate-limiting step at 25 °C. However, various electron acceptors possess different k_{cat} values at fixed NAD(P)H concentrations, which indicates that oxidative half-reaction may be limiting. It is important to note, that *E. cloacae* NR reduces tetryl not to *N*-methylpicramide (Scheme 1), but to species absorbing with λ_{max} = 340-420 nm. Nitrite is released not simultaneously, but after their formation, during their convertion into another species with λ_{max} = 375 nm. Concerning inhibitory analysis, it was found that dicoumarol acts as a strong competitive inhibitor to NADH (K_i = 62 nM), and enzyme is also weakly inhibited by benzoic acid derivatives (Koder and Miller, 1998). It is thought that this is determined by positive amino acid residues close to the active site, which attracts negatively charged organic acids.

The E^0_7 of *E. cloacae* NR is equal to -0.19 V (Koder *et al.,* 2002), and its semiquinone form is extremely unstable, *ca.* 0.01% at equilibrium (Haynes *et al.,* 2002). X-ray data show that the unique property of this enzyme is the bent structure of oxidized isoalloxazine (the N5-N10 axis diverts from coplanarity by 16°) (Haynes *et al.,* 2002). Noncoplanarity increases up to 25° in reduced state. Since semiquinones of free flavins are planar, this noncoplanarity may cause extremely great semiquinone instability. Possibly, this explains the two-electron character of reduction of nitroaromatic compounds and quinones with this enzyme.

Polar groups that interact with the pyrimidine ring and N5 include Lys14, and Asn71 and Lys74. On the dimethylbenzene side, Ile164, Tyr144, and Leu145 also follow the bend of the flavin. Ser39 and Ser40 from the other monomer, which sit over the central ring, move very little upon reduction of the flavin. Pro163 on the other side of the central ring shifts (by 0.15 Å) parallel to the plane of the ring, presumably as a

consequence of the shifts at positions 164 and 165 (Haynes *et al.*, 2002). Depending on the type and size of oxidizing substrate, other nearby aromatic residues (Tyr68, Phe70, Tyr123) may also participate in the binding interaction (Haynes *et al.*, 2002).

The stopped-flow studies of *E. cloacae* NR at 4 ^{o}C and pH 7.0 revealed that enzyme is reduced by NADH with V_{max} = 700±20 s^{-1} and K_m = 0.51±0.04 mM. *p*-Nitrobenzoic acid reoxidizes reduced enzyme with the maximal rate of 1.90±0.09 s^{-1}, *i.e.*, by 300 times slower. The k_{cat} in steady-state, 1.7±0.3 s^{-1}, is in line with these data, thus showing that the catalysis is limited by the oxidative half-reaction (Pitsawong *et al.*, 2014). KIE is observed in both reductive and oxidative half-reactions of *E. cloacae* NR (Pitsawong *et al.*, 2017). It shows that the H atom transferred from dihydronicotinamide to N-5 position of isalloxazine, is subsequently transferred to oxidant, *i.e.* the exchange of proton at N-5 position with the solvent is extremely slow.

A third best examined group B enzyme is *Vibrio fischeri* 26 kD NAD(P)H:FMN oxidoreductase (FRase I). Even though homology with E. *coli* NfsB and *E. cloacae* NR is not high (~30 %), the specific amino acids are still conserved in its active site (Phe124, Ser40(42), Asn71(73), Gly166) (Fig. 6). Main function of FRase I is the reduction of free FMN into $FMNH_2$, which is essential for bioluminescence of bacteria. FRase I follows “ping-pong“ scheme (Zenno *et al.*, 1996a). The FMN cofactor is located at the subunit interface, its isoalloxazine ring *re*-side is accessible to the solvent. Each subunit is comprised of 5 β sheets, which are surrounded by 7 α helices.

FRase I reduces nitroaromatic compounds and quinones, however its substrate specificity is not well investigated. It is worth mentioning that this enzyme reduces free FMN much faster than NfsB (Zenno *et al.*, 1996a). This enzyme is also inhibited by dicoumarol, however K_i value

was not determined. According to X-ray data (Fig. 7), dicoumarol binds to FRase I active site in bent conformation, one of its rings interacting with isoalloxazine ring, and another one – with Phe124 (Koike *et al.*, 1998). Since Phe124 is conserved in other group B nitroreductases, it is safe to suggest that this is a universal common dicoumarol binding mechanism.

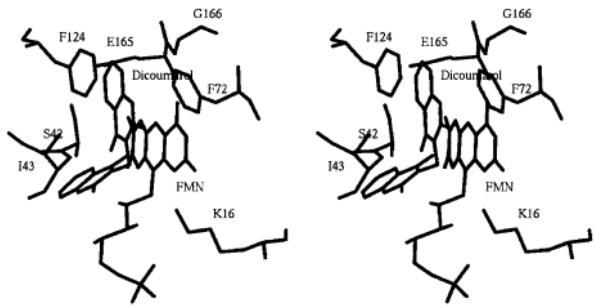

Fig. 7. Dicoumarol binding in *Vibrio fischeri* FRase active site (Koike *et al*., 1998).

2.3.2.3. Reduction of quinones and nitroaromatic compounds with group A nitroreductases.

In contrast to group B nitroreductases that use NADH and NADPH as reducing substrates, group A nitroreductases, of which *E. coli* NfsA is the best characterized member, can use only NADPH. This 27 kD protein is a homodimer, and its subunit is made of 5 β sheets core, surrounded by α helices. FMN cofactor is bound in intersubunit space, its *re*-side is pointed to the another subunit (Kobori *et al.*, 2001; Lovering *et al.*, 2001).

NfsA has a wide spectra of substrates – it can reduce flavin derivatives (FAD, FMN and riboflavin), nitroaromatic compounds (nitrofurazone**,** nitrofurantoin, nitrobenzenes, 4-nitroaniline), quinones, azo-dyes, methylene blue and ferricyanide (Zenno *et al.*, 1996b). As with

other nitrobenzenes, this enzyme can reduce potential antitumor agent CB-1954 to 4-hydroxylamine, which crosslinks DNA and causes cancer cells death. Nitrofurazone reduction by NfsA follows "ping-pong" mechanism with a limiting oxidative half-reaction step (Zenno *et al.*, 1996b). In anaerobic conditions this compound is reduced to open chain nitrile, which acts as an alkylating agent. However, the substrate specificity of this enzyme is insufficiently characterized.

Fig. 8. *E. coli* NfsA and *E. coli* NfsB sequence allignment in Clustal.

E. coli NfsA and NfsB sequence allignment shows a very low their homology (4 %) (Fig. 8). Considering the amino acids in the active site, it is worth mentioning that: a) Phe124 of NfsB is not conserved in NfsA, it coresponds to Ile129; b) Ser40 of NfsB is conserved, it corresponds to Ser41, and c) Asn71 and Gly166 of NfsB are not conserved, they correspond to Gln72 and Pro171 in NfsA. The computer modelling data suggest that Ser40, Ser41 and Phe42 are essential for the binding of oxidizing substrate (CB-1954) (Yang *et al.*, 2013). Phe42 of NfsA corresponds to Thr41 of NfsB or Ile43 of *V. fischeri* FRase, which participate in dicoumarol binding. It was unclear until recently whether

NfsA is inhibited by dicoumarol. However, the presence of hydrophobic Phe42 instead of hydrophobic Ile43 in FRase I indicates that NfsA may also be inhibited by dicoumarol. This residue is also important for NfsA activity and structure stability. Phe42 substitution into Tyr, Asn or Ala resulted in 52, 96, and 99% decrease in nitrofurazon**e** reaction rate (Yang *et al.,* 2013). Phe42Asn and Phe42Ala mutations also decreased k_{cat}/K_m of NADPH to 3-5% of original value (Yang *et al.,* 2013). On the other hand, Tyr42Phe mutation lowered k_{cat}/K_m of NADPH by 40-60%. It is suggested that Phe substitution into short–chain Ala may result in considerable conformational changes, whereas Tyr keeps similar conformation. Therefore, this may indicate that Phe42 does not act as a spacial obstacle, but contributes to the stabilization of the active site (Fig. 9). NfsA redox potential has not been determined until recently. The X-ray analysis of NfsA complex with NADPH was not succesful, however, the enzyme mutagenesis data show that 2‘-phosphate of NADPH binds to Arg203 (Kobori *et al.,* 2001).

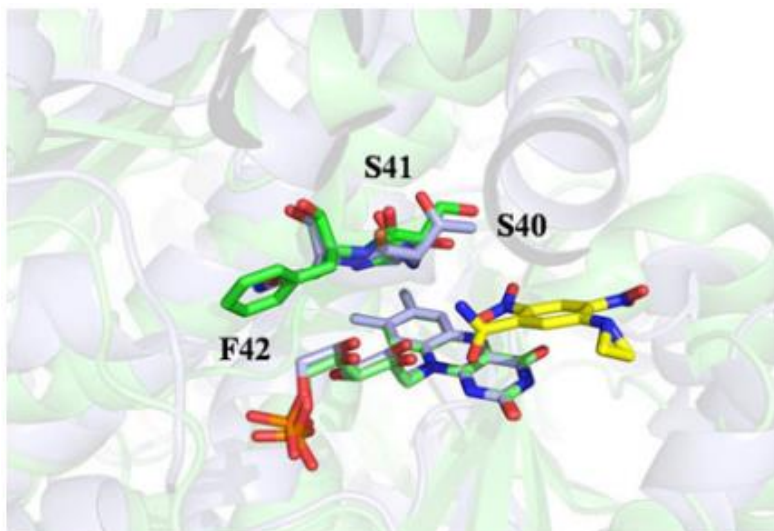

Fig. 9. The computer modelling data of *E. coli* NfsA and CB-1954 complex. Amino acids in enzyme active site are in green, while CB-1954 is in yellow (Yang *et al.,* 2013).

A third well characterized NfsA analogue is 26 kD NADPH:flavin oxidoreductase (Frp) from bioluminescent bacteria *Vibrio harveyi*. Because of this, it is suggested that *E. coli* family of oxygen-insensitive nitroreductases is genetically related to the family of flavin reductases of liuminescent bacteria. The function of these enzymes is to reduce flavin to dihydroflavin, which later participates in luminescence, catalyzed by luciferase (Lei *et al.*, 1994). Like NfsA and NfsB, this enzyme reduces nitroaromatics, quinones and FMN (Zenno *et al.*, 1996b; 1998). However, Frp possesed a much better FMN reductase activity that these enzymes. Structural and functional similarity of Frp and NfsA is evidenced by a 50-fold increased FMN-reductase activity of Glu99Gly mutant of NfsA, whereas this mutation insignificantly affects its activity with other oxidants (Zenno *et al.*, 1998). Frp is exceptional among group A nitroreductases because of the determined its redox potential value, E^{o}_{7} = -0.255 V) (Lei *et al.*, 2005). It was shown that redox equilibrium between $NADP^{+}$/NADPH pair is possible, *i.e.*, this enzyme can be reoxidized with $NADP^{+}$ (Lei *et al.*, 2005). Small absorbance increase in 500-700 nm range was observed during the titration of reduced Frp with $NADP^{+}$, however it is unclear, whether this is due to the formation of FMN semiquinone or $FMNH_2$-$NADP^{+}$ complex.

2.3.2.4 Reduction of quinones and nitroaromatic compounds with *Thermotoga maritima* peroxiredoxin-nitroreductase hybrid enzyme.

Another oxygen-insensitive NR with relatively well examined quinone- and nitroreductase reaction mechanism, is peroxiredoxin-nitroreducrase (Prx-NR) hybrid enzyme of the *Thermotoga maritima.* Prx-NR consists is of 321 amino acids, which form a peroxiredoxin (Prx) domain at the N-terminus (140 amino acids), and an FMN-containing NR domain at the C-terminus (170 amino acids) (Barbey *et al.*, 2008). The

extra 10 amino acids constitute a linker between the two domains. Previous physicochemical and structural characterization of its Prx domain (Barbey *et al.*, 2008) and of the holoenzyme (Couturier *et al.*, 2013) have shown that the Prx and NR domains function independently without the transfer of the redox equivalents between the domains, *i.e.*, NAD(P)H does not provide the electrons for the reduction of Prx-linked oxidants, and the reduction of NR-linked oxidants does not involve the Prx domain. FMN of NR domain is characterized by a standard redox potential of -0.185 V at pH 8.0 (Couturier *et al.*, 2013).

The sequence analysis of NR domain (residues 142-321, GenBank accession number NP_228196) revealed a modest homology, 20–24%, with the sequences of *E. coli* NR-B, and *E. cloacae* NR (Anusevičius *et al.*, 2012) The residues analogous to Phe124, Phe70, Ser40, Lys14 and Lys74 which participate in the binding of nitroaromatic compounds or the inhibitor dicoumarol in *E. coli* NR-B or *E. cloacae* NR, are absent in Prx–NR. On the other hand, the comparison of Prx–NR sequence with that of *E. coli* NR-A also shows a modest homology, 18%, but also points to a possible conservation of several residues participating in the binding of the isoalloxazine ring of FMN, Arg15 (Arg154 in Prx–NR), Gly130,131 (Gly235 and Arg236 residues in Prx–NR), and also Tyr128 (substituted into aromatic Phe260 in Prx–NR). Thus, it is possible that Prx–NR may share some properties of group A nitroreductases as well.

The steady-state kinetics of Prx-NR is characterized by a "ping-pong" scheme with a pronounced quinone-substrate inhibition (Anusevičius *et al.*, 2012). The inhibition constant of naphthazarin, K_{iq}, decreased with a decrease in NADH concentration, thus showing that naphthazarin is a competitive inhibitor with respect to NADH that binds to the oxidized enzyme form. The K_{iq} for naphthazarin at [NADH] = 0 was equal to 95±18 μM. The k_{cat} of this reaction was equal to 28±2.0 s^{-1} . The k_{cat}/K_m

for NADH obtained using 5,8-dihydroxy-, 5-hydroxy-1,4-naphthoquinone, or 9,10- phenanthrenequinone as electron acceptors was equal to $7.2\pm1.5\times10^5$ $M^{-1}s^{-1}$, *i.e.,* close to the apparent second-order reduction rate constant obtained in the presteady-state studies. The maximal rate of reduction of FMN of Prx–NR by NADH was equal to 146 ± 24 s^{-1}. Prx–NR was also inhibited by dicoumarol, which acted as a competitive inhibition with respect to NADH with K_i = 0.70±0.03 μM, thus showing that it competes for the NADH binding site in the oxidized enzyme form.

Prx-NR catalyzes two-electron reduction of quinones and nitroaromatics. The log k_{cat}/K_m of these groups of oxidants increase with their E^1_7 (Anusevičius *et al.,* 2012). Thus, the substrate specificity of Prx-NR is different from that of *E. cloacae* NR, where the reactivity of quinones was by one order of magnitude lower than that of nitroaromatic compounds with the same reduction potential (Nivinskas *et al.,* 2001a, 2002). In addition, in terms of k_{cat}/K_m, the reactivity of quinones and nitroaromatics oxidants towards Prx–NR was by one or two orders of magnitude lower than towards *E. coli* NR-B and *E. cloacae* NR (Nivinskas *et al.,* 2001a, 2002; Jarrom *et al.,* 2009)).

2.3.3. Conclusions

The data analysis shows that the mechanisms of quinone and nitroaromatics reduction by oxygen-insensitive group B nitroreductases are relatively well addressed. They include crystallographic data of the enzyme complexes with oxidants or inhibitors showing the dynamic structure of the active centers. Rapid reaction data point to the rate-limiting nature of oxidative half-reactions. The quantitative structure-activity relationships in steady-state reactions are established, although it is unclear where they could be the same in reactions of other groups of

nitroreductases. The available potentiometric data point to a low stability of FMN semiquinone state. At the same time, some aspects of catalysis of group A nitroreductases are less understood. They include the characterization of steady-state mechanisms, quantitative structure-activity relationships, and potentiometric studies. A common insufficiently understood problem of both enzyme groups is the mechanism of a net four-electron reduction of nitroaromatics into hydroxylamines, including the characterization of the roles of enzymatic and nonenzymatic reduction.

2.4. Reduction of Q ir $ArNO_2$ with C-S dehydrogenases-transhydrogenases

Section 2.4 addresses a broad topic, and contain the description of the mechanisms of enzyme reactions with their physiological electron oxidants. These data are necessary for better understanding of their mechanisms of interaction with nonphysiological oxidants, quinones and nitroaromatics.

2.4.1. Reduction of quinones with mammalian lipoamide dehydrogenase

Mammalian lipoamide dehydrogenase (LipDH, NADH:lipoamide oxidoreductase) is the E_3 component of the pyruvate dehydrogenase, α-ketoglutarate dehydrogenase, and glycine reductase multienzyme complexes. *In vivo,* it catalyzes the NAD^+-dependent oxidation of the dihydrolipoate that is covalently bound to the acyltransferase (E_2) components of these multienzyme complexes (Williams, 1992). LipDH are homodimers containing one noncovalently bound FAD and a redox

active disulfide (Cys41, Cys46) per monomer. The latter is located near the N-terminus of the polypeptide chain (Argyrou *et al.*, 2002).

In the reductive half-reaction of LipDH (Fig. 10), NADH binds to the oxidized enzyme (E_{ox}) and reduces the FAD to $FADH_2$ intermediate. The subsequent reduction of catalytic disulfide is thought to proceed via a covalent adduct between Cys46 and the C4a position of the FAD (Williams, 1992). It generates two-electron reduced form of the enzyme (EH_2), the oxidized FAD and reduced disulfide charge-transfer complex with characteristic absorbance at 530-540 nm. The NAD^+ dissociation completes the reductive half-reaction.

In the oxidative half-reaction (Fig. 10), lipoamide binds to the EH_2, forming a mixed disulfide with Cys41. The free thiolate of Cys46 then attacks the mixed disulfide to form dihydrolipoamide and to regenerate E_{ox}. This reaction is catalyzed by the essential and conserved His-Glu pair located at the C-terminus of the adjacent subunit. Release of dihydrolipoamide completes the catalytic cycle of enzyme.

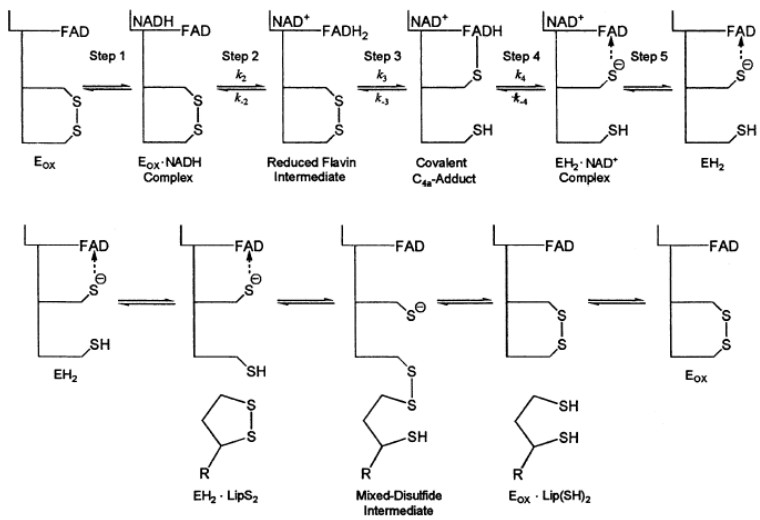

Fig. 10. Reductive and oxidative half-reactions of lipoamide dehydrogenase.

This reaction of pig heart LipDH follows the "ping-pong" mechanism, complicated by the inhibition with high NADH concentrations**.** This is caused by the formation of fraction of LipDH overreduced with NADH, *i.e.,* the formation of $4e^-$-reduced enzyme form (EH_4), possessing reduced FAD and reduced catalytic disulfide. Lipoamide is unable to reoxidize this enzyme form, therefore, the reaction is activated by NAD^+ formed in the course of reaction (Argyrou *et al.,* 2002). At pH 7.0, the standard potentials of E_o/EH_2 and EH_2/EH_4 redox couples are equal to -0.280 V and -0.345 V, respectively (Matthews and Williams, 1976). In steady-state reactions of pig LipDH at pH 7.0, k_{cat} is 420 s^{-1} , the k_{cat}/K_m for NADH is 1.1×10^7 $M^{-l}s^{-1}$, and k_{cat}/K_m for lipoamide is 2.8×10^5 M^{-1} s^{-1} (Vienožinskis *et al.,* 1990). The use of 4(S)-^{2}H NADH as substrate does not decrease the k_{cat} of reaction, thus showing that the reaction is limited by the oxidative, but not reductive half-reaction.

Quinone reductase reaction of pig LipDH is relatively rapid, with k_{cat} reaching 70 s^{-1} at pH 7.0 (Vienožinskis *et al.,* 1990). The reaction follows a "ping-pong" mechanism with k_{cat}/K_m of NADH much lower than in lipoamide reductase reaction, 9.2×10^5 $M^{-1}s^{-1}$. Importantly, the use of 4(S)-^{2}H NADH decrases k_{cat}, thus showing that the reductive half-reaction is rate-limiting. The k_{cat}/K_m of quinones increase with their E^1_7, reaching 10^6 $M^{-1}s^{-1}$ in the case of 1,4-benzoquinone and 2-methyl-1,4-benzoquinone. The reaction is characterized by 23% single-electron flux. Interestingly, the use of deuterated NADH decreases k_{cat}/K_m of quinones by 1.85-3.0 times, whereas the k_{cat}/K_m of single-electron oxidant ferricyanide is decreased by 1.35 times. This shows that ^{2}H transferred from NADH to N5 position of isoalloxazine is transferred to quinone, most probably during its two-electron reduction. The mixed character of inhibition of quinone reductase reaction by NAD^+ is consistent with the

reoxidation of enzyme with low NAD^+ concentrations, and with its competition with NADH for oxidized enzyme form. It shows that this reaction is performed mainly by the EH_4 enzyme form, whose fraction is formed in the presence of NADH and in the absence of NAD^+ and lipoamide. However, the EH_2 form of LipDH also participates in quinone reduction, although at lower rate.

There also exists a rapid redox equilibrium between the NAD^+/NADH and the E_o/EH_2 (E^0_7 = –0.285 V), and EH_2/EH_4 (E^0_7 = –0.345 V) redox couples of LipDH (Matthews and Williams, 1976, Matthews *et al.*, 1979), which is attained much faster than the rate of quinone reduction. Thus, the role of EH_2 in the quinone reduction rate by LipDH may be estimated at $[NAD^+]/[NADH] = 4.7$, which, according to the Nernst equation, corresponds to the redox potential of the medium of –0.300 V. Under these conditions, EH_4 is not formed, and EH_2 is present at the amount of ca. 75% (Anusevičius and Čėnas, 1993). The rates of LipDH-catalyzed reduction of quinones under the physiological conditions are by 8–20 times lower than in the steady-state assays of LipDH at $[NAD^+] = 0$ (Nivinskas *et al.*, 2014).

2.4.2. Interaction of quinones and nitroaromatic compounds with glutathione reductase and trypanothione reductase

Glutathione reductase (GR) and trypanothione reductase (TryR) are 2×55 kD homodimers containing one FAD and catalytic disulfide per subunit. GR catalyzes the reduction of glutathione disulfide (GSSG), and TryR catalyzes the reduction of trypanothione, a glutathione-spermidine conjugate (TS_2) at the expense of NADPH. The crystal structure and reaction mechanism of both enzymes are very similar, except the differences in the structure and electrostatic charge of disulfide oxidant binding site, which will be discussed below. The best studied

representatives of GR are those from yeast, human erythrocytes, and malaria parasite *Plasmodium falciparum* (Kanzok *et al.*, 2000). In these objects, GR perform antioxidant functions, regenerating reduced glutathione (GSH). TR is found exclusively in trypanosomes and leishmania, the causative parasites of several tropical diseases, including African sleeping sickness and Chagas disease. The best studied are TryRs from *Trypanosoma brucei*, *T. congolense*, *T. cruzi*, and *Crithidia fasciculata*. These parasites do not contain GSSG/GSH, and their antioxidant defence relies mainly on TryR-catalyzed regeneration of $T(SH)_2$ (Fairlamb and Cerami, 1992).

The crystal structure of GR (Pai and Shulz, 1983; Karplus *et al.*, 1989; Sarma *et al.*, 2003) and TryR (Kuriyan *et al.*, 1991) reveals the presence of a NADPH-binding site at the *si*-face of isoaloxazine ring, and a catalytic disulfide at its *re*-face, *e.g.*, Cys58, Cys63 (erythrocyte GR), Cys39, Cys44 (*P. falciparum* GR), and Cys52, Cys57 (*C. fasciculata* TR). The reduction of GR and TryR with NADPH proceeds analogously to LipDH (Williams, 1992) (Fig. 10), with the final formation of enzyme EH_2 form (λ_{max} = 530-540 nm). In human erythrocyte GR, Cys63 is close to the flavin C_{4a} and is responsible for the flavin–thiolate charge-transfer complex formation, while a solvent-accessible Cys58 forms a mixed disulfide intermediate with GSSG. The amino acid composition at the disulfide-oxidant binding domain of GR and TryR possess certain differences, enabling to discriminate between the negatively charged GSSG and positively charged TS_2. The main residues responsible for the selectivity are Ala34, Arg77 and Arg347 in erythrocyte GR, which correspond to Glu18, Trp21 and Ala323 in *T. congolense* TryR (Karplus *et al.*, 1989; Sullivan *et al.*, 1991).

The redox potentials of E_o/EH_2 couple of GR and TryR are more positive than that of pig heart LipDH. At pH 7.0 they are equal to -0.227

V (erythrocyte GR), -0.237 V ÷ -0.255 V (yeast GR) (Veine *et al.*, 1998; Rakauskienė *et al.,* 1989), -0.206 V (*P. falciparum* GR, pH 6.9, 4 ^{o}C, Böhme *et al.,* 2000), and -0.273 V (*T. congolense* TR, pH 7.5, Zheng *et al.,* 1995). The E^{0}_{7} for EH_2/EH_4 redox couple of erythrocyte GR is equal to -0.325 V (Veine *et al.,* 1998). It is important to note that although this value is more positive than that of EH_2/EH_4 couple of pig LipDH (Vienožinskis *et al.*, 1990), the superreduced form of GR is not formed during the enzyme turnover. This is attributed to the tight binding of NADPH, which stabilizes the EH_2 state of GR (see below).

The NADPH-dependent reduction of GSSG by GR and TryR of various sources various proceeds according to a "ping-pong" mechanism with k_{cat} = 120 ÷ 240 s^{-1}, and k_{cat}/K_m for NADPH of 1.0 ÷ 5.0×10^7 $M^{-1}s^{-1}$ at pH 7.0 and 25 ^{0}C (Čėnas *et al.*, 1989, 1994; Grellier *et al.,* 2010). The reaction rate-limiting step is reductive half-reaction. One may note, however, that the "ping-pong" mechanism of GR should be classified as "hybrid ping-pong", because during turnover, GSSG reoxidizes not free EH_2 form, but its tight complex with repeatedly bound NADPH (K_d = 2.1 μM, yeast GR, Bulger and Brandt, 1971). In this case, GSSG oxidizes free EH_2 and its complexes with NADPH and $NADP^+$ with sufficiently close rates. The complex of two-electron reduced GR with $NADP^+$ possesses flat absorbance from 500 nm to above 800 nm (Williams, 1976**),** it is formed at high $NADP^+$/NADPH ratio (K_d = 40-60 μM, yeast GR, Čėnas *et al.,* 1989). The formation of EH_2-$NADP^+$ complex is also characteristic for *T. congolense* TryR (Čėnas *et al.,* 1994). The reverse reaction - the reduction of $NADP^+$ with GSH, is best characterized for yeast GR (Rakauskienė *et al.,* 1989). Its k_{cat} increases with pH, reaching 25 s^{-1} at pH 8.0.

The k_{cat} of reduction of quinones by yeast GR, 4-5 s^{-1}, and TryR of *T. congolense,* 1.6÷24 s^{-1}, comprise several percent of the maximal

reduction rates of their physiological disulfide oxidants (Čėnas *et al.*, 1989, 1994). The reduction of model benzo-, naphtho- and phenanthrene-quinones proceeded nonspecifically, *i.e.*, their log k_{cat}/K_m increased with E^1_7. The reaction proceeded with 3.6% single-electron flux (yeast GR), and 44% single-electron flux (*T. congolense* TryR). The presence of acidic, basic, or aromatic substituents in quinone or nitrofuran ring conferred them certain specificity towards erythrocyte or *P. falciparum* GR, or TryR of other sources (Henderson *et al.*, 1988; Belorgey *et al.*, 2013), however, the maximal rates of their reduction did not exceed the above presented limits.

A specific feature of quinone reductase reaction of GR and TryR is their activation by the reaction product, $NADP^+$. At $[NADP^+]/[NADPH] = 100$, the k_{cat} of reduction of quinones by yeast GR increased up to 30-33 s^{-1} with concomitant increase in k_{cat}/K_m of quinones by several times, and an increase in single-electron flux up to 44% (Čėnas *et al.*, 1989). The same events took place in the reactions of *T. congolense* TryR, where at $[NADP^+]/[NADPH] >10$ the rates of quinone reduction were enhanced by 1.4-3.6 times, and the single-electron flux increased up to 80% (Čėnas *et al.*, 1994). This phenomenon is explained by the participation of reduced FAD of EH_2 enzyme form in the reaction. Although the main electron density in FAD-thiolate charge-transfer complex is localized on thiolate, its minor part remains on FAD. The binding of $NADP^+$ to EH_2 with a concomitant displacement of NADPH causes further bleaching of 460 nm absorbance, *i.e.*, increases the electron density on FAD (Williams, 1976), which may accelerate the quinone reduction. In accordance with this, the rapid reaction experiments demonstrate the following order of reactivity of TryR: $EH_2 < EH_2$-NADPH $< EH_2$-$NADP^+$ (Čėnas *et al.*, 1994). Similar results were obtained in the case of *P. falciparum* GR. Using 150 μM menadione as

oxidant, the turnover number of 0.09 s^{-1} was obtained at pH 7.0 and 25 ^oC (Grellier *et al.,* 2010). In stopped-flow experiments, the same concentration of menadione reoxidized the EH_4 form of enzyme to EH_2 with k = 6.0 s^{-1}, and EH_2 to E_o with $k \leq 0.01$ s^{-1} (Bauer *et al.,* 2006). Because NADPH was absent in the rapid reaction experiments, it shows that the enzyme form, participating in steady-state reaction, is the complex of NADPH with EH_2, *i.e.*, the reactivity order is EH_4 > EH_2-NADPH > EH_2.

Another important aspect of interaction of quinones and nitroaromatics with GR and TryR is the inhibition of the reduction of their physiological disulfide oxidants (Henderson *et al.,* 1988; Čėnas *et al.*, 1994; Sarma *et al.,* 2003; Tyagi *et al.,* 2015, Belorgey *et al.,* 2013)**.** In these cases, compounds act as non- or uncompetitive inhibitors with respect to these substrates, and bind at the intersubunit domain of GR or TryR close to the binding sites of their disulfide oxidants. The amino acid residues of this domain of GR are strikingly different, *e.g.*, His75, Glu77, Phe78, Val174, Leu438, and Gly439 (erythrocyte GR), and Ser55, Val56, Asp58, Ile59, Leu455, and Asn456 (*P. falciparum* GR) (Sarma *et al.*, 2003). On the other hand, the different but functionally analogous domain, Ser14, Leu17, Glu18, Trp21, Asn22, Ser109, Tyr110, Met113, and Phe114, is conserved in trypanothione reductases of different origin, *T. congolense, T. cruzi* and *T. brucei* (Taylor *et al.,* 1994). Currently, the significant efforts are devoted to the studies of efficient and specific inhibitors targeted to this domain, with an aim of development of new antimalarial or trypanocidal drugs. It seems, however, that the binding of these compounds to this domain is unrelated to their reduction by GR and TryR.

2.4.3. Interaction of quinones and nitroaromatic compounds with thioredoxin reductases

2.4.3.1. Thioredoxin reductases and their physiological oxidants, thioredoxins and glutaredoxins

NAD(P)H-thioredoxin reductases (TR) and thioredoxins (Trx) comprise the redox systems found in both prokaryotic and eukaryotic organisms (Arner and Holmgren, 2000). Like in other C-S dehydrogenases-transhydrogenases, the obligatory redox cofactors of TrxRs are FAD and catalytic disulfide. However, TRs are classified into two groups with different structure and redox properties:

1) High molecular mass proteins (2×54÷58 kD subunit, H-TR), which have FAD, catalytic disulfide and selenocysteine in its active centre (various mammalian TrxRs). On the other hand, *P. falciparum* TR contains additional cysteine redox center (Tamura and Stadtman, 1996);
2) Low molecular mass proteins (2×35 kD, L-TR), which are found in eukaryotes, bacteria and archea (Hirt *et al.,* 2002).

Apart from thioredoxins, TRs in certain cases may reduce other physiological disulfide oxidants, glutaredoxins (Grx), whose properties and functions are addressed below.

The main physiological functions of Trxs and Grxs is to reduce disulfide bridges of their protein targets (Holmgren, 1989). In addition, these proteins perform antioxidant functions, act as autocrine growth factors, and participate in the reductive regulation of transcription factors and hormones. These functions consist of the maintainance of reduced state of cellular thiolate pool and the reparation of erroneous disulfides or other groups, formed under the oxidative stress. Trxs and Grxs are found in both prokaryotic and eukaryotic organisms.

Thioredoxins are low m.w. (10-12 kD) proteins, containing redox active disulfide motif CXXC, whose redox reactions are reversible. In Trx-catalyzed disulfide reduction, the -SH group of the *N*-side of CxxC motif attacks –S-S- bridge of a target protein, forming a mixed disulfide and free target –SH group. Then the thiol of the *C*-side of CxxC motif disrupts a mixed disulfide, forming fully reduced target protein and oxidized Trx **(**Biaglow and Miller, 2005).

Two Trxs are found in human genome, cytosolic Trx1 and mitochondrial Trx2. The E^0_7 of human Trx1 is equal to -0.230 V (Watson *et al.,* 2003). In mammalians, Trxs expression is enhanced during spermatogenesis (Jimenez *et al.,* 2006). Knockout of Trxs in mice causes early embryo death, which demonstrates its essential role, most probably arising from the participation in embryonal RNA reduction (Nonn *et al.,* 2003; Meyer *et al.,* 2009). In plants, thioredoxins participate in regulation of photosynthesis and germination (Florencio *et al.,* 1988; Buchanan *et al.,* 1994).

The genome of *E. coli* also contains two Trxs. The E^0_7 of *E. coli* Trx1 is equal to -0.270 V (Watson *et al.,* 2003). Its catalytic motif Cys-Gly-Pro-Cys is located at the C-terminal end of a β-strand and in the first turn of a long bent α-helix (α_2) (Holmgren, 1989). The area containing residues 33-34, 75-76, and 91-93 is involved in its binding with other proteins.

The knockout of Trx1 is not lethal for bacteria (Liang *et al.,* 2016). Among the targets of Trx in *E. coli*, RNA reductase I can be reduced by Trx1 and Trx2 (Sengupta and Holmgren, 2014). Trx1 is an efficient reductant of 3-phosphoadenylsulfate (PAPS) reductase, an enzyme essential in sulfate metabolism (Krone *et al.,* 1990). Trx1 regenerates the reduced form of methionine sulfoxide reductase (MSR) by reduction of –S-S- bridge formed after the enzymatic reduction of methionine

sulfoxide. The later is formed in proteins subjected to oxidative stress (Boschi-Muller *et al.,* 2008). An important target for Trx are peroxyredoxins, which catalyze the reduction of H_2O_2 and fatty acid hydroperoxides (Poole, 2005).

Glutaredoxins (Grx) with m.w. 10-12 kD, are divided into dithiol- and monotiol-containing ones. Dithiol Grxs possess an Cys-Pro-Tyr-Cys motif, and catalyze thiol-disulfide exchange, being directly (nonenzymatically) reduced by GSH. Monothiol Grxs possess a Cys-Gly-Phe-Ser motif, and are, with few exceptions, inactive in classical enzymatic Grx activity assays. They participate in iron metabolism with currently poorly understood mechanism (Berndt and Lillig, 2017).

Two dithiol-containing Grxs, cytosolic Grx1 and mitochondrial Grx2 were found in humans (Lonn *et al.*, 2008) and other mammalian species. Grx1 knockout in mice did not have any visible consequences except the elevated concentration of gluathionylated proteins (Ho *et al.,* 2007). Enhanced Grx1 expression caused higher tolerance of heart anoxia in mice (Malik *et al.,* 2008). On the other hand, enhanced human Grx2 expression lead to the death of myocardial cells (Nagy *et al.*, 2008). Three Grxs and two Grx-like proteins (Grx4 and NrdH) are found in *E. coli*. However, their knockout is not lethal (Vlamis-Gardikas *et al.*, 2002). The putative targets of Grx1, Grx3 and NHrdH in *E. coli* are RNA reductase I and PAPS reductase (Russel *et al.,* 1990; Gon *et al.,* 2006).

2.4.3.2. Reactions of quinones and nitroaromatic compounds with mammalian thioredoxin reductase

Mammalian (rat, human) TR is comprised of two 54-58 kD subunits (Oblong *et al*, 1993; Zhong *et al.*, 2000; Nordberg and Arner, 2001), its mechanism is similar to glutathion**e** reductase**.** In addition to FAD and catalytic disulfide, TR contains selenylsulfide, which is located at the

extension of 16 residues of C-end of the protein, within a tetrapeptide motif (-Gly-Cys-Sec-Gly-COOH). The catalysis of TR involves the reduction of FAD by NADPH and subsequent transfer of two electrons to disulfide (Cys59, Cys64) in the N-terminal domain, containing a sequence identical to that of GR (CVNVGC), Subsequently, the electrons are transferred from dithiolate to a selenenylsulfide of another subunit (Fig. 11). At the same time, TR is repeatedly reduced by a second NADPH molecule. The catalytic selenolthiol is responsible for the reduction of mammalian Trx and other numerous substrates of mammalian TR.

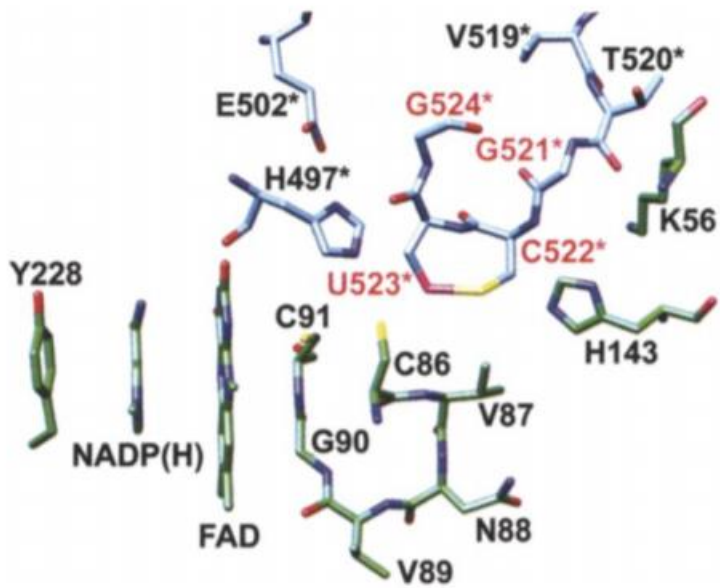

Fig. 11. Model of the C terminus of mitochondrial TR. Carbon atoms from subunit A are colored in green, and those from subunit B are in blue and are designated with asterisks. Modeled residues are labeled in red. For clarity, only the nicotinamide ring of NADP(H) and the isoallozaine ring of FAD are presented (Biterova *et al.*, 2005).

During catalysis, enzyme cycles between $2e^-$ and $4e^-$-reduced states (Arscott *et al.*, 1997; Nordberg and Arner, 2001). 4e- reduced enzyme has an absorbance maximum at 530 nm typical for GR and LipDH, whereas $2e^-$ reduced enzyme possesses half that absorbance. $6e^-$ reduced TR is formed under artificial harsh conditions. FAD is reduced by NADPH very rapidly (>400 s^{-1}), therefore the limiting stange of the reaction may be charge transfer to catalytic selenocysteine, 30-40 s^{-1} (Nordberg and Arner, 2001). The redox potential of the EH_2/EH_4 couple of TR calculated according to the Haldane relationship with $NADP^+$/NADPH was -0.294 V at pH 7.0 (Čėnas *et al.*, 2004). In contrast to L-TRs, mammalian TR may directly reduce 5,5‘-dithio-bis(2-nitrobenzoic acid (DTNB). This reaction is often used to determine TR activity in biological systems and kinetic analysis (Holmgren, 1977; Arner and Holmgren, 2000). The reduction of DTNB and *Chlamydomonas reinhardtii* Trx by TrxR follows “ping-pong“ mechanism (Čėnas *et al.*, 2004).

Mammalian TR possesses a wide range of substrates, including disulfides cystine, lipoic acid, and non-disulfide compounds alloxan, dehydroascorbate, vitamin E, coenzyme Q10 and vitamin K, lipid peroxides and H_2O_2 (Bjornstedt *et al.*, 1995; Zhong *et al.*, 2000; Nordberg and Arner, 2001). Because of this property TR can function as an alternative system for detoxication of lipid peroxides. However, the high value of K_m of H_2O_2, 2.5 mM indicates that TR effectively detoxifies it only if its concentration in the media is high (Zhong *et al.*, 2000). For comparison, thioredoxins are reduced with micromolar K_m values. Besides, all these reactions with exception of lipoic acid, proceed at the rates lower than DTNB reduction.

Rat TR reduces quinones and nitroaromatic compounds in a mixed single- and two-electron way (Čėnas *et al.*, 2004, 2006). During the

reaction, enzyme cycles between four- and two-electron reduced states. 2,3-Dichloro-1,4-naphthoquinone (k_{cat} = 9.6 s^{-1} and k_{cat}/K_m = 6.1×10^6 $M^{-1}s^{-1}$) and 9,10-phenanthrene quinone (k_{cat} = 17.3 s^{-1} and k_{cat}/K_m = 1.9×10^6 $M^{-1}s^{-1}$) turned out to be the best substrates. Among nitroaromatics, tetryl displayed the highest activity (k_{cat} = 1.8 s^{-1} and k_{cat}/K_m = 1.4×10^4 $M^{-1}s^{-1}$), whereas k_{cat}/K_m of other compounds varied in 10^2-10^3 $M^{-1}s^{-1}$ range (Čėnas *et al.,* 2004; 2006). In general, the reactivity of compounds increases with their E^1_7, but the linear log k_{cat}/K_m *vs.* E^1_7 relationship is poorly expressed.

The most important feature of reduction of quinones and nitroaromatics with TR is that in addition to reduced FAD, it is performed by reduced selenocysteine. The rates of reduction of DTNB or fully substituted 9,10-phenanthrene quinone were decreased by 95% after 10 min incubation of reduced TR with 1.0 μM gold thioglucose, which specifically reacts with selenol. At the same time, the reduction rate of juglone decreased by 25-30% (Čėnas *et al.,* 2004). The binding of phenanthrene quinone and tetryl close to selenocysteine was demonstrated by their action as competitive to DTNB inhibitors with K_i of 6.3 μM and 12.5 μM, respectively (Čėnas *et al.,* 2004, 2006). The participation of selenocysteine in these reactions may be explained by the relative ease of its single-electron oxidation, since E_7($Sec^{\cdot}$/Sec^-) is equal to 0.43 V, whereas E_7($Cys^{\cdot}$/CysH) is equal to 0.92 V (Nauser *et al.,* 2006).

The rate of TR-catalyzed NADPH oxidation by partly substituted 1,4-benzoquinones sharply decreases after 0.5 min, and the incubation of reduced enzyme for the same time with 50 μM 1,4-naphthoquinone or its 5-hydroxy- and 5,8-dihydroxy-derivatives resulted in a 50–60% decrease of the DTNB reduction rate. Similar, although slower inactivation was observed during the incubation of reduced TR with tetryl, which react with –SH groups forming trinitrophenylthiones (Marozienė *et al.,* 2001).

In contrast, the activity of reduced TR was unchanged after incubation with phenanthrene quinone (Čėnas *et al.,* 2004). These data show that the reduction of certain quinones and nitroaromatics with TR may be accompanied by their covalent modification, like in the previously described alkylation of reduced enzyme with 1-chloro-2,4-dinitrobenzene (Arner *et al.,* 1995). In this case, Sec^- is a possible target for alkylation due to its high nucleophilicity. Because the antitumour/cytotoxic activity of nitrosoureas and various gold and platinum derivatives is partly attributed to their inactivation of TR (Nordberg and Arner, 2001), it is possible, that the cytotoxicity of partly substituted quinones and certain nitroaromatics may be also partly manifested through this mechanism.

2.4.3.3. Reactions of quinones and nitroaromatic compounds with bacterial and plant thioredoxin reductases

Escherichia coli thioredoxin reductase is the most thoroughly studied representative of L-TRs. *E. coli* TR is 2×33 kD homodimer, which has one FAD molecule and one active disulfide group in per subunit. In catalysis, NADPH transfers hydride to FAD, which subsequently reduces catalytic disulfide. The later transfers redox equivalents to Trx disulfide (Williams, 1995).

In contrast with GR and TryR, *E. coli* TR and other L-TRs do not form FAD-thiolate charge transfer complex in $2e^-$ reduced state (Williams, 1995). This is determined by the specific structure of L-TRs – the enzyme consists of FAD-binding domain and NADPH-binding domain, whereas the catalytic disulfide -Cys135-Ala-Thr-Cys138- is a part of the NADPH-binding domain (PN domain, Fig. 12) (Williams, 1995). It was assumed that in solution, the enzyme exists in an equilibrium between two conformers, nonfluorescent FO (catalytic

disulfide adjacent to FAD), and fluorescent FR (NADP(H) binding site adjacent to FAD) (Waksman *et al.*, 1994; Williams, 1995; Wang *et al.*, 1996; Mulrooney and Williams, 1997). After the NADPH binding to the catalytic disulfide domain, the nicotinamide ring is at 17 Å distance from the isoalloxazine ring (FO conformation, Fig. 12). In order for NAD(P)H to reach FAD, or for Trx to reach catalytic disulfide, the rotation of NAD(P)H domain with the adoption of FR conformation, is necessary (Williams, 1995; Wang *et al.*, 1998).

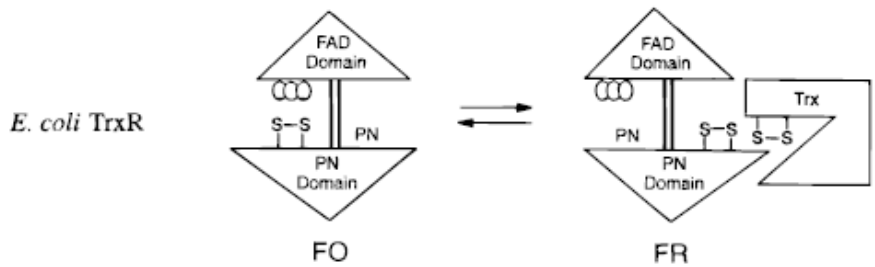

Fig. 12. Conformational changes of *E. coli* L-TR in NADPH (PN) and thioredoxin (Trx) binding (Wang *et al.*, 1998).

When NADPH-binding domain is rotated by 66°, leaving its FAD domain fixed, the nicotinamide ring of NADPH is brought in close contact to the isoalloxazine ring system with the nicotinamide C-4 above the isoalloxazine N-5 (Waksman *et al.*, 1994). With this rotation, the redox active dithiol moves to the surface of the protein where it is now accesible to thioredoxin. Interestingely, a cluster of charged residues (Arg181, Glu183, Lys184) are now allowed to fit into a charged pocket formed on the other monomer by the tip of C-terminal helix and loop connecting residue 24 to residue 29. This dimer interface interaction stabilizes NADPH domain onto the FAD domain in its rotated conformation (Waksman *et al.*, 1994). Cys135 is assumed to be the TR interchange thiol, whereas Cys138 interacts more closely with FAD.

This was confirmed by FAD fluorescence quenching experiments by various pyridine nucleotides (Mulrooney and Williams, 1997).

It was determined that the reduction of FAD is very fast, 590 s^{-1} at pH 7.0, therefore the catalytic cycle being characterized by k_{cat} = 25-30 s^{-1}, is limited by the rate of comformational change or Trx reduction (Lennon and Williams, 1996). Reduction of *E. coli* TR followed "ping-pong" scheme and k_{cat}/K_m was determined to be 1.76 x 10^7 $M^{-1}s^{-1}$ (NADPH) and 7.6 x 10^6 $M^{-1}s^{-1}$ (thioredoxin) (Williams, 1992). In catalysis, *E. coli* TR cycles between two- or four- electron reduced forms, $FADH_2/S_2$ and $FADH_2/(SH)_2$ (Lennon and Williams, 1996; Wang *et al.*, 1996). The E^0_7 values of $FAD/FADH_2$ and $S_2/(SH)_2$ couples are very close to each other. The E_7 values at 12 °C of the four redox couples of thioredoxin reductase are: $(S)_2$-enzyme-$FAD/FADH_2$ = -0.243 V, $(SH)_2$-enzyme-$FAD/FADH_2$ = -0.260 V, (FAD)-enzyme-$(S)_2/(SH)_2$ = -0.254 V, and ($FADH_2$)-enzyme-$(S)_2/(SH)_2$ = -0.271 V. This is why the $4e^-$ reduction of *E. coli* TR is relatively easy (O'Donnell and Williams, 1984). The complexes of reduced FAD with $NADP^+$ absorbing above 700 nm may be observed during enzyme titration with $NADP^+$/NADPH (Lennon and Williams, 1997).

An interesting feature of *E. coli* TR is that in spite of obligatory two-electron character of physiological reactions, it forms neutral (blue) FAD semiquinone during irradiation under anaerobic conditions (Zanetti *et al.*, 1968). The $FADH^\bullet$ of TR cannot be reoxidized by thioredoxin or reduced by NADPH, and may exist in the presence of oxidized catalytic disulfide.

According to the best of our knowledge, the reactions of *E. coli* TR with quinones and nitroaromatics have not been investigated, although this may represent a potentially important way of manifestation of antibacterial action of these compounds. However, these reactions were

studied using its plant analogue, *Arabidopsis thaliana* TR (Bironaitė *et al.,* 1998; Miškinienė *et al.,* 1998).

The dimeric *A. thaliana* TR contains 333 amino acid residues in each dimer, and is structurally similar to the *E. coli* enzyme (Dai *et al.,* 1996). The FAD-binding domain consists of residues 1-117 and 244-316, the NADPH-binding domain consists of residues 118-243, and the catalytic disulfide is formed from Cys135,138. When the FAD domains of both enzymes are superimposed, the NADPH-binding domain of *A. thaliana* TR must be rotated by 8^{o} to superimpose on the corresponding domain of the *E. coli* enzyme. In spite of significant structural similarity, *E. coli* Trx possesses a weak affinity for *A. thaliana* TR (K_m of 80 μM versus 1÷3 μM for plant type Trx-h) (Jacquot *et al.,* 1994). Conversely, plant thioredoxin h is a poor substrate for *E. coli* TR (Decottignies *et al.,* 1991).

The enzymatic reduction of *A. thaliana* Trx with NADPH proceeded according to "ping-pong" mechanism with k_{cat} = 6.2 s^{-1} and K_m = 1.2 μM for Trx, and K_m = 1.8 μM for NADPH (Bironaitė *et al.,* 1998). The E^{o}_{7} of this enzyme, -0.244 V, was found to be close to that of FAD of *E. coli* TR (Bironaitė *et al.,* 1998). The FAD fluorescence changes of TR after addition of pyridine nucleotides or Trx pointed to its conformational changes like in *E. coli* enzyme (Nivinskas *et al.,* 2001b).

The reduction of quinones and nitroaromatics with *A. thaliana* proceeded with 12-16% and 70-90% single-electron flux, respectively (Bironaitė *et al.,* 1998; Miškinienė *et al.,* 1998). Their log k_{cat}/K_m increased with E^{1}_{7}, and the reactivity of nitroaromatics was systematically by 1 order of magnitude lower than that of quinones (Bironaitė *et al.,* 1998; Miškinienė *et al.,* 1998). The reduction of quinones with relatively high potential, E^{1}_{7} = 0.09 V - -0.11 V, was characterized by k_{cat} of 7÷22.2 s^{-1}, *i.e.,* close or above the rate of Trx

reduction. The reaction product $NADP^+$ possessed different inhibition patterns in quinone- and thioredoxin reductase reactions, thus pointing to a possible participation of different redox states in the reactions. Like in the case of mammalian TR, the incubation of reduced enzyme with partly-substituted quinones and tetryl caused time-dependent loss of Trx reductase activity.

In view of a relatively high quinone reductase activity of *A. thaliana* TR and important role of thioredoxin reductase/thioredoxin system in plant metabolism (Buchanan *et al.,* 1994), plant thioredoxin reductase may be an important potential target of redox cycling pesticide action. This type of reactions can convert an antioxidant enzyme into a pro-oxidant one.

Another representative of L-TRs is *Thermotoga maritima* TR, a 2×34.3 kD protein (Nelson *et al.,* 1999). According to the best of our knowledge, its crystal structure is unavailable. Its amino acid sequence matched the sequences of TRs from other hyperthermophilic archea (*Thermotoga neapolitana, Thermotoga sp.* (strain RQ2), and *T. petrophila* RKU-1) by 94-98%, As other L-TrxR, *T. maritima* TR possesses two active cysteine residues (Cys147-AlaThr-Cys150), FAD bonding motif, and NAD(P)H bonding motif (Gly164-GlyGlyAspSer-Ala169) (Yang and Ma, 2010; Hirt *et al.,* 2002). Eventhough most of the TRs utilize NADPH as a reducing substrate, *T. maritima* TR K_m value for NADH is 11 times lower that NADPH. This may be determined by the absence of specific arginine/lysine residues in adenosine-binding domain, which are necessary for binding of 2‘-phosphate group of NAD(P)H (Scrutton *et al.,* 1990). The standard redox potential (E^0) of catalytic disulfide is –0.295 V at pH 7.0 (Couturier *et al.,* 2013). According to the best of our knowledge, the redox potential of FAD of *T. maritima* TR is unavailable.

The physiological oxidant of *T. maritima* TR is a 25.2 kD Grx-like protein, whose gene is coded next to TR gene. It contains two possible redox active motifs, Cys37-GlnTyr-C40 in the N-terminus and Cys147-ProTyr-Cys150 in C-terminus (Yang and Ma, 2010). *T. maritima* Grx may be reduced by GSH under artificial conditions. However, there are no data about the synthesis of glutathione or glutathione reductase homologues, and no classical Trx protein genes with single CxxC motif in *T. maritima* (Nelson *et al.,* 1999). This may indicate that *T. maritima* TR and Grx is the only one protein disulfide oxidoreductase system in this bacteria. They can function as a typical thioredoxin system, because TrxR catalyzed the Grx-dependent reduction of insulin disulfide bridges (Yang and Ma, 2010). Disulfide bridges are one of main factors maintaining the protein structure, which may be disrupted by hyperthermic environment. Therefore, the restoration of disulfide bridges and the maintenance of native protein structure with the participation of Trx/TR or analoguos repair system, is important in hyperthermophilic organisms (Ladenstein and Ren, 2006; 2008).

Among other oxidants, *T. maritima* TR does not reduce *Spirulina* Trx, GSSG, lipoic acid, lipoamide and Na_2SeO_3, and the rate of reduction of DTNB is very low (0.2 U/mg) (Yang and Ma, 2010). The later property is characteristic for H-TR, but not for bacterial L-TRs. On the other hand, some L-TRs from hyperthermophilic archea like *S. solfataricus* (Masullo *et al.,* 1996; Ruocco *et al.,* 2004) and *A. pernix* K1 (Jeon and Ishikawa, 2003) can directly reduce DTNB. This shows that *T. maritima* TR shares some properties of archeal L-TRs.

T. maritima TR reduces benzyl viologen (BV^{2+}) with low rate which significantly increases with temperature, being equal to 3.7 s^{-1} at 30 ^oC, and 50 s^{-1} at 95 ^oC. Using NADH as an electron donor, the highest enzyme activity was observed at pH 9.5, while using NADPH,

the optimal pH shifted to 6.5. The ratios between the rates of NADH and NADPH oxidation were equal to 70 at pH 9.5, and 9 at pH 7.0 (Yang and Ma, 2010). K_m ir V_{max} values for NADH were 73 μM and 65 s^{-1}, respectively (pH 7.0. 95 ^oC)**.**

2.4.4. Conclusions

The currently available data point to a variety of redox states/forms, participating in quinone reductase reactions of C-S dehydrogenases-transhydrogenases: a mixture of two- and four-electron reduced enzyme forms (lipoamide dehydrogenase), complexes of two-electron reduced enzyme with NADPH (glutathione reductase, trypanothione reductase), and four-electron reduced mammalian thioredoxin reductase. In the latter case, the reduced selenylsulfide also participates in the reduction of quinones and nitroaromatics. These reactions proceed in a mixed single- and two-electron way. In most cases, the reactivity of quinones increases with their E^1_7. The structure-activity relationships in the reduction of nitroaromatics are less clear. The relatively poorly understood problem is the mechanism of reduction of quinones and nitroaromatics by low m.w. thioredoxin reductases. An important point is the examination of a possible role of FAD semiquinone in these reactions because of their mixed single- and two-electron character.

3. MATERIALS AND METHODS

3.1. Enzymes and chemicals

E. coli NfsA was a generous gift by Dr. David Ackerley (Victoria University of Wellington, New Zealand) and was purified as described (Prosser *et al.,* 2010). The concentration of NfsA was determined according to the absorbance of FMN using ε_{460} = 12.5 $mM^{-1}cm^{-1}$.

T. maritima TR was was a generous gift by Dr. Nicolas Rouhier (University of Lorraine, Nancy, France) obtained as described (Couturier *et al.,* 2013). The concentration of TmTR was determined according to the absorbance of FAD (ε_{460}=10.9 $mM^{-1}cm^{-1}$).

T. maritima Grx1 was a generous gift by Dr. Nicolas Rouhier (University of Lorraine, Nancy, France). The concentration of Grx1 was determined according to ε_{280} = 145 mM^{-1} cm^{-1} (Couturier *et al.*, 2013).

Quinones (1,4-benzoquinone, 2-methyl-1,4-benzoquinone, 2,3-dichloro-1,4-naphthoquinone, 2,6-dimethyl-1,4-benzoquinone, 5-hydroxy-1,4-naphthoquinone, 5,8-dihydrokxy-1,4-naphthoquinone (naphthazarine), 9,10-phenantrenequinone, 1,4-naphthoquinone, 2-methyl-1,4-naphthtoquinone, tetramethyl-1,4-benzoquinone, 1,4-dihydrokxy-9,10-anthraquinone, 1,8-dihydroxy-9,10-anthraquinone, 9,10-anthraquinone-2-sulfonic acid, 2-hydroxy-3-methyl-1,4-naphthoquinone, 2-hydroxy-1,4-naphthoquinone), 1,1‘-dibenzyl-4,4‘–bipyridinium, riboflavin, nitroaromatic compounds (*p*-, *o*-, *m*-dinitrobenzenes, *p*-nitrobenzaldehyde, *p*-nitroacetophenone, *p*-nitrobenzoic acid, nitrobenzene, nitrofurantoin, nifuroxime), dicoumarol, 3-acetylpyridine adenine dinucleotide (APADH), 3-acetylpyridine adenine dinucleotide phosphate (APADPH), ADP ribose, 5,5'-dithiobis-(2-nitrobenzoic acid) (DTNB), *p*-chloromercuribenzoic acid (pCMB),

glucose-6-phosphate, glucose-6-phosphate dehydrogenase, ferricyanide, $Fe(EDTA)^-$, $NAD(P)^+$, NAD(P)H, cytochrome *c*, *E. coli* NfsB**,** formiate dehydrogenase and superoxide dismutase (SOD) were obtained from Sigma-Aldrich and Fluka. 2,4,6-Trinitrotoluene (TNT), 2,4,6-trinitrophenyl-*N*-methylnitramine (tetryl), and nitrosobenzene were synthesized as described previously (Čėnas *et al.*, 2001), and were the generous gift of Dr. Jonas Šarlauskas (Institute of Biochemistry, Vilnius). CB-1954 was synthesized as described previously (Miškinienė *et al.*, 1999), and was a generous gift of Dr. Vanda Miškinienė (Institute of Biochemistry, Vilnius). The purity of synthesized compounds was characterized by TLC, ^{1}H NMR, UV, and IR spectroscopy and elemental analysis.

3. 2. Steady-state kinetic studies

Steady-state kinetic measurements were performed spectrophotometrically in 0.1 M K-phosphate (pH 7.0), containing 1 mM EDTA, at 25 ^{o}C, using a PerkinElmer Lambda 25 spectrophotometer. The initial rates of enzymatic NADPH-dependent quinone- or nitro-reduction were determined by monitoring the oxidation of NADPH ($\Delta\varepsilon_{340}$ = 6.2 mM^{-1} cm^{-1}). Data were corrected for the intrinsic NAD(P)H:oxidase activity of the enzyme in the reaction medium, and for the nonenzymatic oxidation of NADPH by high potential 1,4-benzoquinone and 2-methyl-1,4-benzoquinone. In particular cases, the data were corrected for the spectral changes at 340 nm, occurring during the two(four)-electron reduction of nitrobenzenes. The steady-state parameters of reactions, the catalytic constants (k_{cat}) and the bimolecular rate constants (k_{cat}/K_m) of the oxidants at fixed concentration of NADPH correspond to the reciprocal intercepts and slopes of Lineweaver–Burk plots, [E]/*V vs.* 1/[Q], where *V* is the reaction rate, [E] is the enzyme concentration, and [Q] is the

concentration of quinone or nitroaromatic oxidant. Throughout this work, k_{cat} represents the number of molecules of NADPH oxidized by a single active center of the enzyme per second. The rates of enzymatic reduction of $APAD^+$ with NADH were monitored following the formation of APADH ($\Delta\varepsilon_{363}$ = 5.6 $mM^{-1}cm^{-1}$) (Weber and Kaplan, 1957). For kinetic studies, APADH was prepared *in situ* by reduction of $APAD^+$ with 100 mM formiate and 1 mg/ml formiate dehydrogenase. APADH concentration was determined according to ε_{365} = 7.8 $mM^{-1}cm^{-1}$ (Kaplan and Ciotti, 1956). The kinetics of reduction of CB-1954 were assessed according to $\Delta\varepsilon_{420}$ = 1.2 $mM^{-1}cm^{-1}$ (Race *et al.*, 2007). The kinetic parameters were obtained by the fitting of kinetic data to the parabolic expression using SigmaPlot 2000 (version 11.0, SPSS Inc.). Single-electron flux in the reduction of quinones was determined by monitoring the 1,4-benzoquinone-mediated reduction of cytochrome *c* (50 μM) in the presence of 100 μM NADPH and 50 μM 1,4-benzoquinone according to $\Delta\varepsilon_{550}$ = 20 $mM^{-1}cm^{-1}$. The same conditions were used for the monitoring the enzyme-mediated reduction of cytochrome *c* by 50 μM tetryl or TNT in the presence of 100 μM NADPH and in the absence or the presence of 100 U/ml SOD. Tetryl reduction was monitored using an NADPH regeneration system (10 mM glucose-6-phosphate and 1 mg/ml glucose-6-phosphate dehydrogenase), recording the absorbance at 200-550 nm. In some experiments, NADH regenerative system (20 μM NADPH, 100 mM HCOONa, and 1mg formate dehydrogenase). Also, for pH-dependency studies, 0.1 M K-phosphate buffer solutions with pH ranging from 5.5 to 8.0 were used, as well as 0.1 M Tris-acetate buffer solutions with pH 5.5 and 8.0. APAD(P)H kinetics were monitored and redox potentials were calculated according to the Haldane relationship.

The data were fitted to Eq. (19) corresponding to the “ping-pong“ kinetic mechanism, where [NADPH] stands for [S]:

$$\frac{V}{[E]} = \frac{k_{cat}[S][Q]}{K_{m(S)}[Q] + K_{m(Q)}[S] + [S][Q]} \quad (19)$$

In the inhibition studies, the data were fitted to Eqs. (20)-(22), which describe competitive, uncompetitive and mixed-type inhibition by the reaction product $NADP^+$ or another inhibitor [I], respectively. The inhibition constants K_{is} and K_{ii} describe the effects of inhibitors on the slopes of Lineweaver-Burk plots and their intercepts with y-axis, respectively:

$$\frac{V}{[E]} = \frac{k_{cat}[S]}{K_{m(S)}\left(1 + \frac{[I]}{K_{is}}\right) + [S]}, \quad (20)$$

$$\frac{V}{[E]} = \frac{k_{cat}[S]}{K_{m(S)} + [S]\left(1 + \frac{[I]}{K_{ii}}\right)}, \quad (21)$$

$$\frac{V}{[E]} = \frac{k_{cat}[S]}{K_{m(S)}\left(1 + \frac{[I]}{K_{is}}\right) + [S]\left(1 + \frac{[I]}{K_{ii}}\right)} \quad (22)$$

3.3. Fluorescence measurements

The fluorescence spectra of FMN, NfsA, and NfsB (5 µM) were recorded using a Hitachi MPF-7 fluorimeter at an excitation wavelength of 460 nm at pH 7.0 and 25 ^oC.

3.4. Presteady-state kinetic studies

The presteady-state kinetic measurements of reduction of NfsA by excess NADPH were carried out by using a stopped-flow SX.17 MV spectrophotometer (Applied Photophysics) at pH 7.0 and 25 ^oC. The

concentration of the enzyme after mixing was 5.0 µM. The kinetics of absorbance decrease at 460 nm were analyzed according to the single exponent fit using SigmaPlot software.

Kinetics of 5 µM *T. maritima* TR reduction with 50 µM NADH and its reoxidation was carried out by using a stopped-flow SX.17 MV spectrophotometer (Applied Photophysics). Spectra of intermediate compounds formed during 5 µM *T. maritima* TR reoxidation by duroquinone were recorded after 0.2 s, 2 s, 3 s, 4 s and 6 s.

Because nitrosobenzene possesses significant absorbance at 340 nm, the initial rates (0–5 s) of oxidation of NADPH by nitrosobenzene were determined according to $\Delta\varepsilon_{370}$ = 2.5 $mM^{-1}cm^{-1}$ using a stopped-flow SX.17 MV spectrophotometer (Applied Photophysics, Leatherhead, UK). When necessary, NfsA was added to a syringe containing nitrosobenzene, and ascorbate was added to a syringe containing NADPH. NO_2^- formation was determined using Griess reagent. When sulfanilamide is added (or sulphanilic acid), the nitrite ion reacts to form a diazonium salt. Then azo dye agent (*N*-alpha-naphthyl-ethylenediamine) is formed and a pink color develops (Beda and Nedospasov, 2005). Oxygen consumption during the reactions of TNT, tetryl and naphthoquinones with ascorbate was monitored using a Digital Model 10 Clark electrode (Rank Brothers Ltd., Bottisham, UK). The initial O_2 concentration at 25 ^oC was assumed to be 250 µM.

3.5. Photoreduction studies

NfsA photoreduction was carried out with 5 µM of 5-deazaflavin in the presence of NADPH regenerative system (20 µM NADPH, 10 mM glucose-6-phosphate, and 0.5 mg/mL glucose-6-phosphate dehydrogenase). Spectra were recorded for 80 minutes and measured in 4 minute intervals and a 50 W lamp.

3.6. Determination of reaction activation enthropy and enthalpy

Enthalpies and enthropies of various quinones and nitroaromatic compounds were determined by measuring bimolecular rate constants at various temperatures (10 ^{o}C - 40 ^{o}C) and then calculating them using Eyring equation (23):

$$\ln \frac{k}{T} = \frac{-\Delta^{\ddagger} H^{\ominus}}{R} \cdot \frac{1}{T} + \ln \frac{\kappa k_{\mathrm{B}}}{h} + \frac{\Delta^{\ddagger} S^{\ominus}}{R} \qquad (23)$$

4. RESULTS AND DISCUSSION

4.1. Reduction of quinones and nitroaromatic compounds by *E. coli* NfsA

4.1.1. The two-electron character of reduction of quinones and nitroaromatic compounds by NfsA

The proportion of single-electron flux during the reduction of quinones by NAD(P)H-oxidizing flavoenzymes may be determined via the 1,4-benzoquinone-mediated reduction of added cytochrome *c*, and is equal to the ratio between the cytochrome c reduction rate and a doubled rate of NAD(P)H oxidation (Iyanagi *et al.*, 1990). This is based on a negligibly low rate of cytochrome c reduction by 1,4-hydroquinone at pH<7.2, whereas 1,4-benzosemiquinone, formed during single-electron reduction, reduces cytochrome c at high rate ($k \sim 10^6$ $M^{-1}s^{-1}$). During NfsA-catalyzed reduction of 1,4-benzoquinone by NADPH the single-electron flux post-correction for enzymatic reduction of cytochrome c was measured as 3 %, consistent with a very low level of single-electron transfer. In accordance with this, at pH 7.0 and excess NADPH, 1,4-benzoquinone oxidized stoichiometrical amount of NADPH (ΔA_{340} = -0.3÷-0.4) in a NfsA-catalyzed reaction. The reaction rate of a second phase is close to NADPH-oxidase activity of enzyme (Fig. 13A).

At pH 7.0, 50 μM 1,4-naphthoquinone also oxidized a stoichiometric amount of NADPH in a first phase, but also an excess NADPH in a second phase (Fig. 13A). On the other hand, 50 μM 5,8-dihydroxy-1,4-naphthoquinone oxidized 300 μM NADPH in a single phase (Fig. 13B). This is explained by the following: a) two-electron reduction product of 1,4-benzoquinone, hydroquinone (E^o_7 = 0.28 V) is very slowly reoxidized by O_2 at pH 7.0, therefore, 1,4-benzoquinone is unable to oxidize more

that the stechiometric amount of NADPH; b) two-electron reduced 1,4-naphthoquinone (E^{o}_{7} = 0.04 V) is reoxidized at a moderate rate, thus, it may oxidize excess NADPH in a second phase; c) two-electron reduced 5,8-hydroxy-1,4-naphthoquinone (E^{o}_{7} = -0.06 V) is reoxidized very rapidly (O'Brien, 1991), and excess NADPH is oxidized in a single phase. At pH 5.5, the reoxidation rate of 1,4-naphthohydroquinone becomes much slower, and it is able to oxidize just a stoichiometric amound of NADPH (Fig. 13B), whereas the rate of reoxidation of reduced 5,8-dihydroxy-1,4-naphthoquinone remains high enough to ensure the oxidation of excess NADPH in a single phase (O'Brien, 1991) (Fig. 13B).

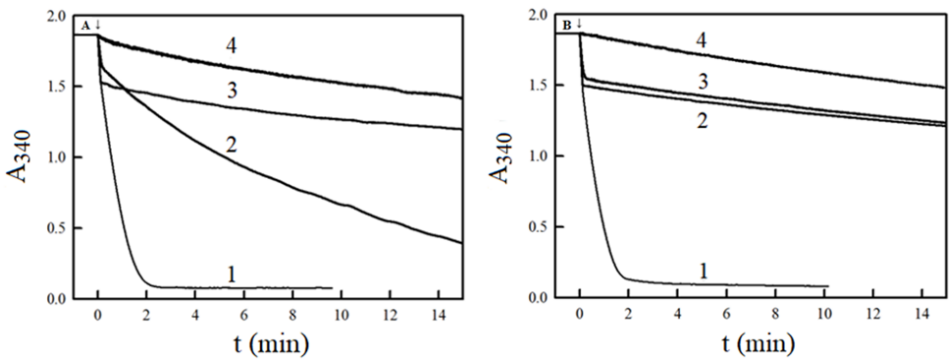

Figure 13. A) Kinetics of NfsA-catalyzed oxidation of 300 µM NADPH at pH 7.0 using 50 µM naphtazarine (1), 50 µM naphthoquinone (2), and (3) 50 µM benzoquinone (3) as oxidants, (4) NADPH-oxidase reaction of NfsA, enzyme concentration, 100 nM. B) The same experiment repeated at pH 5.5.

The determination of single-electron flux during the enzymatic reduction of aromatic nitrocompounds is complicated, because both nitroanion-radicals and aromatic hydroxylamines reduce cytochrome *c*, although the latter reaction is relatively slow. When tetryl or TNT were used as NfsA oxidants, the reduction rate of added cytochrome *c* was equal to 16% of NADPH oxidation rate after the correction for a direct

enzymatic reduction of cytochrome *c*. The reaction rate decreased by 30-40% post addition of SOD (100 U/ml), which inhibits the reduction of cytochrome c by superoxide, that is formed during the redox cycling of nitroaromatic anion-radicals. These data show that NfsA reduces tetryl and TNT predominantly via two-electron transfer. Additionally, during the tetryl reduction by NfsA in the presence of an NADPH regeneration system, the products absorbing at 380-385 nm are formed (Fig. 14A). Their spectra are close to those previously observed during the two-electron reduction of tetryl by *E. cloacae* NR and *T. maritima* peroxiredoxin-nitroreductase hybrid enzyme (Nivinskas *et al.,* 2001a; Anusevičius *et al.,* 2012) (Fig. 14A). The structure of these products is not characterized so far. This contrasts with the single-electron reduction of tetryl with NQO1 (Scheme 1), where the reduction product *N*-methylpicramide possesses λ_{max} = 340 nm and absorbance shoulder at 400-450 nm (Anusevičius *et al.,* 1998). Further, the reduction of tetryl with NfsA was not accompanied by enhanced O_2 consumption, and the amount of formed nitrite is far below the amount of used tetryl (Fig. 14B).

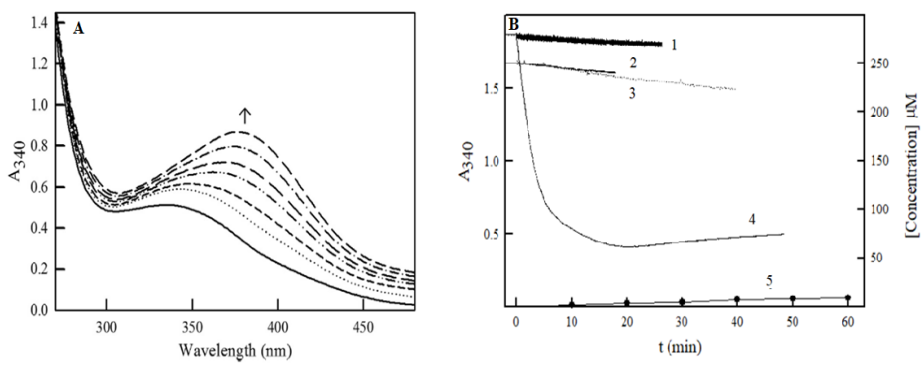

Figure 14. A) Spectra of reduction products of 100 µM tetryl in the presence of 20 µM NADPH, 5 nM NfsA, and the NADPH regeneration system. Spectra were recorded in 12 min interval, with the arrow indicating the direction of progression of the spectra over time, pH 7.0. B) Oxidation of NADPH (1,4), consumption of oxygen (2,3) and

formation of nitrite (5) during the NfsA-catalyzed oxidation of 300 μM NADPH by 50 μM tetryl (2,4,5) and in control experiments (2,3), enzyme concentration, 20 nM, pH 7.0.

Collectively, our data are consistent with NfsA catalyzing predominantly the two-electron reduction of various groups of quinones and nitroaromatic compounds, including their *N*-nitramine derivatives.

4.1.2. Steady-state kinetics and substrate specificity of NfsA

Steady-state reaction kinetics for NfsA were examined using 16 quinones with single-electron reduction potentials ranging from -0.46 V to +0.09 V, and 12 nitroaromatic oxidants, whose potentials ranged from -0.49 V to -0.16 V (Table 2). At fixed NADPH concentrations, a series of parallel plots was observed in Lineweaver-Burk graphs, when the most reactive nitroaromatic compounds - tetryl (Fig. 15) or TNT (Fig. 16) were used as the oxidants. This indicates that these reactions follow "ping-pong" scheme. The bimolecular reaction rate constants (k_{cat}/K_m) for the reduction of tetryl and TNT were 7.9 ± 0.7 x 10^6 M^{-1} s^{-1}, and 2.7 ± 0.4 x 10^6 M^{-1} s^{-1}, respectively (Table 2). The k_{cat}/K_m for NADPH oxidation obtained according to "ping-pong" scheme was equal to 3.4 ± 0.5 x 10^6 M^{-1} s^{-1}. The calculated maximal values of k_{cat} at infinite concentrations of NADPH and electron acceptor were equal to 110 ± 13 s^{-1} for tetryl, and 135 ± 12 s^{-1} for TNT.

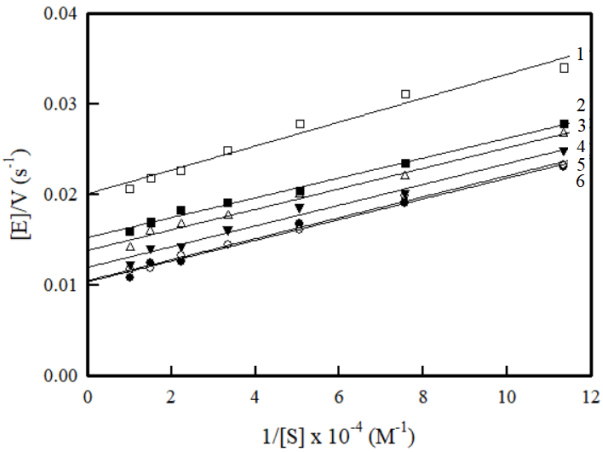

Fig. 15. The steady-state kinetics of *E. coli* NfsA catalyzed oxidation of NADPH using tetryl as an oxidant. The concentrations of NADPH: 20 μM (1), 30 μM (2), 50 μM (3), 100 μM (4), 150 μM (5), and 200 μM (6).

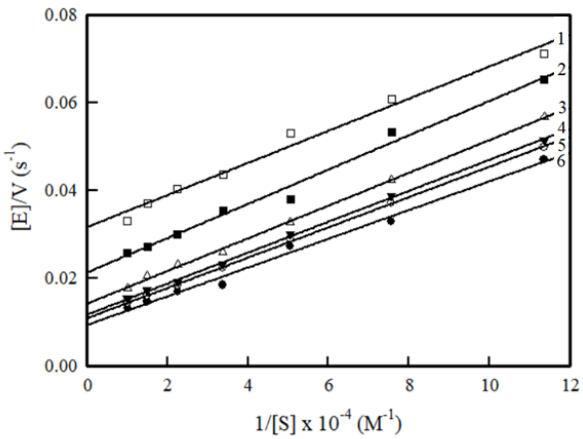

Fig. 16. The steady-state kinetics of *E. coli* NfsA catalyzed oxidation of NADPH using TNT as an oxidant. The concentrations of NADPH: 20 μM (1), 30 μM (2), 50 μM (3), 100 μM (4), 150 μM (5), and 200 μM (6).

Our results indicate that the reactivity of nitroaromatic compounds increased with an increase in their single-electron reduction potential (E^1_7) (Table 2; Fig. 17). Their log k_{cat}/K_m were characterized by a linear but scattered positive dependence on their E^1_7 values (r^2 = 0.8313). The introduction of their VdWvol as the second variable in a two-parameter regression did not improve the correlation (r^2 = 0.8386). The reactivity of

nitroaromatics was 10-fold higher than that of quinones with similar E^1_7 values. The reactivity of 7-trifluoromethyl-3-amino-1,2,4-benzotriazine-1,4-dioxide (7-CF_3-TPZ), which is a derivative of an experimental anticancer drug tirapazamine, was close to that of quinones with similar potentials.

Table 2. Hydride transfer potentials (E_7 (Q/QH$^-$)) of quinones, single-electron reduction potentials of quinones ($E^1{}_7$) and pK$_a$ of their semiquinones (pK$_a$ (QH$^\cdot$)) (Čėnas *et al.*, 2004), and $E^1{}_7$ of nitroaromatic compounds (Wardman, 1989), Van der Waals volumes of quinones and nitroaromatic compounds (VdWvol), catalytic constants (k_{cat}), bimolecular rate constants (k_{cat}/K_m) in NfsA-catalyzed reactions at pH 7.0 and 25 ^{o}C in the presence of 100 μM NADPH.

No.	Compound	E_7 (Q/QH$^-$) (V)	$E^1{}_7$ (V)	pK$_a$ (QH$^\cdot$)	VdWvol (Å^3)	k_{cat} (s^{-1})	k_{cat}/K_m (M^{-1}s^{-1})
	Quinones						
1	1,4-Benzoquinone	0.20	0.09	4.10	124	62±6	5.8±0.6 × 10^6
2	2-Methyl-1,4-benzoquinone	0.12	0.01	4.45	142	54±6	6.8±0.7 × 10^6
3	2,3-Dichloro-1,4-naphthoquinone	-	-0.04	-	187	61±5	2.8±0.3 × 10^6
4	2,6-Dimethyl-1,4-benzoquinone	0.06	-0.08	4.75	160	51±6	3.2±0.4 × 10^6
5	5-Hydroxy-1,4-naphthoquinone	-0.06	-0.09	3.65	180	22±3	1.4±0.2 × 10^7
6	5,8-Dihydroxy-1,4-naphthoquinone	-0.08	-0.11	2.80	192	12±2	1.3±0.1 × 10^7
7	9,10-Phenantrenequinone	-0.03	-0.12	-	218	54±6	4.7±0.5 × 10^6
8	1,4-Naphthoquinone	-0.03	-0.15	4.10	168	46±5	1.4±0.2 × 10^6
9	2-Methyl-1,4-naphthoquinone	-0.11	-0.20	4.50	187	36±4	2.8±0.3 × 10^5
10	Tetramethyl-1,4-benzoquinone	-0.09	-0.26	5.10	197	2.5±3	2.3±0.2 × 10^3
11	1,4-Dihydroxy-9,10-anthraquinone	-	-0.30	-	245	0.7±0.1	1.0±0.15 × 10^5

12	Riboflavin	-0.21	-0.32	8.50	423	4.2±0.6	$2.6\pm0.2 \times 10^5$
13	1,8-Dihydroxy-9,10-anthraquinone	-	-0.33	3.95	245	1.6±0.2	$1.1\pm0.1 \times 10^5$
14	9,10-Anthraquinone-2-sulfonic acid	-0.25	-0.38	3.25	266	1.4±0.15	$1.9\pm0.2 \times 10^4$
15	2-Hydroxy-1,4-naphthoquinone	-0.20	-0.41	4.70	180	72±8	$1.1\pm0.1 \times 10^7$
16	2-Hydroxy-3-methyl-1,4-naphthoquinone	-0.24	-0.46	-	200	56±5	$8.8\pm1.5 \times 10^6$
	Nitroaromatic compounds						
1	Tetryl	-	-0.16	-	218	85±9	$7.9\pm0.9 \times 10^6$
2	2,4,6-Trinitrotoluene	-	-0.25	-	182	89±10	$2.7\pm0.3 \times 10^6$
3	Nifuroxime	-	-0.26	-	133	180±20	$5.9\pm0.6 \times 10^6$
4	Nitrofurantoin	-	-0.26	-	202	136±18	$7.2\pm1.0 \times 10^6$
5	*p*-Dinitrobenzene	-	-0.26	-	143	27±3	$7.4\pm0.7 \times 10^5$
6	*o*-Dinitrobenzene	-	-0.29	-	142	60±6	$3.4\pm0.3 \times 10^6$
7	*p*-Nitrobenzaldehyde	-	-0.32	-	142	30±3	$1.8\pm0.2 \times 10^5$
8	*m*-Dinitrobenzene	-	-0.35	-	143	55±6	$1.2\pm0.1 \times 10^6$
9	*p*-Nitroacetophenone	-	-0.36	-	160	59±5	$1.5\pm0.2 \times 10^5$
10	CB-1954	-	-0.39	-	217	15±2	$6.5\pm1.4 \times 10^4$

11	*p*-Nitrobenzoic acid	-	-0.43	-	149	64±7	$2.5\pm0.2 \times 10^4$
12	Nitrobenzene	-	-0.49	-	123	14±2	$9.6\pm0.8 \times 10^3$
	Other compounds						
1	Ferricyanide	-	0.41	-	-	89±6	$8.6\pm1.4 \times 10^6$
2	Fe(EDTA)	-	0.12	-	-	43±5	$6.5\pm1.1 \times 10^4$
3	7-Trifluoromethyl-3-amino-1,2,4-benzotriazine-1,4-dioxide (7-CF_3-TPZ)	-	-0.345	-	-	6.6±0.7	$2.9\pm0.5 \times 10^3$

[a]monitored at 420 nm.

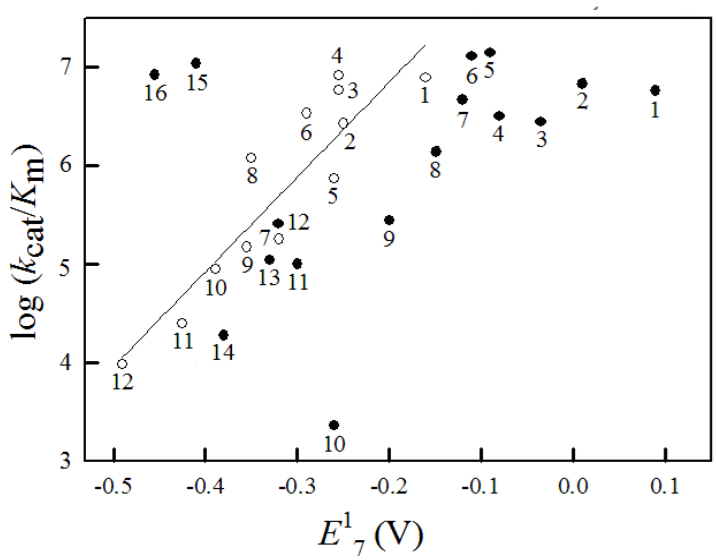

Fig. 17. Reactivity of quinones and nitroaromatic compounds in *E.coli* NfsA-catalyzed reactions. Relationship between log k_{cat}/K_m of quinones (solid circles) and nitroaromatic compounds (blank circles) in NfsA catalyzed reaction and their single-electron reduction potentials at pH 7.0 (E^1_7) is shown. Numbers refer to quinones and nitroaromatic compounds whose redox potentials and reduction rate constants are given in Table 2.

The correlations between log k_{cat}/K_m and E^1_7 or $E^7(Q/OH^-)$ (potential of single-step hydride transfer, Eq. (11)) of quinones are absent (r^2 is equal to 0.1675 and 0.2261, respectively). The exclusion of the data of 2-hydroxy-1,4- naphthoquinone and 2-methyl-3-hydroxy-1,4-naphthoquinone, which possess significantly increased reactivity (Fig. 17) improves the statistics (r^2 = 0.6236 for E^1_7 and r^2 = 0.3302 for $E_7(Q/OH^-)$. However, the further introduction of VdWvol, or, in the case of E^1_7, VdWvol and pK_a($QH^{\cdot}$) as additional variables did not significantly improve the correlation data. Our previous studies (Anusevičius *et al.*, 2002*;* Misevičienė *et al.*, 2006) have shown that nitroaromatics, being much less efficient oxidants of NQO1 in comparison with quinones, possess less negative activation enthropies

than quinones. This points to their weaker electronic coupling with reduced FAD during the reaction. However, the studies of temperature dependence of k_{cat}/K_m of reduction of oxidants with NfsA did not reveal significant and unequivocal differences between $\Delta S^{\neq}$ for reduction of nitroaromatics and quinones, or between 2-hydroxy-3-methyl-1,4-naphthoquinone and 2-methyl-1,4-naphthoquinone (Table 3). Thus, the causes of these anomalies are still not understood, however, they are also observed in *E. cloacae* group B nitroreductase (Nivinskas *et al.*, 2001a, 2002). Therefore, it can be concluded that NfsA shows similar substrate specificity as the other group B members of its family.

Table 3. Calculated activation enthropies and enthalpies of reduction various quinones and $ArNO_2$ during the reduction by NfsA (pH 7.0, 25 ^oC).

Compound	$\Delta H^{\neq}$ (kJ/ mol)	$\Delta S^{\neq}$ (J/mol× ^oK)
TNT	29.9±5.0	-15.1±16.7
Menadione	22.8±3.1	-56.0±10.4
p-Nitrobenzaldehyde	26.5±3.1	-57.4±12.0
2-Hydroxy-3-methyl-1,4-naphthoquinone	35.5±4.5	14.4±15.0
o-Dinitrobenzene	32.8±4.7	-30.0±11.0

We also found that the reactivity of NfsA with riboflavin, 2-methyl-1,4-naphthoquinone, and 2,6-dimethyl-1,4-benzoquinone increased upon an increase in pH (Fig. 18). For all three compounds investigated, the coefficient $\Delta\log k_{cat}/K_m$ /ΔpH was similar, however, it was significantly lower than unity (Fig. 18), *i.e.*, 0.11±0.03 (riboflavin), 0.14±0.03 (2-methyl-1,4- naphthoquinone), and 0.18±0.04 (2,6-dimethyl-1,4-benzoquinone). The same reactivity trend has been observed for

riboflavin and 2,6-dimethyl-1,4-benzoquinone in Tris-acetate, pH 5.5 and 8.0 (data not shown).

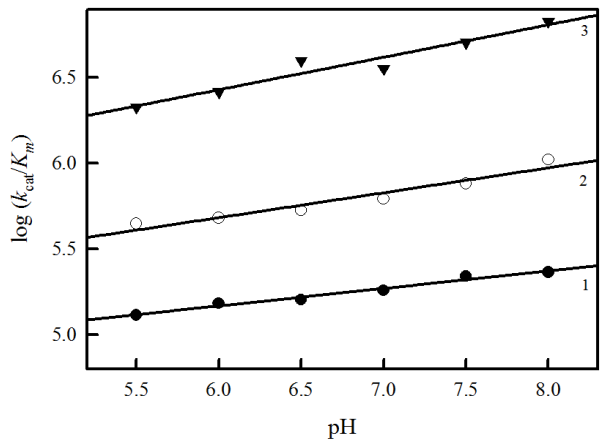

Figure 18. pH dependence of the reactivity of NfsA with riboflavin (1), 2-methyl-1,4-naphthoquinone (2), and 2,6-dimethylbenzoquinone (3).

Further studies of pH dependence of k_{cat}/K_m of oxidants involved single-electron acceptor ferricyanide, nitroaromatic compound TNT, and quinone with enhanced reactivity, 2-hydroxy-1,4-naphthoquinone. The data of Fig. 19 show that the pH profile of reactivity of ferricyanide was similar to those of 2-methyl-1,4-naphthoquinone and 2,6-dimethylbenzoquinone (Fig. 18). The reactivity of TNT possessed flat optimum between pH 6.5 and 7.5, and the reactivity of 2-hydroxy-1,4-naphthoquinone sharply decreased at pH<5.75. This may point to a possibility of their binding at separate active site domains of NfsA.

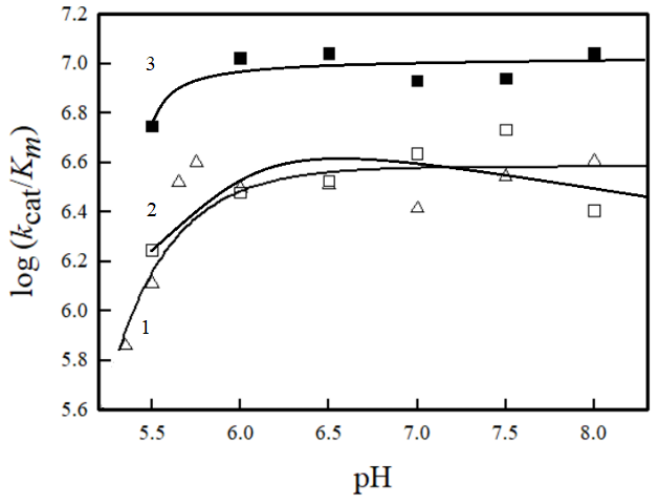

Fig. 19. pH dependence of the reactivity of NfsA with TNT (1), 2-hydroxy-1,4-naphthoquinone (2), or ferricyanide (3).

In order to provide additional insight on the interaction of the oxidants and inhibitors (see 4.1.3) with the active site of NfsA, we examined their effects on the fluorescence of FMN in the active center (Fig. 20A, B).

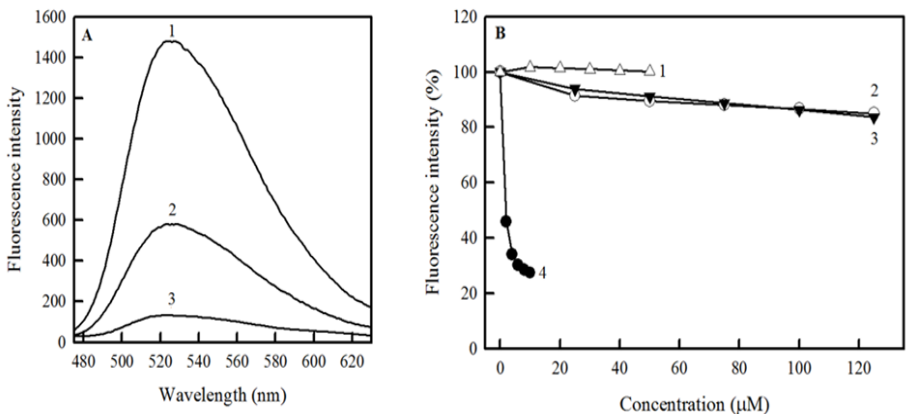

Figure 20. A) Fluorescence spectra of 5 μM FMN (1), 5 μM NfsA (2) and 5 μM NfsB (3). B) The effects of dicoumarol (1,4), TNT (2), and tetryl (3) on the fluorescence intensity of FMN of 5 μM NfsA (1), and NfsB (2-4). Excitation - 460 nm, emission - 525 nm.

The intensity of the fluorescence of FMN of NfsA was 40% as compared with free FMN (Fig. 20A), this value being higher than the fluorescence intensity of FMN in NfsB, 12% (Fig. 20A), and in *E. cloacae* NR, 17% (Nivinskas *et al.,* 2002). Dicoumarol at concentrations exceeding its K_i, 10-50 μM (see 4.1.3), did not quench the fluorescence of NfsA (Fig. 20B), nor did reaction product $NADP^+$ (100-500 μM), tetryl or TNT (50-250 μM), 1,4-benzoquinone (100-400 μM), or 2,3-dichloro-1,4-naphthoquinone (10-40 μM) (data not shown). In contrast, micromolar concentrations of dicoumarol quenched the fluorescence of FMN of *E. coli* NfsB by ~70%, which is in line with the its much lower K_i. (see 4.1.3) Tetryl and TNT (10-125 μM) also quenched the fluorescence of NfsB by a small extent up to 20% (Fig. 20B). $NADP^+$ (50-250 μM) quenched the fluorescence of FMN to an even smaller extent, 12% (data not shown).

4.1.3. The studies of inhibition of NfsA

We found that the reaction product, $NADP^+$, acted as a competitive inhibitor with respect to NADPH at fixed concentration of tetryl (K_i = 160 ± 30 μM according to the slopes in the Lineweaver-Burk plot) (Fig. 21A).

It also acted as a mixed close to uncompetitive inhibitor towards tetryl at fixed NADPH concentration (Fig. 21B), being characterized by K_{is} = 1500 ± 200 μM, and by K_{ii} = 450 ± 70 μM according to the intercepts in the Lineweaver-Burk plot. It shows that $NADP^+$ mainly competes with NADPH for the binding to the oxidized enzyme form (Fig. 25A). However, $NADP^+$ also binds to the reduced enzyme although with much lower affinity, competing with the nitroaromatic oxidant and thus decreasing its k_{cat}/K_m. Redox inactive adenosine 2',5'-diphosphate also

acts as a competitive inhibitor to NADPH (K_i = 660 ± 100 μM, data not shown).

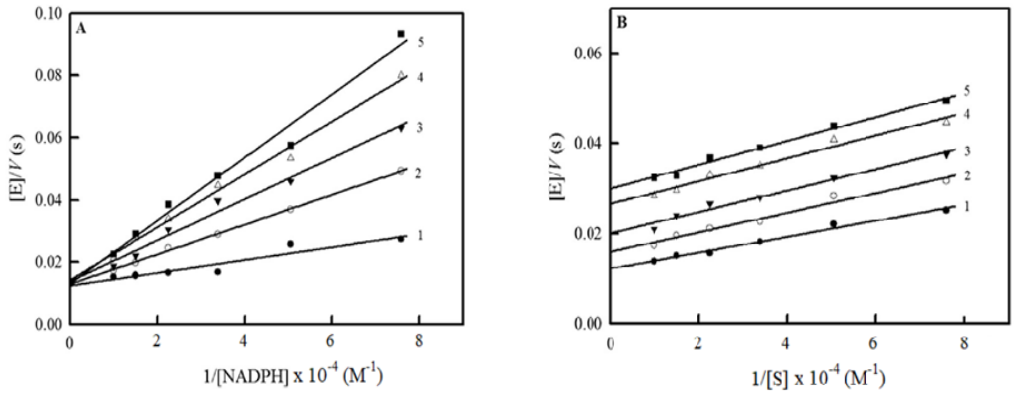

Fig. 21. A) The inhibition of NfsA-catalyzed tetryl reduction by $NADP^+$ - varied NADPH concentrations in the presence of 100 μM tetryl and varying $NADP^+$ concentrations as numbered according to the following scheme: 0 mM (1), 0.125 mM (2), 0.25 mM (3), 0.5 mM (4), and 0.75 mM (5). B) The inhibition of NfsA-catalyzed tetryl reduction by $NADP^+$ - varied tetryl concentrations in the presence of 100 μM NADPH and varying $NADP^+$ concentrations as numbered according to the following scheme: 0 mM (1), 0.125 mM (2), 0.25 mM (3), 0.5 mM (4), and 0.75 mM (5).

Dicoumarol, a classical inhibitor of mammalian NQO1 and group B nitroreductases, inhibits NfsA by acting as a competitive (K_{is} = 18.0±1.6 μM) inhibitor towards NADPH (Fig. 26A), and an uncompetitive inhibitor towards the oxidant tetryl (Fig. 26B). Our data indicate that the affinity of dicoumarol for the oxidized form of NfsA is much higher than for the reduced enzyme form. In a parallel experiment, we found that dicoumarol inhibits *E. coli* NfsB far more strongly than NfsA, by acting as a competitive inhibitor towards NADPH (K_i = 1.8±0.2 μM, data not shown). The latter value is in agreement with the previous data (Anlezark *et al*., 1992).

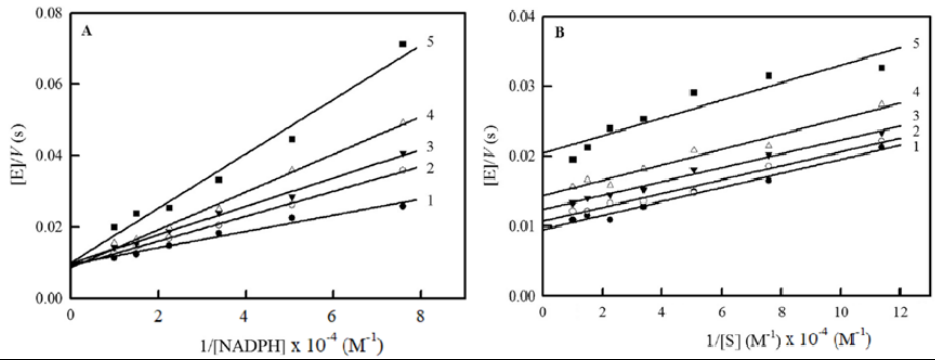

Fig. 22. A) The inhibition of NfsA-catalyzed tetryl reduction by dicoumarol - varied NADPH concentrations in the presence of 100 μM tetryl and varying dicoumarol concentrations as numbered according to the following scheme: 0 μM (1), 5 μM (2), 10 μM (3), 20 μM (4), and 30 μM (5). B) The inhibition of NfsA-catalyzed tetryl reduction by dicoumarol - varied tetryl concentrations in the presence of 100 μM NADPH and varying dicoumarol concentrations as numbered according to the following scheme: 0 μM (1), 5 μM (2), 10 μM (3), 20 μM (4), and 30 μM (5).

Another classical inhibitor of NAD(P)H-dependent enzymes, Cibacron blue, inhibits NfsA very efficiently, acting as a competitive inhibitor to NADPH (K_i = 0.09 ± 0.01 μM, data not shown).

4.1.4. The mechanism of two/four-electron reduction of nitroaromatics with NfsA

In spite of extensive studies of two(four)-electron reduction of nitroaromatics by NRs (Eq. (15,16), the pathways of formation of Ar-NHOH from Ar-NO intermediates are not well understood. Nitroso compounds possess higher redox potentials than the parent nitrocompounds (Kovacic *et al.*, 1990). Consistent with this, nitrosobenzene was suggested to be by 10^3-10^4 times faster than nitrobenzene in oxidation of *Enterobacter cloacae* NR or *Escherichia*

coli NfsB (Koder and Miller, 1998; Race *et al.*, 2005). For this reason, it was suggested that Ar-NO intermediates are reduced in a second faster enzyme catalytic cycle (Scheme 2, pathway (a)). However, accurate determination of the kinetic parameters of this cycle was complicated by a rapid parallel direct oxidation of NADH by nitrosobenzene (Race *et al.*, 2005). Thus, it is possible that this reaction (Scheme 2, pathway (b)) plays a significant role in the formation of Ar-NHOH during the catalysis of NRs. Further evidence for this supposition is provided by reports of the direct oxidation of NAD(P)H by 1-nitroso-2-naphthol (Leskovac *et al.*, 1989), and 5-(aziridin-1-yl)-2-nitro-4-nitrosobenzamide (Knox *et al.*, 1992).

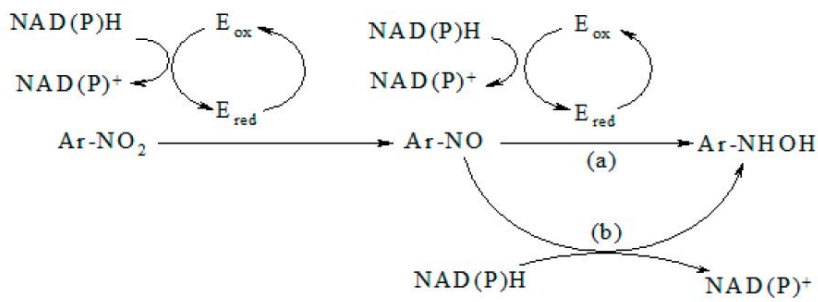

Scheme 2. Pathways of enzymatic (a) and nonenzymatic (b) formation of Ar-NHOH from Ar-NO.

Our data provide evidence that some steps of two(four)-electron reduction of nitroaromatics by nitroreductases are largely enzyme-independent, namely the pathway of formation of Ar-NHOH from Ar-NO. First, we have examined the oxidation of NADPH by nitrosobenzene. As expected for a bimolecular process, the initial reaction rates at fixed NADPH were proportional to concentration of nitrosobenzene (Fig. 23A). The obtained rate constant, 124.3±4.5 $M^{-1}s^{-1}$, was close to the previously established values (Race *et al.*, 2005;

Leskovac *et al.*, 1989). The presence of NfsA accelerated the reaction (Fig. 23A), however, the effect was modest at ≤40 nM enzyme concentrations. Thus, one may conclude that at NfsA concentrations typically used in steady-state assays, the rate of nonenzymatic NADPH oxidation by nitrosobenzene may even exceed the rate of enzymatic oxidation. The rate constants of NfsA-catalyzed reduction of nitrosobenzene were obtained from the differences in reaction rates in the presence and absence of enzyme (Fig. 23A). We obtained values of $k_{cat(app.)}$ = 55.0 ± 9.5 s^{-1} at 100 μM NADPH, and k_{cat}/K_m = 5.7 ±1.1 x 10^5 $M^{-1}s^{-1}$. The latter value is below the suggested range of k_{cat}/K_m for the reaction of nitrosobenzene with *E. coli* NfsB, 2.2 ÷ 15.2 x 10^6 $M^{-1}s^{-1}$ (Race *et al.*, 2005). It is likely that this reflects in part the different reactivity of NfsA and NfsB. However, it is also likely that use of the stopped-flow method (which eliminates delays in monitoring the reaction due to mixing time) has enabled a more accurate determination of the rate constants. The introduction of ascorbate into the reaction mixture rapidly suppressed the oxidation of NADPH (Fig. 23B). Ascorbate would be expected to outcompete NADPH because it reduces nitrosobenzene much faster, with k = 2.8 x 10^3 M^{-1} s^{-1} (Ursic *et al.*, 1998).

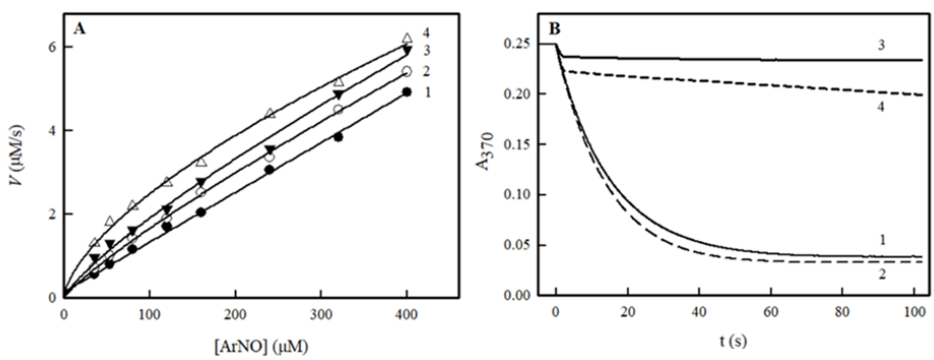

Fig. 23. A) Rates of oxidation of 100 μM NADPH by nitrosobenzene in the absence (1) and presence of NfsA (2–4). Enzyme concentration - 10 nM (2), 20 nM (3), and 40 nM (3). B) Kinetics of oxidation of 100 μM

NADPH by 400 μM nitrosobenzene in the absence (1,3) and presence (2,4) of 40 nM NfsA. Ascorbate (final concentration - 2 mM) was added into a syringe containing NADPH (3,4).

Because NfsA reduces nitrobenzene at a relatively slow rate, we conducted further studies of its reactions with faster oxidants possessing higher E^1_7 values (Table 2).

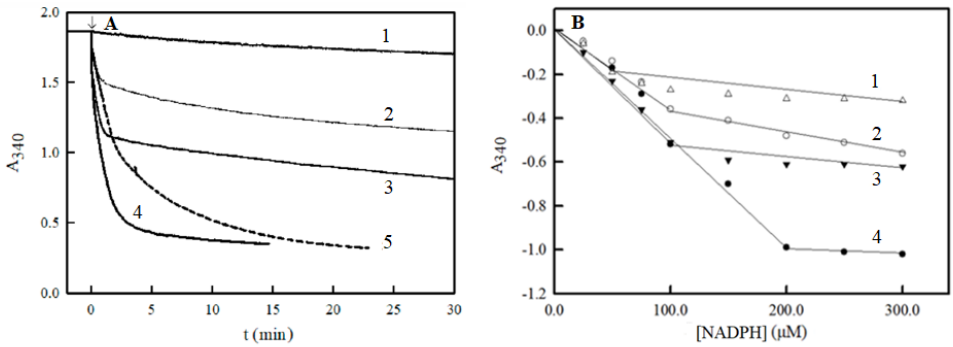

Fig. 24. A) Kinetics of oxidation of 300 μM NADPH by 50 nM NfsA in the absence of electron acceptor (1), or in the presence of 50 μM TNT (2,3), or 50 μM tetryl (4,5). The reaction mixture additionally contained 2.0 mM ascorbate in two of the reactions (2,5). B) The changes in absorbance at 340 nm during the first phase of oxidation. Oxidant: 50 μM TNT (1,2), 50 μM tetryl (3,4), 2.0 mM ascorbate was present (1,3).

It was found that under standard reaction conditions 2 moles of NADPH were oxidized per mole of TNT in a first reaction phase (Fig. 24A), with the rate of a second phase being close to the intrinsic NADPH:oxidase activity of NfsA. This is consistent with formation of 2(4)-monohydroxyl-amino dinitrotoluene as the product of reduction of TNT by NfsA (Yang *et al.*, 2013). The product(s) of tetryl reduction by NfsA were not identified, however, 4 moles of NADPH were oxidized per mole of tetryl, which points to a possible formation of dihydroxylamine. A similar multiphasic oxidation of excess NADH by TNT and tetryl has been observed in reactions catalyzed by *E. cloacae*

NR (Nivinskas *et al.*, 2001a). In the absence of enzyme and the presence of an NADPH regeneration system, 50 μM TNT did not form 340 nm absorbing products, and 50 μM tetryl reduction products increased the 340 nm absorbance only marginally, by ~0.05 in 10 min. The 2:1 and 4:1 ratio of NADPH oxidized per mole of oxidant was further confirmed by the dependence of the amplitude of the first oxidation phase on NADPH concentration (Fig. 24B). Importantly, the presence of ascorbate changed the NADPH/$ArNO_2$ stoichiometry to 1:1 (TNT) and 2:1 (tetryl), and decreased the reaction rate (Fig. 24B). In empirical pilot tests, maximal inhibition was observed at 0.5-0.7 mM ascorbate, therefore, in all subsequent experiments 2.0 mM ascorbate was used. The effect of ascorbate on the NADPH/$ArNO_2$ stoichiometry is consistent with the rapid reduction of Ar-NO intermediates by ascorbate (Uršič *et al.*, 1998) which withdraws them from further oxidation of NADPH. Reactivity of a series of nitrosobenzenes towards ascorbate and synthetic NADH derivative increases with an increase in their electron-accepting properties, and follows Hammett-type relationships with the value of ρ close to 1.0 (Uršič *et al.*, 1998).

Using different nitroaromatic oxidants, ascorbate decreased the initial reaction rate in a uniform way across a wide range of NfsA concentrations (Fig. 25).

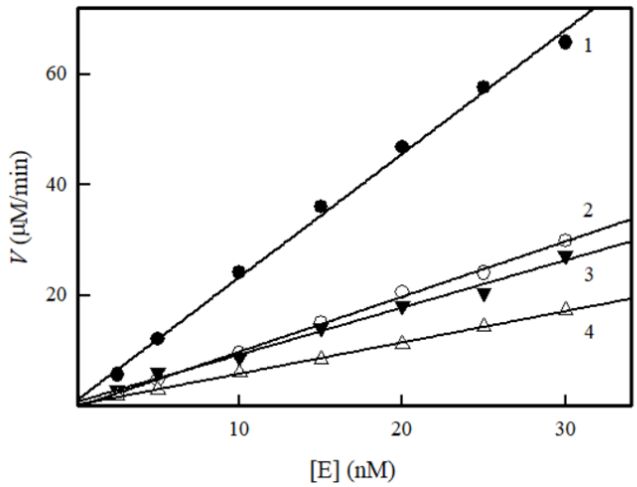

Fig. 25. Dependence of NADPH oxidation rate on NfsA concentration in the absence (1,3) or presence (2,4) of 2.0 mM ascorbate. NADPH concentration, 200 μM, 50 μM TNT (1,2) or 2.0 mM *p*-nitrobenzoic acid (3,4) were used as oxidants.

The ratios of reaction rate in the absence of ascorbate and its presence were independent of the concentration of NADPH used in the experiments (15-250 μM), being equal to 1.63±0.04 (nitrobenzene), 1.72±0.05 (*p*-nitrobenzoic acid), 2.34± 0.09 (*p*-nitroacetophenone), 2.32± 0.03 (TNT), and 2.57± 0.02(tetryl).

We next examined the effects of ascorbate on the steady-state kinetic parameters, $k_{cat(app.)}$ and k_{cat}/K_m, of NADPH oxidation by NfsA at fixed concentrations of oxidant. We obtained similar values of k_{cat}/K_m for NADPH using different nitroaromatic oxidants (Table 4). Importantly, it was observed that addition of ascorbate decreased both k_{cat}/K_m and $k_{cat(app.)}$ of the reactions (Table 4).

Table 4. The steady-state rate constants of NADPH oxidation by NfsA using various oxidants in the absence and presence of 2.0 mM ascorbate.

No.	Oxidant	-ascorbate		+ascorbate	
		$k_{cat(app.)}$ (s^{-1})	k_{cat}/K_m ($M^{-1}s^{-1}$)	$k_{cat(app.)}$ (s^{-1})	k_{cat}/K_m ($M^{-1}s^{-1}$)
1.	TNT (50 µM)	52.0±5.5	3.85±0.36×10^6	23.0±3.5	1.56±0.22×10^6
2.	Tetryl (50 µM)	41.8±7.0	3.78±0.50×10^6	16.1±3.0	2.08±0.23×10^6
3.	*p*-Nitroaceto-phenone (0.5 mM)	50.8±6.2	3.20±0.4×10^6	20.1±3.5	1.62±0.21×10^6
4.	*p*-Nitrobenzoic acid (2.0 mM)	30.6±4.5	3.30±0.42×10^6	19.7±1.2	2.05±0.30×10^6
5.	Nitrobenzene (1.5 mM)	4.6±0.3[1]	n.d.[2]	3.1±0.2[1]	n.d.[2]
6.	5-OH-1,4-NQ (50 µM	19.4±2.9	1.60±0.22×10^6	18.3±2.2[1]	n.d.[3]
7.	1,4-NQ (50 µM)	26.0±3.2	1.52±0.18×10^6	22.0±3.0[1]	n.d.[3]
8.	2-OH-1,4-NQ (20 µM)	26.5±1.4	1.70±0.22×10^6	26.2±3.7	1.46±0.23×10^6

[1] The rate at saturating NADPH concentration, 250 µM;
[2] Not determined due to low K_m values for NADPH;
[2] Not determined due to data scattering.

Interestingly, when various quinones were used as oxidants, the k_{cat}/K_m measured for NADPH were consistently ~2-fold lower than those obtained using $ArNO_2$ (Table 4). Such a difference is inconsistent with the "ping-pong" reaction mechanism, where the reductive and oxidative half-reactions proceed independently, and the k_{cat}/K_m value for the reducing substrate should not depend on the nature of the oxidant (Cleland, 1970). Ascorbate did not substantially affect the initial rate of NfsA-catalyzed NADPH oxidation by 1,4-NQ and 5-OH-1,4-NQ, but its presence resulted in a significant data scattering. This may be explained by the single-electron reduction of naphthoquinones by ascorbate and reoxidation of their anion-radicals by oxygen (O'Brien, 1991; Roginsky *et al.*, 1999). In the presence of 2.0 mM ascorbate and 50 µM quinone in control experiments, the O_2 uptake rates were ≥200 µM/min (5-OH-1,4-NQ) and 70 µM/min (1,4-NQ). Therefore, for these reactions only the

$k_{cat(app.)}$ values at saturating NADPH concentration were determined accurately (Table 4). On the other hand, the low redox cycling rate of 2-OH-1,4-NQ, ≤ 0.1 μM/min, enabled us to demonstrate that in this case ascorbate decreased the k_{cat}/K_m of NADPH only by 16% (Table 4).

Taken together, our data argue against significant involvement of NfsA in the reduction of nitroso derivatives of examined compounds, and for the major role of its direct reduction by NADPH (Scheme 2, pathway (b)). A possible occurrence of a second faster catalytic cycle, the reduction of Ar-NO by repeatedly reduced enzyme (Scheme 2) should not change the k_{cat}/K_m for NADPH, because in both cycles NADPH reacts with the same enzyme form. Because nitroaromatics and other aromatic compounds bind at the nicotinamide binding pocket close to the isoalloxazine ring of FMN (Lovering *et al.*, 2001), it is unlikely that Ar-NO can participate in a ternary complex formation with NR. Ascorbate should also not affect the k_{cat} of NfsA, because this is limited by the slowest catalysis step, oxidation of the reduced enzyme by oxidants. Thus, Ar-NO should simply amplify the rate and stoichiometry of enzymatic NADPH oxidation with nitroaromatics by ~2-fold. The quantitative analysis of competition between NAD(P)H and NR for the reduction of nitroso compounds other than nitrosobenzene is complicated by the absence of relevant kinetic data. However, our findings show that the inhibition by ascorbate takes place at a wide range of NfsA concentrations (Fig. 25). Our preliminary data show that the effects of ascorbate same take place in the reactions of *E. cloacae* NR, and are not observed during the single-electron reduction of nitroaromatics by NADP:cytochrome P-450 reductase.

4.1.5. The studies of photoreduction and rapid reduction of NfsA

Like other flavoenzymes, NfsA may be photoreduced in the presence of catalytic amount of 5-deazaflavin (Fig. 26). However, the long irradiation time, >60-80 min, caused protein precipitation and sample turbidity. Thus, we were able to reach maximal 70% photoreduction extent according to the absorbance spectra of reduced *E. cloacae* NR (Koder *et al.,* 2002). However, even in this case, we were unable to observe the formation of anionic (λ_{max} = 380 nm) or neutral (λ_{max} = 600 nm) FMN semiquinone, which points to its instability like in *E. cloacae* NR (Koder *et al.*, 2002).

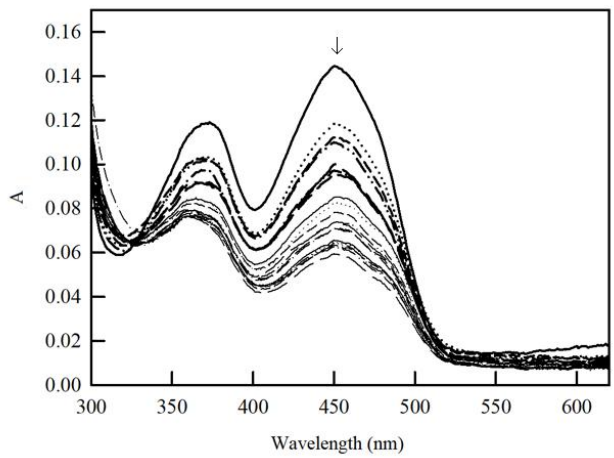

Figure 26. The photoreduction of 11.6 µM NfsA with 1 µM 5-deazaflavin under anaerobic conditions in the presence of 5 mM glucose and glucose oxidase. Spectra were recorded for 80 minutes.

The rapid reaction studies of reduction of NfsA by excess NADPH monitored at 460 nm in an aerobic medium show that in almost all cases, the reaction rates were ≥400 s^1 estimated according to the single-exponent fit, which is close to the detection limits of the stopped-flow spectrophotometer (Fig. 27A). Therefore, it was impossible to determine the reaction kinetic parameters. The reduction which corresponded to

~90% extent, was followed by a subsequent slow phase of the enzyme reoxidation by O_2, 0.2-0.3 s^{-1}, which was evident at low concentrations of NADPH, 50 µM, *i.e.*, conditions with an excess of O_2 over NADPH in the medium (Fig. 27B). The mixing of enzyme, NADPH and excess quinone resulted in much lower extent of FMN reduction and its rapid reoxidation (Fig. 27B). In this process, we failed to observe the transient formation of species with absorbance above 460 nm.

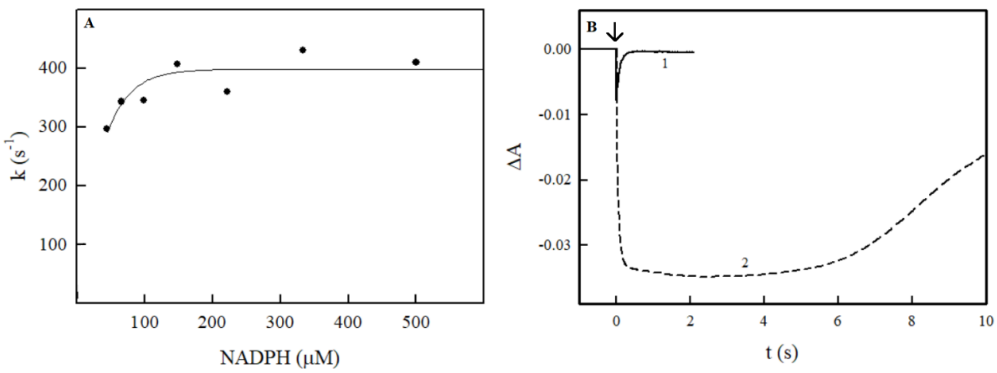

Fig. 27. A) The first-order rate constants of reduction of 5 µM NfsA with NADPH. B) The 460 nm absorbance changes after mixing 5 µM NfsA with 50 µM NADPH and 200 µM 2,6-dimethyl-1,4-benzoquinone (1), and with 50 µM NADPH in control experiment.

4.1.6. Determination of NfsA redox potential

In most cases, the redox potentials of flavoenzymes may be determined using slow reductive titration, monitoring the establishment of redox equilibrium between flavin cofactor and redox indicator. This may be performed spectrophotometrically, or, in an alternative way, spectroelectrochemically, using the mixture of catalytic amounts of redox mediators. On the other hand, according to the Haldane relationship, the reaction equilibrium constant (*K*) is equal to the ratio of forward and

reverse reaction rate constants, if the reactions proceed via the same reaction intermediate. This approach was used for the determination of standard redox potentials (E^0_7) of glutathione reductase and rat H-TR (Rakauskienė *et al.,* 1989; Čėnas *et al.,* 2004) from their bimolecular reaction rate constants (k_{cat}/K_m) with NADPH and $NADP^+$. According to the Nernst equation for a two-electron (hydride) transfer, $\log K = \Delta E^0_7$ (V)/0.0295.

The estimation of kinetic parameters of reduction of $NADP^+$ by NfsA is complicated by the absence of appropriate electron donor. For this reason, we examined the enzyme reactions with oxidized and reduced NADP(H) analogue, 3-acetylpiridine adenine dinucleotide phosphate (APADPH, E^0_7 = -0.258 V).

The data of Fig. 28 show that the transhydrogenase reaction of NfsA, reduction of $APADP^+$ at the expense of NADPH, proceeds according to a "ping-pong" mechanism, which is complicated by the inhibition by $APADP^+$. In this case, $APADP^+$ acts as a competitive to NADPH inhibitor (K_i = 150 μM), binding to the oxidized enzyme form. The reaction is characterized by $k_{cat} = 25\pm4.2\ s^{-1}$ and $k_{cat}/K_m = 4.3\pm0.6\times10^4\ M^{-1}\ s^{-1}$ for $APADP^+$. In the reverse reaction, APADPH was prepared *in situ* using glucose-6-phosphate/glucose-6-phosphate dehydrogenase system. The rate of its oxidation with NfsA was monitored using ferricyanide as an electron acceptor, because its absorbance did not overlap with that of APADPH. The reaction rate did not depend on ferricyanide concentration, 0.2-1.0 mM, and was characterized by $k_{cat} = 5.5\pm0.6\ s^{-1}$ and $k_{cat}/K_m = 1.35\pm0.29\times10^6\ M^{-1}\ s^{-1}$ for APADPH (on two-electron base) (Fig. 29). These results give $K = 31.4\pm11.1$, which in turn gives E^0_7 = -0.215±0.005 V.

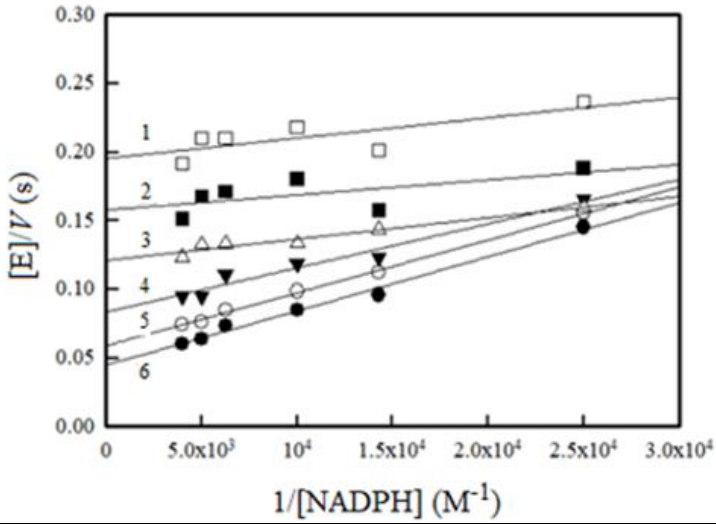

Figure 28. Dependence of the role of transhydrogenase reaction of NfsA on NADPH concentration at fixed $APADP^+$ concentration. $APADP^+$ concentrations are as follows: (1) 0.132 mM, (2) 0.198 mM, (3) 0.296 mM, (4) 0.444 mM, (5) 0.667 mM, (6) 1.0 mM;

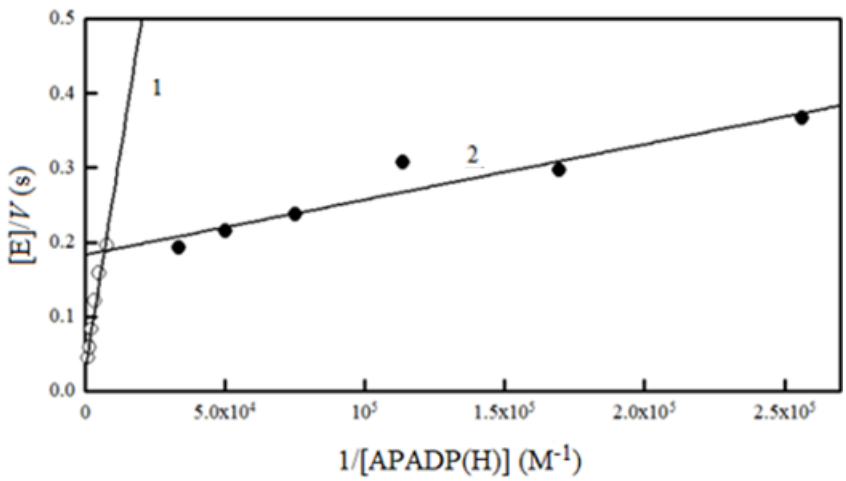

Figure 29. The rates of reactions of $APADP^+$/APADPH with NfsA: the maximal rates of $APADP^+$ reduction with NADPH (1), and the rates of APADPH-dependent reduction of 0.5 mM ferricyanide (2).

4.1.7. Discussion

The present study discloses several important findings on the mechanism of catalysis and oxidant substrate specificity of NfsA, which are relavant also to understanding of general principles of nitroreductase catalysis:

a) NfsA acts as a generic two-electron reductase by showing that it reduces previously uncharacterized compounds such as polynitromatic *N*-nitramine tetryl, and various quinones via two-electron (hydride) transfer (Fig. 13,14). The products of tetryl reduction are similar to those observed in *E. cloacae* NR and *T. maritima* peroxiredoxin-nitroreductase-catalyzed reactions (Nivinskas *et al.*, 2001a; Anusevičius *et al.*, 2012). In this case, the formation of *N*-methylpicramide by NQO1, proceeding with a high level of single-electron transfer and redox cycling (Anusevičius *et al.*, 1998) may be attributed to the higher stability of the flavin semiquinone in NQO1, 8-10% at redox equilibrium (Tedeschi *et al.*, 1995), in comparison to *E. cloacae* NR, ca. 0.01% (Haynes *et al.*, 2002). The data on the tetryl reduction (Fig. 14A) may indirectly imply that the $FMN^{-\bullet}$ state in NfsA is also extremely unstable. This assumption is further supported by the data of NfsA photoreduction (Fig. 26). The possibility of a single-step (H^-) hydride transfer mechanism (Eq. 13) is also supported by the observed pH dependence of reactivities of quinones and riboflavin, with the reaction k_{cat}/K_m increasing slightly with increasing pH for each of these compounds (Fig. 18). This would not be expected for a three-step (e^-,H^+,e^-) hydride transfer as per Eq. 14, because of the divergent pK_a values for the quinones versus riboflavin. The pK_a of riboflavin semiquinone is 8.5 (Hemmerich *et al.*, 1977), which means that the single-electron reduction potential of riboflavin decreases with increasing pH with a coefficient of -0.059 V/ΔpH. In contrast, the E^1

values of used quinones are pH-independent in this range. Thus, the data of Fig. 18 are inconsistent with a three-step hydride transfer, for which reactivity of riboflavin would be expected to increase relative to the reactivity of quinones at lower pH. A similar pH dependence was obtained during the reduction of riboflavin and several quinones by the group B nitroreductase of *E. cloacae* (Nivinskas *et al.*, 2002);

b) NfsA follows a "ping-pong" mechanism with tetryl and TNT (Fig. 15, 16), as previously observed for another nitroaromatic oxidant, nitrofurazone (Zenno *et al.*, 1996b). For NfsA, the oxidative half-reaction (*i.e.*, the reoxidation of $FMNH^-$ by the oxidant substrate) should be a rate-limiting step, because the values of k_{cat} at infinite concentrations of tetryl or TNT are substantially lower than the lowest rate of the reductive half reaction (the reduction of FMN by NADPH) measured in the rapid reaction experiments (>400 s^{-1}) (Fig. 27). Moreover, the k_{cat} of reactions at fixed NADPH concentrations (Table 2) were also lower than the reduction rate of FMN at the same NADPH concentration (Fig. 27). A "ping-pong" mechanism with a rate-limiting oxidative half-reaction is also characteristic for NfsB of *E. coli* (Race *et al.*, 2005; Jarrom *et al.*, 2009), *E. cloacae* NR (Nivinskas *et al.*, 2002; Pitsawong *et al.*, 2014), and the peroxiredoxin-nitroreductase of *T. maritima* (Anusevičius *et al.*, 2012). The data of $NADP^+$ inhibition (Fig. 21) enable to propose the mechanism of catalysis of NfsA, where $NADP^+$ (P) binds relatively tightly to the oxidized enzyme form (E_{ox}), but weakly binds or does not bind or rapidly dissociates from the reduced enzyme form (E_{red}):

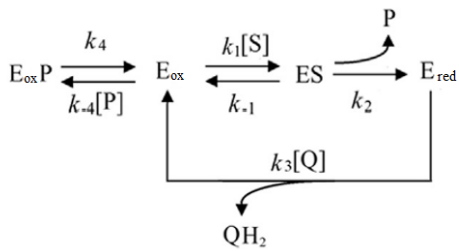

Scheme 3. The „ping-pong“ mechanism for NfsA.

In this case, the reaction rate is expressed as:

$$\frac{[E]}{V} = \frac{1}{k_2} + \frac{1}{k_3[Q]} + \frac{k_{-1} + k_2}{k_1 k_2 [S]} \left(1 + \frac{k_{-4}[P]}{k_4}\right) \quad (24)$$

In the absence of $NAD(P)^+$ (P), Eq. 24 it is transformed to a simple “ping-pong“ scheme:

$$\frac{[E]}{V} = \frac{1}{k_2} + \frac{1}{k_3[Q]} + \frac{k_{-1} + k_2}{k_1 k_2 [S]} \quad (25)$$

c) Our data provide some insight on the specificity of NfsA towards nitroaromatic and quinoidal oxidants. The quantitative structure-activity relationships of single-electron reduction of quinones and nitroaromatic compounds by flavoenzymes are relatively easy to understand, because they follow an “outer-sphere“ electron transfer mechanism (Marcus and Sutin, 1985). In this case, the reactivity of oxidants is not strongly influenced by their structure, the reactivity increases with an increase in their E^1_7, and also by the reactivity of quinones is typically higher than that of nitroaromatics that possess similar values of E^1_7 (Anusevičius *et al.*, 2013, and references therein) In contrast, the reaction characteristics of flavoenzyme-catalyzed two-electron reduction of quinones and nitroaromatics are more complex and individual (Nivinskas *et al.*, 2001a, 2002; Anusevičius *et al.*, 2002, 2012; Misevičienė *et al.*, 2006).

Our data show that the oxidant substrate specificity for NfsA is generally similar to that of *E. cloacae* NR (Nivinskas *et al.,* 2001a, 2002), *i.e.,* the log k_{cat}/K_m of nitroaromatics increased with increasing E^1_7, and was systematically higher than the reactivities of quinones with the notable exception of the significantly enhanced reactivity of the 2-hydroxy-1,4-naphthoquinones (Fig. 17). The best studied NR of B group, *E. coli* NfsB, which is strongly homologous with *E. cloacae* NR, possesses several partly overlapping domains that provide alternative binding possibilities for nitroaromatic oxidants and other ligands (Parkinson *et al.,* 2000; Johansson *et al.,* 2003; Race *et al.,* 2005). In spite of low sequence homology between NfsB, *E. cloacae* NR and NfsA, several important amino acid residues are also conserved in the active center of NfsA, including Ser40, Ser41, and Phe42 (hydrophobic substitute for Thr41 in *E. coli* NfsB and *E. cloacae* NR) which, according to molecular docking and mutagenesis studies, may be involved in the binding of CB-1954 and TNT (Yang *et al*. 2013; Bai *et al.,* 2015). These data may partly explain the similar oxidant specificity profiles of NfsA and *E. cloacae* NR. On the other hand, the absence of FMN fluorescence quenching of NfsA by dicoumarol and $NADP^+$, which efficiently bind to the oxidized enzyme form, contrasts with the fluorescence quenching observed for *E. coli* NfsB (Fig. 20B) and *E. cloacae* NR (Nivinskas *et al.,* 2002), which may suggest that certain oxidants and other ligands bind to the oxidized form of NfsA in a different conformation compared to NfsB or *E. cloacae* NR, *e.g.* at a greater distance from the isoalloxazine ring. Further research that takes into account the flexibility of the active centers of these NRs and the possibility of conformational transitions between their oxidized and reduced forms will be required to comprehensively resolve these issues;

d) We for the first time determined the E^0_7 value of NfsA, -0.215±0.005 V, which is more positive than that of another A group nitroreductase, *V. harveyi* Frp, -0.255 V (Lei *et al.*, 2005), and is closer to E^0_7 of *E. cloacae* NR, -0.190 V (Koder *et al.*, 2002). However, it is currently impossible to characterize the factors determining the values of redox potentials of nitroreductases because of a limited amount of potentiometric data for their other representatives, and

e) We for the first time characterized the role of nonenzymatic reduction of nitroso intermediates in the net four-elctron reduction of nitroaromatics with nitroreductases (Fig. 23-25). Apart from clarifying the reaction mechanism, our data may be helpful in the modification of biodegradation pathways of polynitroaromatic compounds. Although nitrosobenzene is not transiently accumulated during the reduction of nitrobenzene by NR in the presence of an NADH regeneration system (Koder *et al.*, 1998), aerobic incubation of TNT with *Pseudomonas* sp. leads to close to 25% yield of azoxyarenes, the condensation products of nitroso- and hydroxylamine metabolites (Haidour *et al.*, 1996). Nitroso metabolites of dinitrotoluene were transiently formed by *Salmonella typhimurium* with a close to 50% yield even under anaerobic conditions (Sayama *et al.*, 1991). In addition to reoxidation of Ar-NHOH by O_2, a possible cause is limited NAD(P)H regeneration. In our opinion, the addition of ascorbate could significantly reduce the transient accumulation of the above groups of metabolites.

4.2. Reduction of quinones and nitroaromatic compounds by *T. maritima* TR

4.2.1. Steady-state kinetics of *T. maritima* TR

The maximal rate of reduction of a putative physiological oxidant of TmTR, Grx1, at pH 7.0 was 0.2-0.3 s^{-1} (0.1 M K-phosphate, 100 µM NADH, 3–10 µM Grx1, 0.10 mM DTNB), which is close to the intrinsic NADH oxidase activity of the enzyme, 0.05 s^{-1}. In agreement with the previous data (Yang and Ma, 2010), an increase in pH to 8.0 (0.03 M Tris-HCl) increased the reactivity of Grx1. Under these conditions, k_{cat} was equal to 2.1±0.6 s^{-1}, and the k_{cat}/K_m for Grx1 was $6.3\pm0.6\times10^5$ $M^{-1}s^{-1}$. On the other hand, the TmTR-catalyzed oxidation of NADH by a number of quinones and nitroaromatic compounds at pH 7.0 was much faster (Table 5). Using varied concentrations of 5,8-dihydroxy-1,4-naphthoquinone (naphthazarin) as an electron acceptor at several fixed concentrations of NADH, the reaction was characterized by a series of parallel Lineweaver-Burk plots (Fig. 30). It corresponds to a "ping-pong" scheme, which was also characteristic for the quinone- and nitroreductase reactions of *A. thaliana* TR (Bironaitė *et al.*, 1997; Miškinienė *et al.*, 1998). In our case, k_{cat}/K_m for naphtazarin was $3.3\pm0.3\times10^5$ $M^{-1}s^{-1}$, the k_{cat}/K_m for NADH was $1.7\pm0.2\times10^6$ $M^{-1}s^{-1}$, and k_{cat}, obtained by extrapolation to infinite concentrations of NADH and napthhazarin, was equal to 39.1±3.5 s^{-1}.

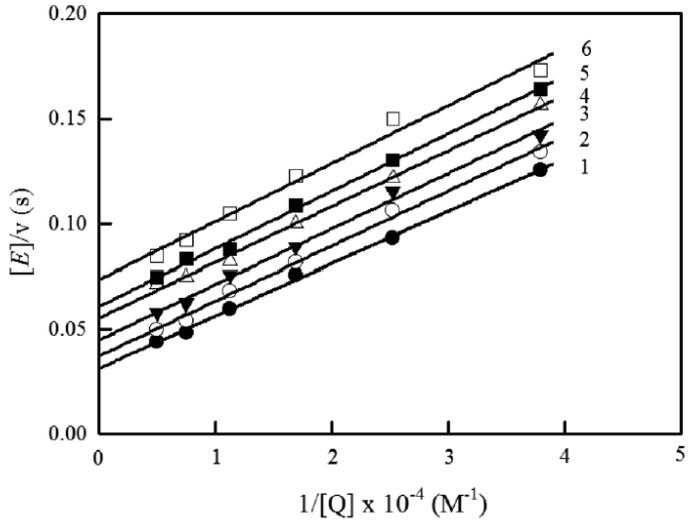

Fig. 30. "Ping-pong" scheme of *T. maritima* TR catalyzed oxidation of NADH by 5,8-dihydroxy-1,4-naphtoquinone (naphthazarin). NADH concentration was 100 μM (1), 66.6 μM (2), 44.4 μM (3), 29.6 μM (4), 19.8 μM (5), and 13.2 μM (6).

Table 5. Kinetic parameters of reduction of quinones and nitroaromatic compounds by *T. maritima* thioredoxin reductase. The catalytic constants (k_{cat}) and bimolecular rate constants (k_{cat}/K_m) of electron acceptors in TmTR catalyzed reactions at pH 7.0 and 25°C were obtained in the presence of 100 μM NADH. Their single-electron reduction potentials at pH 7.0 (E^1_7) are taken from Wardman (1989).

No	Compound	E^1_7 (V)	k_{cat} (s^{-1})	k_{cat}/K_m (M^{-1} s^{-1})
	Quinones			
1	1,4-Benzoquinone	0.09	35.7±3.4	4.05±0.5 x 10^5
2	2-Methyl-1,4-benzoquinone	0.01	19.8±2.2	1.26±0.15 x 10^6
3	2,3-Dichloro-1,4-naphthoquinone	-0.035	56.4±6.5	1.35±0.14 x 10^6
4	2,6-Dimethyl-1,4-benzoquinone	-0.08	35.4±4.5	2.79±0.3 x 10^5
5	5-Hydroxy-1,4-naphthoquinone	-0.09	47.7±6.0	1.2±0.13 x 10^6
6	5,8-Dihydroxy-1,4-naphthoquinone	-0.11	29.1±3.2	3.3±0.4 x 10^5
7	9,10-Phenanthrenequinone	-0.12	58.5±4.8	5.1±0.45 x 10^5
8	1,4-naphthoquinone	-0.15	18.9±1.8	6.6±0.8 x 10^5
9	2-methyl-1,4-naphthoquinone	-0.20	24.6±3.7	1.38±0.15 x 10^5
10	Tetramethyl-1,4-benzoquinone	-0.26	3.9±0.4	1.3±0.11 x 10^5
11	1,4-Dihydroxy-9,10-anthraquinone	-0.30	2.9±0.2	2.9±0.3 x 10^5

12	1,8-Dihydroxy-9,10-anthraquinone	-0.33	1.5±0.2	$1.1\pm0.12 \times 10^5$
13	1,1‘ –Dibenzyl-4,4‘ –bipyridinium	-0.35	3.7±0.4	$1.5\pm0.2 \times 10^3$
14	9,10-Anthraquinone-2-sulfonic acid	-0.38	0.96±0.2	$6.0\pm0.5 \times 10^4$
15	2-Hydroxy-1,4-naphthoquinone	-0.41	0.75±0.1	$5.1\pm0.45 \times 10^3$
	Nitroaromatic compounds			
1	2,4,6-Trinitrophenylmethylnitramine (tetryl)	-0.16	6.3±0.6	$6.6\pm0.7 \times 10^4$
2	2,4,6-Trinitrotoluene	-0.25	4.2±0.4	$1.5\pm0.2 \times 10^4$
3	1,4-Dinitrobenzene	-0.26	n.d.	$5.1\pm0.4 \times 10^4$
4	1,2-Dinitrobenzene	-0.29	4.2±0.3	$1.5\pm0.1 \times 10^4$
5	4-Nitrobenzaldehyde	-0.32	n.d.	$5.1\pm0.45 \times 10^3$
6	1,3-Dinitrobenzene	-0.35	2.4±0.25	$1.2\pm0.2 \times 10^4$
7	4-Nitroacetophenone	-0.355	5.1±0.4	$3.9\pm0.5 \times 10^3$
8	4-Nitrobenzoic acid	-0.425	1.8±0.3	$1.5\pm0.1 \times 10^3$
9	Nitrobenzene	-0.49	0.4±0.05	$1.5\pm0.2 \times 10^2$

	Other compounds			
1	Ferricyanide	0.41	2.2±0.1	$1.5\pm0.4 \times 10^4$
2	7-trifluoromethyl-3-amino-1,2,4-benzotriazine-1,4-dioxide (7-CF_3-TPZ)	-0.345	0.3±0.05	$3.3\pm0.4 \times 10^2$

The log k_{cat}/K_m of oxidants generally increased with an increase in their single-electron reduction potential (E^1_7) (Fig. 31). The reactivity of nitroaromatics was systematically lower than that of quinones with similar E^1_7 values.

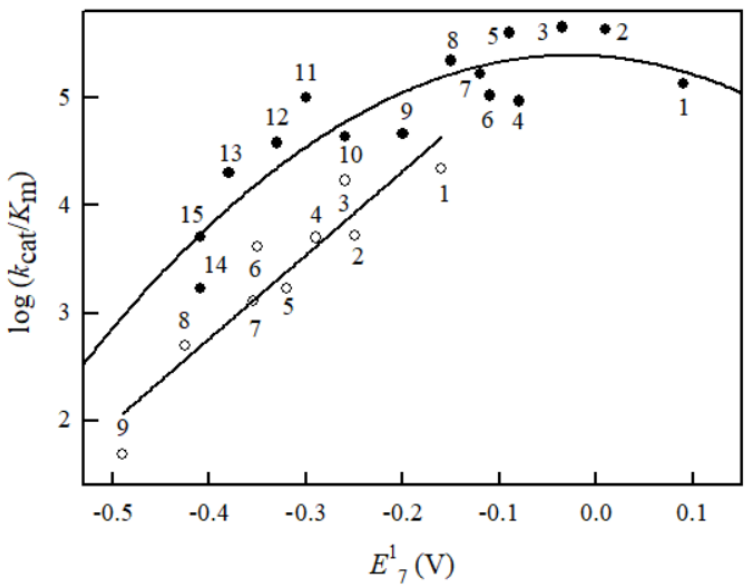

Fig. 31. Reactivity of quinones and nitroaromatic compounds in *T. maritima* TR-catalyzed reactions. Relationship between log k_{cat}/K_m of quinones (solid circles) and nitroaromatic compounds (blank circles) in TmTR catalyzed reaction and their single-electron reduction potentials at pH 7.0 (E^1_7) is shown. Numbers refer to quinones and nitroaromatic compounds whose redox potentials and reduction rate constants are given in Table 5.

Next we aimed at characterizing the possible single-electron transfer events in the reduction of quinones and nitroaromatics by *T. maritima* TR. The percentage of the single-electron flux in the reduction of quinones by TmTR was determined by a benzosemiquinone-mediated reduction of cytochrome *c* (Iyanagi *et al.*, 1990, and references therein). During the enzymatic reduction of 50 μM 1,4-benzoquinone by 150 μM

NADH, the rate of reduction of added 50 μM cytochrome *c* was equal to 50% of NADH oxidation rate. This shows that single-electron flux makes up 25% of the overall electron flux in this case. The quantitation of single-electron flux in the nitroreductase reactions of flavoenzymes is less straightforward, because both nitroaromatic anion-radicals and the products of their two(four)-electron reduction (hydroxylamines) reduce cytochrome *c* (Šarlauskas *et al.*, 2004). During the TmTR-catalyzed oxidation of 100 μM NADH by 100 μM *p*-dinitrobenzene or tetryl, the rate of reduction of added 50 μM cytochrome *c* was 160% and 182% of NADH oxidation rate, respectively. The cytochrome *c* reduction was inhibited by 100 U/mg superoxide dismutase (SOD) by 25% (*p*-dinitrobenzene) and 31% (tetryl). In this case, the $ArNO_2/ArNO_2^{\bullet}$ and $O_2^{-\bullet}/O_2^{-\bullet}$ redox couples are under rapid equilibrium, and only the $O_2^{-\bullet}$-mediated, but not the nitroradical-mediated, cytochrome *c* reduction is inhibited by SOD. Nevertheless, it points to an at least 20-27% share of single-electron flux in the reduction of nitroaromatic compounds by TR. Tetryl and menadione oxidize excess NADH, the reactions are accompanied by O_2 uptake (Fig. 32).

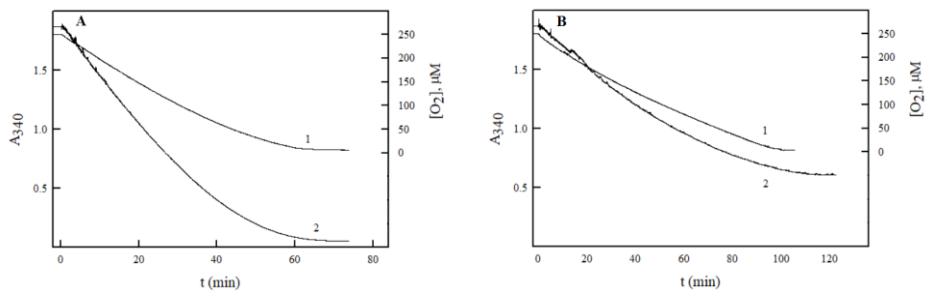

Fig. 32. Oxygen consumption (curves 1) and NADH oxidation (curves 2) during reduction of 100 μM menadione (A) and 100 μM tetryl (B) with TmTR. [NADH] = 300 μM, [TmTR] = 40 nM, pH 7.0. Oxygen consumption was monitored by Clark electrode, NADPH oxidation was monitored in an open spectrophotometer cell.

The reduction of tetryl in the presence of NADH regeneration system is accompanied by the formation of *N*-methylpicramide, which is indicated by the rise in absorbance with λ_{max} = 340 nm and a shoulder at 400-450 nm, and formation of nitrite (Fig. 33). It shows that the reaction proceeds with the involvement of single-electron transfer (Scheme 1).

It is commonly accepted that quinoidal compouds are reduced by the reduced FAD of flavoenzymes containing a catalytic disulfide, including *A. thaliana* TR (Čėnas *et al.*, 1994; 2004; 2006; Bironaitė *et al.*, 1997; Miškinienė *et al.*, 1998; and references therein). This may also be true for TmTR, because a 40–50 min incubation of the reduced enzyme with the thiol alkylating agent *p*-chloromercury benzoate (*p*-CMB) resulted in a 95% inhibition of the reduction of Grx1 (Fig. 34). In contrast, the reduction of naphthazarin was inhibited by 40–50%. In control experiments, incubation of TR with NADH resulted in the inhibition of Grx1 and naphthazarin reduction activity by 10-20%.

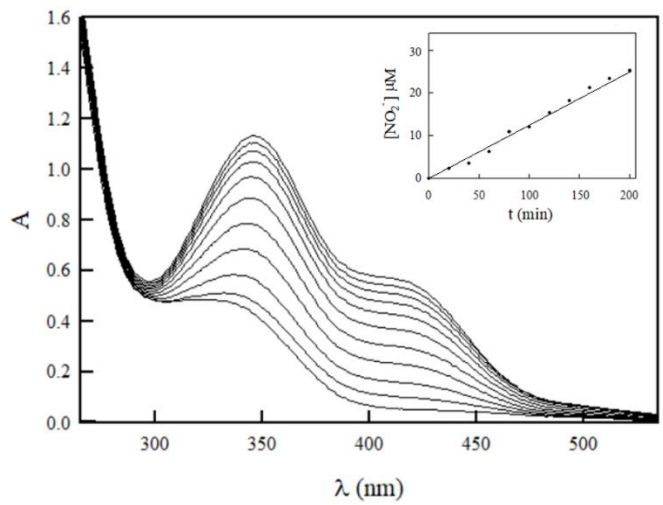

Fig. 33. Spectra of reduction products of 100 mM tetryl in the presence of 40 nM TmTR, and the NADH regeneration system. Spectra were recorded in 20 min interval. NO_2^- formation is demonstrated in the inset.

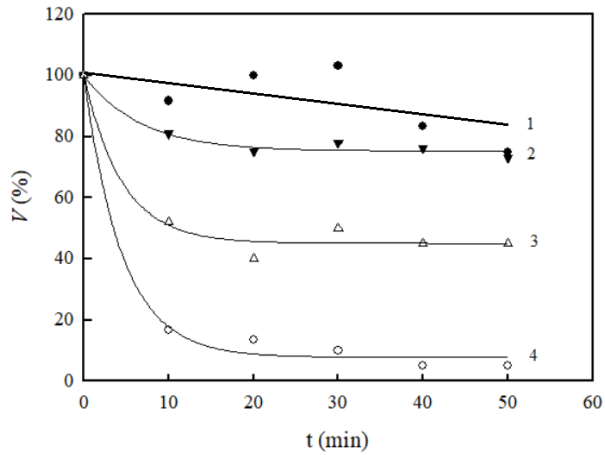

Fig. 34. Changes of naphthazarin and Grx1-reductase activity during the incubation of reduced TmTR with *p*-CMB. Enzyme was incubated in the presence of 200 µM NADH in the absence (1,2) and in the presence of 100 µM *p*-CMB (3,4). Oxidants: 100 µM naphthazarin (1,3) and 4 µM Grx1 (2,4).

The sequence of TmTR (Genbank accession number TM_0869 or AAD35951) shows that apart from the similarity of its catalytic disulfide motif (Cys147, Ala148, Thr149, and Cys150) which likely participates in the reduction of glutaredoxin-1 to the disulfide motif of *E. coli* TR (Lennon *et al.*, 1999), its interdomain sequence motif Gly251, Pro254 is similar to the motifs Gly244, Pro247 of *E. coli* TR and Gly298, Pro301 of *A. thaliana* TR, which participate in domain rotation (Fig. 12). These data indirectly point to a possible similarity in the catalysis of those TRs, involving a transition between the nonfluorescent flavin-to-disulfide- and fluorescent flavin-to-NAD(P)H-binding site conformations (Dai *et al.*, 1996; Lennon *et al.*, 1997; 1999). For this reason, we further examined the effects of various ligands on the fluorescence intensity of FAD of TmTR.

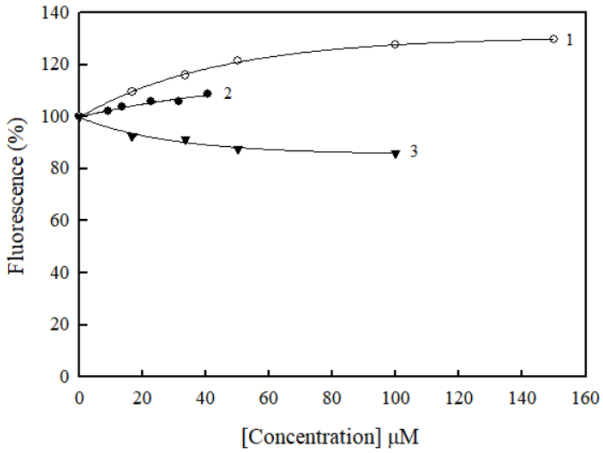

Fig. 35. Fluorescence changes of FAD of TmTR after addition of of ADP-ribose (1), Grx1 (2) and $NADP^+$ (3). Enzyme concentration = 4 µM, excitation wavelengh – 460 nm, emission – 560 nm.

We found that the fluorescence intensity of FAD in TmTR makes up to 20% of that of free FAD, which is close to 25% in *A. thaliana* TR (Nivinskas *et al.*, 2001b). The addition of ADP-ribose or Grx1 increased its fluorescence intensity by max. 30% and 12%, respectively, and addition of NAD^+ decreased its intensity by ~10% (Fig. 35). These ligands also affect the fluorescence intensity of FAD of A. *thaliana* TR, but in different way (Nivinskas *et al.*, 2001b) (discussed in 4.2.5).

4.2.2. Rapid reaction studies of TmTR

The prestady-state measurements of reduction of TR by excess NADH monitored at 460 nm show that the kinetics of the reaction are best described by a single-exponent fit. The reduction of FAD is characterized by a maximum rate of 82±3.0 s^{-1}, and the apparent bimolecular rate constant of *T. maritima* TR reduction by NADH, 1.6±0.15 × 10^6 $M^{-1}s^{-1}$ (Fig. 36). The latter value is close to the k_{cat}/K_m for NADH, obtained in the steady-state experiments. Typically, the

absorbance of FAD at 460 nm decreased by 70–80% at the end of the reaction, as in the case of *E. coli* TR (Lennon *et al.*, 1997). Reduced 3-acetylpyridine adenine dinucleotide (APADH) reduces TmTR with much lower maximum rate, 1.3±0.3 s^{-1}, and the aparent bimolecular rate constant of 3.3±0.5×10^5 $M^{-1}s^{-1}$ (data not shown).

In order to characterize the redox states of FAD participating in this process, we monitored the multiple turnover of FAD during TmTR-catalyzed oxidation of NADH by duroquinone.

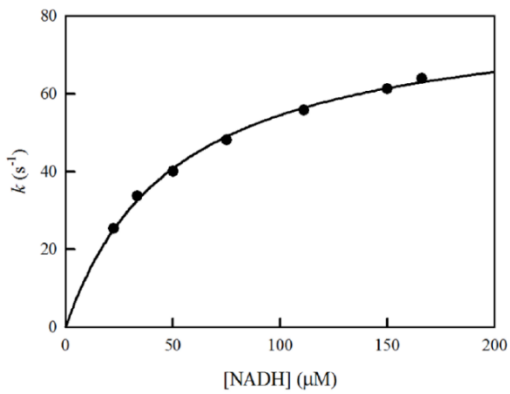

Fig. 36. The dependence of pseudofirst-order presteady-state reduction rate constant (*k*) of reduction of *T. maritima* TR on NADH concentration.

In control experiments performed in the absence of quinone, the initial fast phase of FAD reduction by NADH monitored at 460 nm was followed by a slower reoxidation by oxygen (Fig. 37A). The addition of duroquinone significantly accelerated the reoxidation (Fig. 37A). Importantly, addition of quinone caused a transient increase in absorbance at 600 nm at the same time scale, which was almost not evident in control experiments (Fig. 37A).

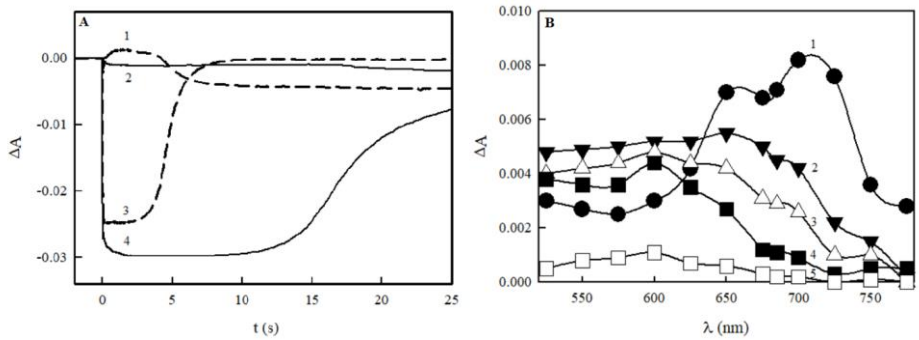

Figure 37. A) The TmTR FAD absorbance changes during enzyme turnover monitored at 600 nm (1,2) and 460 nm (3,4) in the presence of 100 µM duroquinone (1,3) or in its absence (2,4). Enzyme concentration, 5.0 µM. B) Spectra of reaction intermediates formed during the turnover of 5.0 µM *T. maritima* TR with 50 µM NADH and 100 µM duroquinone. Spectra were recorded after 0.2 s (1), 2.0 s (2), 3.0 s (3), 4.0 s (4), and 6.0 s (5).

The data collected at different wavelengths show that the absorbance initially increased in the range of 525-775 nm and above, and was characterized by λ_{max} ~700 nm (Fig. 37B). Subsequently, the formation and decay of a secondary absorbance with λ_{max} ~600 nm has taken place (Fig. 37B). The latter resembles the absorbance of the neutral (blue) FAD semiquinone ($FADH^{\cdot}$) of *E. coli* TR, which is formed during the enzyme irradiation under anaerobic conditions, but not in physiological reactions (Zanetti *et al.*, 1968). The transient accumulation of $FADH^{\cdot}$ during the turnover may indicate that its oxidation is the rate-limiting (slower) step in the reoxidation of two-electron reduced FAD with quinones. However, the other reaction intermediates, *e.g.*, the $FADH_2$-NAD^+ complex absorbing above 700 nm (Lennon and Williams, 1997) may be formed at the beginning of the turnover, as shown in Fig. 37B.

4.2.3. The inhibition studies of TmTR

The inhibition of NAD(P)H-oxidizing flavoenzymes by the reaction product, $NAD(P)^+$, gives some information on the binding of NAD(P)H/$NAD(P)^+$ to the different redox states of the enzyme, and, in certain cases, on its redox equilibrium with the $NAD(P)^+$/NAD(P)H couple (Vienožinskis *et al.*, 1990; Bironaitė *et al.*, 1997; Čėnas *et al.*, 2004). In the case of *T. maritima* TR, NAD^+ acted as a mixed-type inhibitor towards NADH (Fig. 38A), *i.e.*, it decreased both the maximal rate of the reaction and the k_{cat}/K_m for NADH. This means that NAD^+ not only competes with NADH for the binding to the oxidized enzyme form, but also competes with the quinoidal electron acceptor for the binding to the reduced enzyme form, or even reoxidizes the reduced enzyme (Rudolph *et al.*, 1979). In agreement with this, NAD^+ acts as a mixed-type inhibitor towards naphthazarin (Fig. 38B), decreasing both its k_{cat}/K_m and the maximum reaction rate.

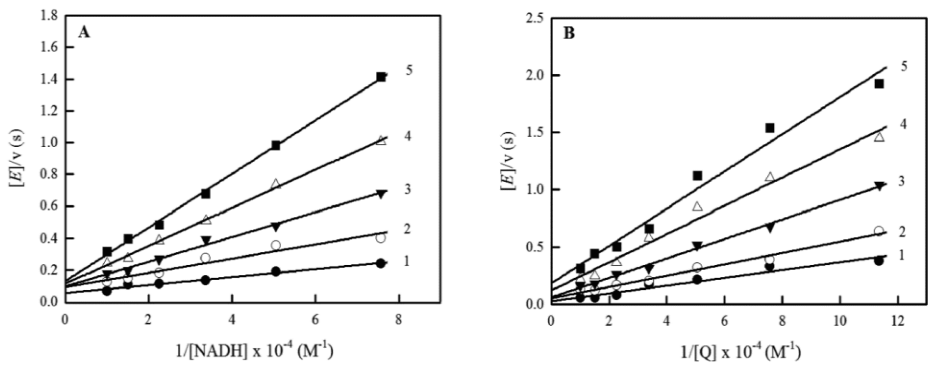

Fig. 38. Inhibition of TmTR by NAD^+. (A) TmTR quinone reductase reaction inhibition by NAD^+ at varied NADH concentrations in the presence of 100 μM naphtazarin. NAD^+ concentrations: 0 mM (1), 0.2 mM (2), 0.4 mM (3), 0.6 mM (4), and 1.0 mM (5). (B) TmTR quinone reductase reaction inhibition by NAD^+ at varied naphthazarin concentrations in the presence of 100 μM NADH. NAD^+ concentrations: 0 mM (1), 0.2 mM (2), 0.4 mM (3), 0.6 mM (4), and 1.0 mM (5).

Importantly, the inhibitory effect of NAD^+ towards the k_{cat}/K_m of naphthazarin decreased with an increase in NADH concentration from 30 μM to 100 μM (Fig. 39A). Besides, in the presence of 600 μM NAD^+, varied naphthazarin concentrations at several fixed concentrations of NADH give a series of converging Lineweaver-Burk plots (Fig. 39B). This is in contrast with the series of parallel double-reciprocal plots obtained in the absence of NAD^+ (Fig. 30). Thus, based on the general effects of the reaction products on the reaction rates (Rudolph and Fromm, 1979; Rudolph, 1979), the data of Fig. 39A,B indicate that NAD^+ not only competes with naphthazarin for the binding to the reduced enzyme, but also possibly reoxidizes the reduced enzyme (Rudolph *et al.*, 1979; Rudolph, 1979) (Scheme 4).

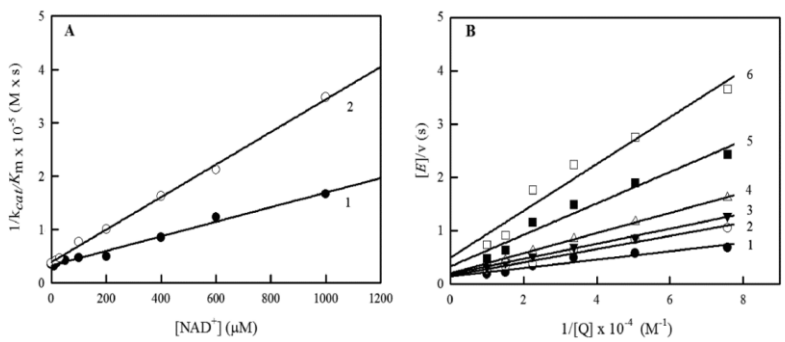

Fig. 39. Inhibition of TmTR by NAD^+. (A) Decrease of naphthazarin k_{cat}/K_m by NAD^+ at [NADH]=100 μM (1), and [NADH]=30 μM (2); (B) Influence of 600 μM NAD^+ on rate of TmTR-catalyzed oxidation of NADH by naphthazarin. NADH concentrations: 100 μM (1), 66.7 μM (2), 44.4 μM (3), 29.6 μM (4), 19.8 μM (5), 13.2 μM (6).

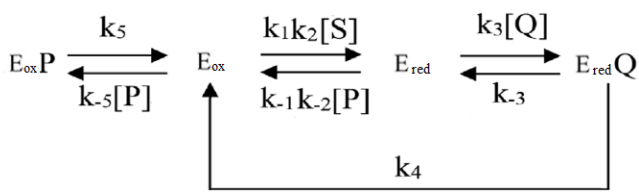

Scheme 4. The reaction mechanism for TmTR.

Assuming a rapid equilibrium between the oxidized (E_{ox}) and reduced (E_{red}) enzyme forms and NADH (S) and NAD^+ (P), Scheme 4 gives the following steady-state rate equation (Eq. 26), where Q is the electron acceptor:

$$\frac{[E]}{V} = \frac{1}{k_4} + \left(1 + \frac{k_{-3}}{k_4}\right)\left(\frac{1}{k_3[Q]} + \frac{k_{-1}k_{-2}k_{-5}[P]^2}{k_1k_2k_3k_5[S][Q]} + \frac{k_{-1}k_{-2}[P]}{k_1k_2k_3[S][Q]}\right) + \frac{1}{k_1k_2[S]}\left(1 + \frac{k_{-5}[P]}{k_5}\right) \quad (26)$$

In the absence of NAD^+ ([P]=0), Eq. 26 is reduced to Eq. 27, which corresponds to a simple „ping-pong“ scheme:

$$\frac{[E]}{V} = \frac{1}{k_4} + \left(1 + \frac{k_{-3}}{k_4}\right)\frac{1}{k_3[Q]} + \frac{1}{k_1k_2[S]} \quad (27)$$

Importantly, Eq. 26 shows that the k_{cat}/K_m of reduction of quinone ($k_3k_4/(k_{-3} + k_4)$) should decrease with an increase in the [P]/[S] ratio (*i.e.*, the $[NAD^+]/[NADH]$ ratio) which, in the case of the rapid redox equilibrium, corresponds to the redox potential of the medium, E_h. We summarized the data in Fig. 38,39, expressing k_{cat}/K_m for naphthazarin as a function of E_h, and taking the standard redox potential for $[NAD^+]/[NADH]$ couple as –0.32 V. The data of Fig. 40 show that 50% inhibition of quinone reductase activity expressed as k_{cat}/K_m takes place at E_h= –0.31±0.03 V, which formally may be equal to the standard potential of enzyme.

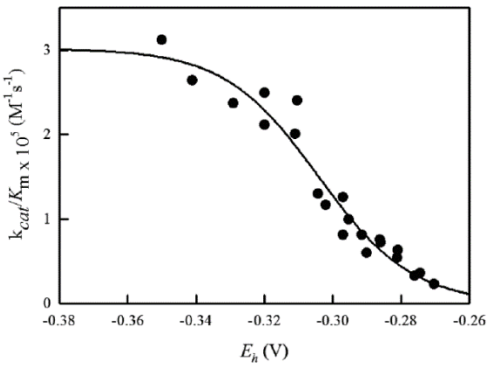

Fig. 40. Dependence of k_{cat}/K_m of naphthazarin on the redox potential of medium (E_h) at pH 7.0, *i.e.* [NAD^+]/[NADH] ratio.

However, the control experiments show that varied naphthazarin concentrations at several fixed concentrations of NADH give a series of converging Lineweaver-Burk plots also in the presence of redox inactive ADP-ribose (Fig. 41).

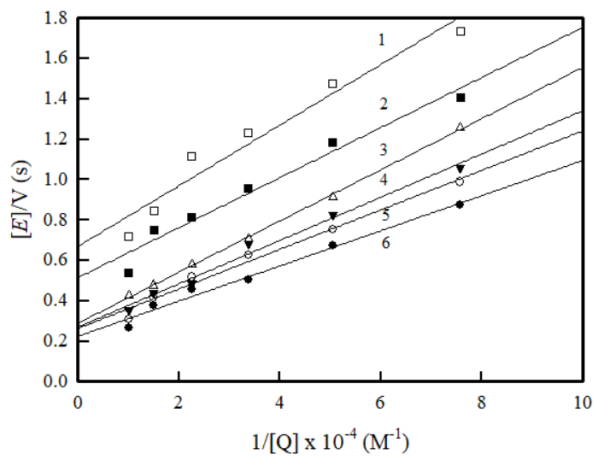

Fig. 41. TmTR quinone reductase reaction inhibition by 0.5 mM ADP-ribose at varied NADH and naphthazarin concentrations. NADH concentrations: 13.2 μM (1), 19.8 μM (2), 29.6 μM (3), 44.4 μM (4), 66.7 μM (5), and 100 μM (6).

4.2.4. Determination of redox potential of TmTR.

The redox potential of TmTR may be determined using the Haldane relationship. Because Grx1 is a slow substrate for TmTR, the studies of NAD^+ enzymatic reduction using reduced Grx1 as a substrate is problematic. For this reason, we examined the reactions of TmTR with 3-acetylpyridine adenine dinucleotide ($APAD^+$/APADH) redox couple with E^0_7 = -0.258 V. During the TmTR-catalyzed reduction of $APAD^+$ by NADH, the substrate inhibition by NADH takes place, *i.e.*, at fixed $APAD^+$ concentration, the reaction rates decrease with an increasing NADH concentration (Fig. 42A). The data linearization in Cleland plots (Fig. 42A) enables to determine the substrate inhibition constants (K_i) of NADH. Their increase with $APAD^+$ concentration (Fig. 42B) demonstrates the competitive character of inhibition. This means that after TmTR reduction, NADH repeatedly binds to the reduced enzyme form thus competing with $APAD^+$. Importantly, NADH substrate inhibition does not take place using quinone as oxidant (Fig. 30). At [$APAD^+$] = 0, K_i of NADH is equal to 140±15 μM. The oxidation of TmTR by $APAD^+$ is characterized by k_{cat} = 2.7±0.2 s^{-1}, and k_{cat}/K_m = 3.8±0.1×10^4 $M^{-1}s^{-1}$ (Fig. 43).

The steady-state studies of enzymatic APADH oxidation give k_{cat} = 1.0±0.2 s^{-1}, and k_{cat}/K_m = 3.2±0.6×10^5 $M^{-1}s^{-1}$, which are similar to the kinetic parameters obtained in presteady-state experiments (Fig. 43). Finally, using K = 8.68±1.54, *i.e.*, the ratio of k_{cat}/K_m of forward and reverse reactions, and E^0_7 = -0.258 V for $APAD^+$/APADH couple, the Nernst equation gives E^0_7 = -0.230±0.003 V for FAD of TmTR, with an understanding that the catalytic disulfide/dithiol does not participate in the reactions with $APAD^+$/APADH. This value is close although slightly

higher than E^0_7 of FAD of *E. coli* TR, -0.242÷-0.258 V (O'Donnell and Williams, 1984).

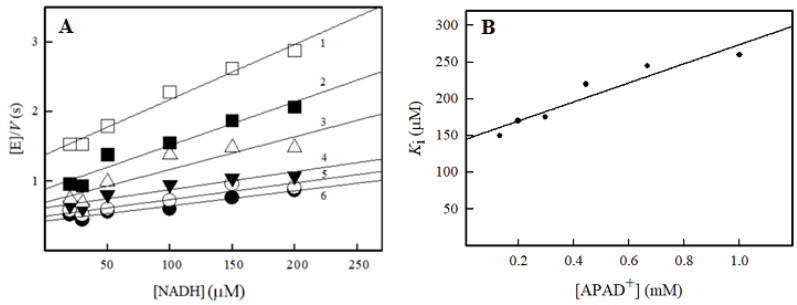

Fig. 42. A) The rates of TmTR-catalyzed reduction of APAD$^+$ by NADH, presented in Cleland coordinates. The concentrations of APAD$^+$: 1.0 mM (1), 0.67 mM (2), 0.44 mM (3), 0.30 mM (4), 0.20 mM (5), and 0.13 mM (6). B) Dependence of NADH substrate inhibition constant on APAD$^+$ concentration.

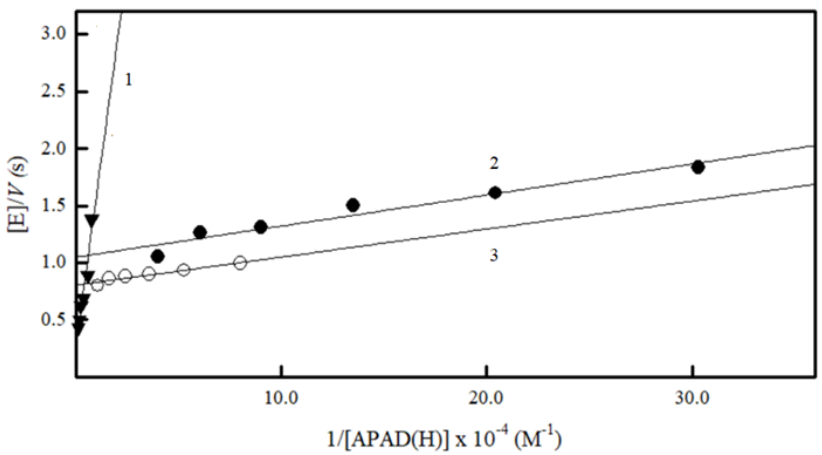

Fig. 43. The rates of reactions of APAD$^+$/APADH with TmTR: TmTR-catalyzed reduction of APAD$^+$ with NADH (1), TmTR-catalyzed oxidation of APADH with ferricyanide (2), and rapid reduction of TmTR with APADH (3).

4.2.5. Discussion

The present study discloses several important findings on the mechanism of catalysis and reduction of nonphysiological oxidants by TmTR;

a) The sequence similarity of intersubumit domains of TmTR and *E. coli* and *A. thaliana* TR, and FAD fluorescence studies (Fig. 35) suggest that the catalysis of TmTR involves the conformational changes similar to other TRs (Wang *et al.*, 1996; Mulrooney and Williams, 1997).

Table 6. The effects of binding of ligands on the fluorescence intensity of TR of various sources.

Enzyme source	Ligand				Reference
	3-AADP^{+a}	NAD(P)$^{+}$	2‘,5‘-ADP/ ADP-ribose	Trx/Grx	
E. coli	-75%	none[b]	n.d.	n.d.	Mulrooney and Williams, 1997
A. thaliana	-20%	+100%	+28%	+30%	Nivinskas *et al.*, 2001b
T. maritima	n.d.	-15%[c]	+30%[d]	+10%[e]	This work

[a]3-Aminopyridine adenine dinucleotide phosphate; [b]C.H. Williams, Jr., personal communication, [c]saturated NAD^{+} concentration 100 µM; [d]saturated ADP-ribose concentration 150 µM; [e]saturated Grx1 concentration 40 µM.

The effects of binding of ligands on the fluorescence intensity of TR of various sources are summarized in Table 6. The binding of Trx/Grx in the vicinity of the catalytic disulfide of TR may cause conformational change increasing the concentration of the fluorescent TR conformer. This is understandable from purely sterical reasons. The different effects of pyridine nucleotides and their analogues on FAD fluorescence may be

explained by the superposition of two opposite factors: i) increased content of fluorescent FR conformer upon binding of $AADP^+$, $NAD(P)^+$ or 2‘,5‘-ADP/ ADP-ribose, and ii) quenching of FAD fluorescence by pyridine ring of $AADP^+$ and $NAD(P)^+$. In our opinion, these effects are quantitative but not qualititative, and may be attributed to some differences in the relative positions of FAD and NAD(P)H-binding domains in enzymes from different sources (Dai *et al.*, 1996);

b) the E^0_7 value of FAD of TmTR, -0.230 V, is close to that of *E. coli* TR, -0.242÷-0.258 V (O‘Donnell and Williams, 1984), and *A. thaliana* TR, -0.244 V (Bironaitė *et al.,* 1998). One may note, that it is significantly higher than E^0_7 of catalytic disulfide of TmTR, -0.295 V (Couturier *et al.,* 2013). Although the mechanism of catalysis of TmTR is not studied in detail, the thermodynamically unfavorable hydride transfer from reduced FAD to catalytic disulfide may be one of the reasons for the slow reduction of Grx1 and other disulfide proteins;

c) although TmTR like other CS dehydrogenases-electrontransferases catalyze obligatory two-electron (hydride) transfer between NAD(P)H and their physiological disulfide oxidants, however, they perform mixed single- and two-electron reduction of quinones via their FAD cofactor. According to the values of k_{cat}/K_m of quinones, their relative reactivity is: yeast GR (Čėnas *et al.,* 1989) < *T. congolense* TryR (Čėnas *et al.,* 1994) < *A.thaliana* TR (Bironaitė *et al.,* 1998) ≤ rat TR (Čėnas *et al.,* 2004) ~ TmTR. However, TmTR reduces quinones and nitroaromatic compounds with higher maximal rates than *A. thaliana* or rat TR (Table 5). The comparison of presteady- and steady-state kinetic data of TmTR (Fig. 31,36, Table 5) shows that the oxidative half-reaction is rate-limiting in the catalysis, with a possible exception of 2,3-dichloro-1,4-naphthoquinone, 5-hydroxy-1,4-naphthoquinone, and 9,10-phenanthrene

quinone, where the reductive reaction may be partly rate-limiting. Thus, TmTR like the previously studied *A. thaliana* TR, may be considered as a potential target for redox active herbicides like 2,3-dichloro-1,4-naphthoquinone, the air pollution agent 9,10-phenanthrene quinone, and the explosives tetryl and TNT (Table 5), which are important soil and groundwater pollutants at their disposal sites (Bironaitė *et al.,* 1998; Miškinienė *et al.,* 1998; and references therein). These compounds may be considered as the "subversive substrates" for *T. maritima* TR because they convert the antioxidant functions of this enzyme into prooxidant ones due to their redox cycling. These reactions may be important in their action against *T. maritima* which, although anaerobic, can proliferate under low O_2 tension as well, and suffer from oxidative stress (Le Fourn *et al.,* 2008). These features may be even more important in view of the recently emerged interest in the use of *T. maritima* spp. in food, paper, biofuel-related applications, and in the synthesis of industrial chemicals (Frock *et al.,* 2010; Zeldes *et al.,* 2015). Although TmTR catalyzes mixed single-electron reduction of quinones and nitroaromatics, the use of *T. maritima* at elevated temperatures may enhance the formation of their two-electron reduction products due to a decreased O_2 concentration;

d) the dependence of reactivity of quinones and nitroaromatics on their E^1_7 and systematically lower reactivity of nitroaromatics (Fig. 31) is analogous to the regularities observed in the reactions of *A. thaliana* TR (Bironaitė *et al.,* 1998; Miškinienė *et al.,* 1998). This is in line with an "outer-sphere" electron transfer pathway (Marcus and Sutin, 1985), or with a mixed one- and two-electron transfer (e^-, H^+, e^-) with a rate limiting first electron transfer (Anusevičius *et al.,* 2005). In this case, the systematic lower reactivity of nitroaromatic compounds may be attributed to their lower single-electron self-exchange rate constants (Meotner and

Neta, 1986; Gramp and Jaenicke, 1987). This contrasts with the likewise single-step (H^-) hydride transfer in reactions of nitroreductases, and with their different substrate specificity (Fig. 17);

e) the data of Fig. 37B show that neutral FAD semiquinone is transiently accumulated during the TmTR-catalyzed reduction of quinone. It shows that the oxidation of $FADH^{\cdot}$ but not of $FADH_2$ may be a rate-limiting step in the reduction of quinones. On the other hand, it is also possible that the reaction is performed by several redox forms of TmTR, including $FADH_2$-NAD^+ complex absorbing at >700 nm (Fig. 37B) (Lennon and Williams, 1997). This may explain the complex character of inhibition of TmTR by NAD^+ and ADP-ribose (Fig. 38-41), which is consistent with the ligand binding at the oxidized and reduced enzyme forms, but also with a possibility of reoxidation by NAD^+. It seems that Scheme 4 and Eq. (26) do not completely describe the reduction of quinones and other nonphysiological oxidants by TmTR. Possibly, the relevant steps in catalysis, which may affect k_{cat}/K_m of oxidants, are also the conformational changes, induced by the ligand binding at NAD(H) binding site (Fig. 35). This probably can explain an uncommon effect of ADP-ribose on the kinetics of quinone reduction (Fig. 41).

In this aspect it is important to note, that although a member of H-TR group, rat thioredoxin reductase, and a structurally related disulfide reductase, TryR, reduce quinones in a mixed single- and two-electron way, FAD semiquinone is not formed in the course of these reactions (Čėnas *et al.,* 1994,2004). In these cases, quinones react with FAD-thiolate charge-transfer complex in the reduced enzyme form (Čėnas *et al.*, 1994,2004). It may follow that in the absence of efficient electronic coupling of FAD with catalytic disulfide/dithiolate like in L-TRs of *E.*

coli (Zanetti *et al.,* 1968) and *T. maritima*, the FAD cofactors in flavoenzymes C-S transhydrogenases may possess considerable semiquinone stability, in spite of obligatory two-electron reduction of their physiological disulfide oxidants. In addition, our findings provide an additional argument challenging the assumption on the obligatory formation of red (anionic) flavin semiquinones in dehydrogenases-transhydrogenases.

Summing up, the data of this work extend the relatively scarce information on the mechanisms and substrate specificity of quinone- and nitroreductase reactions of flavoenzymes dehydrogenases-transhydrogenases. The most credible mechanism of reduction of quinones and, presumably, nitroaromatics by NfsA is a single-step (H^-) hydride transfer, which also may take place in the reactions of group B NR of *E. cloacae* (Nivinskas *et al.,* 2001). However, the most credible mechanism of reduction of the above compounds by mammalian NQO1 is a three-step (e^-, H^+, e^-) hydride transfer (Anusevičius *et al.,* 1998, 2002; Misevičienė *et al.,* 2006). This may be explained by a relatively higher stability of anionic FAD semiquinone state in NQO1 (Tedeschi *et al.,* 1995; Haynes *et al.,* 2002). On the other hand, a mixed single- and two-electron character of reaction of TmTR may be explained by a significant stability of neutral FAD semiquinone in low m.m. TRs (Zanetti *et al.,* 1968). The existence of certain although opposite substrate specificity of NRs and NQO1 (Anusevičius *et al.,* 2002, and references therein) may be attributed to the binding of quinones and nitroaromatics close to the isoalloxazine ring of these enzymes, requiring significant displacement of certain amino acid residues and causing stacking interactions (Faig *et al.,* 2000). In contrast, the data on the reactions of TmTR and related *A.*

thaliana TR (Bironaitė *et al.,* 1998; Miškinienė *et al.,* 1998) with quinones and nitroaromatics point to a greater role of their electron-accepting potency rather to that of structural factors, and, possibly, weaker electronic interaction. Taken together, this shows that the existence of two-electron accepting physiological oxidants of dehydrogenases-transhydrogenases does not imply the two-electron character of reduction of quinones and nitroaromatic compounds. This diversity of mechanisms may expand the significance and areas of application of dehydrogenases-transhydrogenases in biomedicine and ecotoxicology.

CONCLUSIONS

1. Two-electron reduction of quinones and nitroaromatic compounds by *E. coli* nitroreductase A (NfsA) follows "ping-pong" kinetics. The rate-limiting step is the oxidative half-reaction.
2. The experimental data are most consistent with a single-step (H^-) hydride transfer mechanism in the reduction of quinones by NfsA. Substrate specificity of NfsA (selectivity for 2-hydroxy-1,4-naphthoquinones and higher reactivity of nitroaromatic compounds compared with quinones), is similar to that of group B *Enterobacter cloacae* nitroreductase.
3. The obtained data argue against significant involvement of NfsA in the second step of the reduction of nitroaromatic compounds to hydroxylamines (reduction of intermediate nitroso compounds), and for the major role of nitroso compound direct reduction by NADPH.

4. FMN semiquinone formation was not detected during photoreduction of NfsA. The determined E^0_7 value of FMN cofactor of NfsA (-0.215 V) is close to that of *E. cloacae* NR (-0.190 V).

5. *Thermotoga maritima* TR catalyzes mixed $1e^-$ and $2e^-$ reduction of quinones and nitroaromatic compounds. Reaction follows „ping-pong" kinetics with a rate-limiting oxidative half-reaction.

6. The reactivity of quinones and nitroaromatics in TmTR-catalyzed reduction increases with the increase in their single-electron reduction potential. The systematic lower reactivity of nitroaromatic compounds may be attributed to their lower single-electron self-exchange rate constants. Accumulation of FAD semiquinone ($FADH^\bullet$) during the TmTR-catalyzed reduction of quinones indicates that the oxidation of $FADH^\bullet$ may be a rate-limiting step in the reduction of quinones.

7. The redox potential of FAD of TmTR, -0.230 V, is close to redox potentials of other low molecular mass thioredoxin reductases.

REFERENCES

1. Anderson R. Energetics of the one-electron reduction steps of riboflavin, FMN and FAD to their fully reduced forms. *Biochim Biophys Acta.* 1983. 722:158-62. doi: 10.1016/0005-2728(83)90169-x.

2. Angermaier L, Simon H. On the reduction of aliphatic and aromatic nitro compounds by *Clostridia*, the role of ferredoxin and its stabilization. *Hoppe Seylers Z Physiol Chem.* 1983. 364:961-75. doi: 10.1515/bchm2.1983.364.2.961.

3. Anlezark G, Melton R, Sherwood R, Coles B, Friedlos F, Knox R. The bioactivation of 5-(aziridin-1-yl)-2,4-dinitrobenzamide (CB1954)--I. Purification and properties of a nitroreductase enzyme from *Escherichia coli*--a potential enzyme for antibody-directed enzyme prodrug therapy (ADEPT). *Biochem Pharmacol.* 1992. 44:2289-95. doi: 10.1016/0006-2952(92)90671-5.

4. Anusevičius Ž, Čėnas N. Dihydrolipoamide-mediated redox cycling of quinones. *Arch Biochem Biophys.* 1993. 302:420-4. doi: 10.1006/abbi.1993.1234.

5. Anusevičius Ž, Misevičienė L, Medina M, Martinez-Julvez M, Gomez-Moreno C, Čėnas N. FAD semiquinone stability regulates single- and two-electron reduction of quinones by *Anabaena* PCC7119 ferredoxin:$NADP^+$ reductase and its Glu301Ala mutant. *Arch Biochem Biophys.* 2005. 437:144-50. doi: 10.1016/j.abb.2005.03.015.

6. Anusevičius Ž, Misevičienė L, Šarlauskas J, Rouhier N, Jacquot JP, Čėnas N. Quinone- and nitroreductase reactions of *Thermotoga maritima* peroxiredoxin-nitroreductase hybrid enzyme. *Arch Biochem Biophys.* 2012. 528:50-6. doi: 10.1016/j.abb.2012.08.014.

7. Anusevičius Ž, Nivinskas H, Šarlauskas J, Sari MA, Boucher JL, Čėnas N. Single-electron reduction of quinone and nitroaromatic xenobiotics by recombinant rat neuronal nitric oxide synthase. *Acta Biochim Pol.* 2013. 60:217-22.

8. Anusevičius Ž, Šarlauskas J, Čėnas N. Two-electron reduction of quinones by rat liver NAD(P)H:quinone oxidoreductase: quantitative structure-activity relationships. *Arch Biochem Biophys.* 2002. 404:254-62. doi: 10.1016/s0003-9861(02)00273-4.

9. Anusevičius Ž, Šarlauskas J, Nivinskas H, Segura-Aguilar J, Čėnas N. DT-diaphorase catalyzes N-denitration and redox cycling of tetryl. *FEBS Lett.* 1998. 436:144-8. doi: 10.1016/s0014-5793(98)01115-6.

10. Anusevičius Ž, Soffers AE, Čėnas N, Šarlauskas J, Martinez-Julvez M, Rietjens IM. Quantitative structure activity relationships for the electron transfer reactions of *Anabaena* PCC 7119 ferredoxin-$NADP^+$ oxidoreductase with nitrobenzene and nitrobenzimidazolone derivatives: mechanistic implications. *FEBS Lett.* 1999. 450:44-8. doi: 10.1016/s0014-5793(99)00464-0.

11. Argyrou A, Blanchard JS, Palfey BA. The lipoamide dehydrogenase from *Mycobacterium tuberculosis* permits the direct observation of flavin intermediates in catalysis. *Biochemistry.* 2002. 41:14580-90. doi: 10.1021/bi020376k.

12. Arnér ES, Björnstedt M, Holmgren A. 1-Chloro-2,4-dinitrobenzene is an irreversible inhibitor of human thioredoxin reductase. Loss of thioredoxin disulfide reductase activity is accompanied by a large increase in NADPH oxidase activity. *J Biol Chem.* 1995. 270:3479-82. doi: 10.1074/jbc.270.8.3479.

13. Arnér ES, Holmgren A. Physiological functions of thioredoxin and thioredoxin reductase. *Eur J Biochem.* 2000. 267:6102-9. doi: 10.1046/j.1432-1327.2000.01701.x.

14. Arscott L, Gromer S, Schirmer R, Becker K, Williams CH Jr. The mechanism of thioredoxin reductase from human placenta is similar to the mechanisms of lipoamide dehydrogenase and glutathione reductase and is distinct from the mechanism of thioredoxin reductase from *Escherichia coli. Proc Natl Acad Sci U S A.* 1997. 94:3621-6. doi: 10.1073/pnas.94.8.3621.

15. Asher G, Dym O, Tsvetkov P, Adler J, Shaul Y. The crystal structure of NAD(P)H quinone oxidoreductase 1 in complex with its potent inhibitor dicoumarol. *Biochemistry*. 2006. 45:6372-8. doi: 10.1021/bi0600087.

16. Bai J, Zhou Y, Chen Q, Yang Q, Yang J. Altering the regioselectivity of a nitroreductase in the synthesis of arylhydroxylamines by structure-based engineering. *Chembiochem.* 2015. 16:1219-25. doi: 10.1002/cbic.201500070.

17. Barbey C, Rouhier N, Haouz A, Navaza A, Jacquot JP. Overproduction, purification, crystallization and preliminary X-ray analysis of the peroxiredoxin domain of a larger natural hybrid protein from *Thermotoga maritima. Acta Crystallogr Sect F Struct Biol Cryst Commun.* 2008. 64:29-31. doi:

18. Bauer H, Fritz-Wolf K, Winzer A, Kühner S, Little S, Yardley V, Vezin H, Palfey B, Schirmer RH, Davioud-Charvet E. A fluoro analogue of the menadione derivative 6-[2'-(3'-methyl)-1',4'-naphthoquinolyl]hexanoic acid is a suicide substrate of glutathione reductase. Crystal structure of the alkylated human enzyme. *J Am Chem Soc*. 2006. 128:10784-94. doi: 10.1021/ja061155v.

19. Beda N, Nedospasov A. A spectrophotometric assay for nitrate in an excess of nitrite. *Nitric Oxide.* 2005. 13:93-7. doi: 10.1016/j.niox.2005.05.002.

20. Belorgey D, Lanfranchi DA, Davioud-Charvet E. 1,4-naphthoquinones and other NADPH-dependent glutathione reductase-catalyzed redox cyclers as antimalarial agents. *Curr Pharm Des.* 2013. 19:2512-28. doi: 10.2174/1381612811319140003.

21. Berndt C, Lillig CH. Glutathione, Glutaredoxins, and Iron. *Antioxid Redox Signal.* 2017. 27:1235-1251. doi: 10.1089/ars.2017.7132.

22. Biaglow J, Miller R. The thioredoxin reductase/thioredoxin system: novel redox targets for cancer therapy. *Cancer Biol Ther.* 2005. 4:6-13. doi: 10.4161/cbt.4.1.1434.

23. Bianchet M, Faig M, Amzel L. Structure and mechanism of NAD[P]H:quinone acceptor oxidoreductases (NQO). *Methods Enzymol.* 2004. 382:144-74. doi: 10.1016/S0076-6879(04)82009-3.

24. Bironaitė D, Anusevičius Ž, Jacquot JP, Čėnas N. Interaction of quinones with *Arabidopsis thaliana* thioredoxin reductase. *Biochim Biophys Acta.* 1998. 1383:82-92. doi: 10.1016/s0167-4838(97)00190-8.

25. Bironaitė D, Čėnas N, Kulys J. The rotenone-insensitive reduction of quinones and nitrocompounds by mitochondrial NADH:ubiquinone reductase. *Biochim Biophys Acta.* 1991. 1060:203-9. doi: 10.1016/s0005-2728(09)91008-8.

26. Biterova E, Turanov A, Gladyshev V, Barycki J. Crystal structures of oxidized and reduced mitochondrial thioredoxin reductase provide molecular details of the reaction mechanism. *Proc Natl Acad Sci U S A.* 2005. 102:15018-23. doi: 10.1073/pnas.0504218102.

27. Björnstedt M, Hamberg M, Kumar S, Xue J, Holmgren A. Human thioredoxin reductase directly reduces lipid hydroperoxides by NADPH and selenocystine strongly stimulates the reaction via catalytically generated selenols. *J Biol Chem.* 1995. 270:11761-4. doi: 10.1074/jbc.270.20.11761.

28. Bohme C, Arscott L, Becker K, Schirmer R, Williams CH Jr. Kinetic characterization of glutathione reductase from the malarial parasite *Plasmodium falciparum.* Comparison with the human enzyme. *J Biol Chem.* 2000. 275:37317-23. doi: 10.1074/jbc.M007695200.

29. Boschi-Muller S, Gand A, Branlant G. The methionine sulfoxide reductases: Catalysis and substrate specificities. *Arch Biochem Biophys.* 2008. 474:266-73. doi: 10.1016/j.abb.2008.02.007.

30. Bryant D, McCalla D, Leeksma M, Laneuville P. Type I nitroreductases of *Escherichia coli*. *Can J Microbiol.* 1981. 27:81-6. doi: 10.1139/m81-013.

31. Buchanan BB, Schürmann P, Jacquot JP. Thioredoxin and metabolic regulation. *Semin Cell Biol.* 1994. 5:285-93. doi: 10.1006/scel.1994.1035.

32. Bulger J, Brandt K. Yeast glutathione reductase. II. Interaction of oxidized and 2-electron reduced enzyme with reduced and oxidized nicotinamide adenine dinucleotide phosphate. *J Biol Chem.* 1971. 246:5578-87.

33. Carlson B, Miller L, Neta P, Grodkowski J. Oxidation of NADH involving rate-limiting one-electron transfer. *J. Am. Chem. Soc,* 1984. 106:7233–7239.

34. Carlson B, Miller L. Mechanism of the oxidation of NADH by quinones. Energetics of one-electron and hydride routes. *J. Am. Chem. Soc*. 1985. 107:479–485.

35. Čėnas N, Anusevičius Ž, Bironaitė D, Bachmanova GI, Archakov AI, Ollinger K. The electron transfer reactions of NADPH: cytochrome P450 reductase with nonphysiological oxidants. *Arch Biochem Biophys.* 1994. 315:400-6. doi: 10.1006/abbi.1994.1517.

36. Čėnas N, Anusevicius Ž, Nivinskas H, Misevičienė L, Šarlauskas J. Structure-activity relationships in two-electron reduction of quinones. *Methods Enzymol.* 2004a. 382:258-77. doi: 10.1016/S0076-6879(04)82015-9.

37. Čėnas N, Arscott D, Williams CH Jr, Blanchard JS. Mechanism of reduction of quinones by *Trypanosoma congolense* trypanothione reductase. *Biochemistry.* 1994. 33:2509-15. doi: 10.1021/bi00175a021.

38. Čėnas N, Nemeikaitė-Čėnienė A, Šarlauskas J, Anusevičius Ž, Nivinskas H, Misevičienė L, Marozienė A. Mechanisms of the mammalian cell cytotoxicity of explosives. In: *Ecotoxicology of explosives. Sunahara GI, Lotufo G, Kuperman RG, Hawari J, eds. CRC Press, Boca Raton, London, New York.* 2009. 211-227

39. Čėnas N, Nivinskas H, Anusevičius Ž, Šarlauskas J, Lederer F, Arnér ES. Interactions of quinones with thioredoxin reductase: a challenge to the antioxidant role of the mammalian selenoprotein. *J Biol Chem.* 2004b. 279:2583-92. doi: 10.1074/jbc.M310292200.

40. Čėnas N, Prast S, Nivinskas H, Šarlauskas J, Arnér ES. Interactions of nitroaromatic compounds with the mammalian selenoprotein thioredoxin reductase and the relation to induction of apoptosis in human cancer cells. *J Biol Chem.* 2006. 281:5593-603. doi: 10.1074/jbc.M511972200.

41. Čėnas N, Rakauskienė G, Kulys J. One- and two-electron reduction of quinones by glutathione reductase. *Biochim Biophys Acta.* 1989. 973:399-404. doi: 10.1016/s0005-2728(89)80381-0.

42. Chatterjee P, Sternberg N. A general genetic approach in *Escherichia coli* for determining the mechanism(s) of action of tumoricidal agents: application to DMP 840, a tumoricidal agent. *Proc Natl Acad Sci U S A.* 1995. 92:8950-4. doi: 10.1073/pnas.92.19.8950.

43. Chen S, Wu K, Zhang D, Sherman M, Knox R, Yang CS. Molecular characterization of binding of substrates and inhibitors to DT-diaphorase: combined approach involving site-directed mutagenesis, inhibitor-binding analysis, and computer modeling. *Mol Pharmacol.* 1999. 56:272-8. doi: 10.1124/mol.56.2.272.

44. Cleland W. Steady State Kinetics. *The Enzymes*. 1970. 2:1-65

45. Copp J, Mowday A, Williams E, Guise C, Ashoorzadeh A, Sharrock A, Flanagan J, Smaill J, Patterson A, Ackerley D. Engineering a Multifunctional Nitroreductase for Improved Activation of Prodrugs and PET Probes for Cancer Gene Therapy. *Cell Chem Biol.* 2017. 24:391-403. doi: 10.1016/j.chembiol.2017.02.005.

46. Couturier J, Prosper P, Winger AM, Hecker A, Hirasawa M, Knaff DB, Gans P, Jacquot JP, Navaza A, Haouz A, Rouhier N. In the absence of thioredoxins, what are the reductants for peroxiredoxins in *Thermotoga maritima? Antioxid Redox Signal*. 2013. 18:1613-22. doi: 10.1089/ars.2012.4739.

47. Dachs G, Hunt M, Syddall S, Singleton D, Patterson A. Bystander or no bystander for gene directed enzyme prodrug therapy. *Molecules.* 2009. 14:4517-45. doi: 10.3390/molecules14114517.

48. Dai S, Saarinen M, Ramaswamy S, Meyer Y, Jacquot JP, Eklund H. Crystal structure of *Arabidopsis thaliana* NADPH dependent

thioredoxin reductase at 2.5 Å resolution. *J Mol Biol.* 1996. 264:1044-57. doi: 10.1006/jmbi.1996.0695.

49. Danson S, Ward TH, Butler J, Ranson M. DT-diaphorase: a target for new anticancer drugs. *Cancer Treat Rev.* 2004. 30:437-49. doi: 10.1016/j.ctrv.2004.01.002.

50. Darchen A, Moinet C. Mecanisme e.c.e. de reduction du para-dinitrobenzene en para-nitrophenyhydroxylamine. *Journal of Electroan Chem and Interf Electrochem*. 1977. 78:81-88.

51. De Oliveira I, Zanotto-Filho A, Moreira JC, Bonatto D, Henriques J. The role of two putative nitroreductases, Frm2p and Hbn1p, in the oxidative stress response in *Saccharomyces cerevisiae*. *Yeast*. 2010. 27:89-102. doi: 10.1002/yea.1734.

52. Decottignies P, Schmitter JM, Dutka S, Jacquot JP, Miginiac-Maslow M. Characterization and primary structure of a second thioredoxin from the green alga, *Chlamydomonas reinhardtii*. *Eur J Biochem.* 1991. 198:505-12. doi: 10.1111/j.1432-1033.1991.tb16043.x.

53. Faig M, Bianchet MA, Talalay P, Chen S, Winski S, Ross D, Amzel LM. Structures of recombinant human and mouse NAD(P)H:quinone oxidoreductases: species comparison and structural changes with substrate binding and release. *Proc Natl Acad Sci U S A.* 2000. 97:3177-82. doi: 10.1073/pnas.050585797.

54. Fairlamb AH, Cerami A. Metabolism and functions of trypanothione in the *Kinetoplastida*. *Annu Rev Microbiol.* 1992. 46:695-729. doi: 10.1146/annurev.mi.46.100192.003403.

55. Faro M, Gómez-Moreno C, Stankovich M, Medina M. Role of critical charged residues in reduction potential modulation of ferredoxin-$NADP^+$ reductase. *Eur J Biochem.* 2002. 269:2656-61. doi: 10.1046/j.1432-1033.2002.02925.x.

56. Fasco M, Principe L. Vitamin K1 hydroquinone formation catalyzed by DT-diaphorase. *Biochem Biophys Res Commun.* 1982. 104:187-92. doi: 10.1016/0006-291x(82)91957-x.

57. Florencio F, Yee B, Johnson T, Buchanan BB. An NADP/thioredoxin system in leaves: purification and characterization of NADP-thioredoxin reductase and thioredoxin h from spinach. *Arch Biochem Biophys.* 1988. 266:496-507. doi: 10.1016/0003-9861(88)90282-2.

58. Frock AD, Notey JS, Kelly RM. The genus *Thermotoga*: recent developments. *Environ Technol.* 2010. 31:1169-81. doi: 10.1080/09593330.2010.484076.

59. Fukuzumi S, Ishikawa M, Tanaka T. Acid-catalysed reduction of p-benzoquinone derivatives by an NADH analoque, 9,10-dihydro-10-methylacridine. The energetic comparison of one-electron vs. two-electron path-ways. *J Chem Soc. Perk. Trans.* 1989. 2:1811–1816.

60. Fukuzumi S, Ohkubo K, Tokuda Y, Suenobu T. Hydride Transfer from 9-Substituted 10-Methyl-9,10-dihydroacridines to Hydride Acceptors via Charge-Transfer Complexes and Sequential Electron−Proton−Electron Transfer. A Negative Temperature Dependence of the Rates. *J. Am. Chem. Soc.* 2000. 122: 4286–4294.

61. Gon S, Faulkner MJ, Beckwith J. *In vivo* requirement for glutaredoxins and thioredoxins in the reduction of the ribonucleotide reductases of *Escherichia coli. Antioxid Redox Signal.* 2006. 8:735-42. doi: 10.1089/ars.2006.8.735.

62. Grampp G, Jaenicke W. ESR-spectroscopic investigation of the parallel electron and proton exchange between quinones and their radicals: Part I. Measurements at 298 K. *J. Electroanal. Chem.* 1987. 229:297–303.

63. Grellier P, Marozienė A, Nivinskas H, Šarlauskas J, Aliverti A, Čėnas N. Antiplasmodial activity of quinones: roles of aziridinyl substituents and the inhibition of *Plasmodium falciparum* glutathione reductase. *Arch Biochem Biophys.* 2010. 494:32-9. doi: 10.1016/j.abb.2009.11.012. Epub 2009 Nov 15.

64. Grove J, Lovering A, Guise C, Race P, Wrighton C, White S, Hyde E, Searle P. Generation of *Escherichia coli* nitroreductase mutants conferring improved cell sensitization to the prodrug CB1954. *Cancer Res.* 2003. 63:5532-7.

65. HaÏdour A, Ramos JL. Identification of Products Resulting from the Biological Reduction of 2,4,6-Trinitrotoluene, 2,4-Dinitrotoluene, and 2,6-Dinitrotoluene by *Pseudomonas sp*. *Environ. Sci. Technol.* 1996. 30:2365–2370.

66. Hargreaves RH, Hartley JA, Butler J. Mechanisms of action of quinone-containing alkylating agents: DNA alkylation by aziridinylquinones. *Front Biosci.* 2000. 5:172-80. doi: 10.2741/hargreav.

67. Haynes C, Koder RL, Miller AF, Rodgers D. Structures of nitroreductase in three states: effects of inhibitor binding and reduction. *J Biol Chem.* 2002. 277:11513-20. doi: 10.1074/jbc.M111334200.

68. Hemmerich P, Massey V. Flavin and 5-deazaflavin: a chemical evaluation of 'modified' flavoproteins with respect to the mechanisms of redox biocatalysis. *FEBS Lett.* 1977. 84:5-21. doi: 10.1016/0014-5793(77)81047-8.

69. Hemmerich P, Massey V. In: *Proceedings of the 3rd International Symposium on Oxidases and Related Systems (King, T.E., ed.), Albany, New York.* 1979. 1-13.

70. Henderson R, Pickrell J, Jones R, Sun J, Benson J, Mauderly J, McClellan R. Response of rodents to inhaled diluted diesel exhaust:

biochemical and cytological changes in bronchoalveolar lavage fluid and in lung tissue. *Fundam Appl Toxicol.* 1988. 11:546-67. doi: 10.1016/0272-0590(88)90119-4.

71. Hirt R, Müller S, Embley T, Coombs G. The diversity and evolution of thioredoxin reductase: new perspectives. *Trends Parasitol.* 2002. 18:302-8. doi: 10.1016/s1471-4922(02)02293-6.

72. Ho YS, Xiong Y, Ho DS, Gao J, Chua BH, Pai H, Mieyal JJ. Targeted disruption of the glutaredoxin 1 gene does not sensitize adult mice to tissue injury induced by ischemia/reperfusion and hyperoxia. *Free Radic Biol Med.* 2007. 43:1299-312. doi:10.1016/j.freeradbiomed.2007.07.025.

73. Holmgren A. The function of thioredoxin and glutathione in deoxyribonucleic acid synthesis. *Biochem Soc Trans.* 1977. 5:611-2. doi: 10.1042/bst0050611.

74. Holmgren A. Thioredoxin and glutaredoxin systems. *J Biol Chem.* 1989. 264:13963-6.

75. Holtzman J, Crankshaw D, Peterson F, Polnaszek C. The kinetics of the aerobic reduction of nitrofurantoin by NADPH-cytochrome P-450 *c* reductase. *Mol Pharmacol.* 1981. 20:669-73.

76. Hu L, Yu C, Jiang Y, Han J, Li Z, Browne P, Race P, Knox R, Searle P, Hyde E. Nitroaryl phosphoramides as novel prodrugs for *E. coli* nitroreductase activation in enzyme prodrug therapy. *J Med Chem.* 2003. 46:4818-21. doi: 10.1021/jm034133h.

77. Hubig S, Rathore R, Kochi J. Steric Control of Electron Transfer. Changeover from Outer-Sphere to Inner-Sphere Mechanisms in Arene/Quinone Redox Pairs. *J. Am. Chem. Soc.* 1999. 121: 617–626.

78. Iyanagi T, Watanabe S, Anan KF. One-electron oxidation-reduction properties of hepatic NADH-cytochrome b5 reductase. *Biochemistry.* 1984. 23:1418-25. doi: 10.1021/bi00302a013.

79. Iyanagi T, Yamazaki I. One-electron-transfer reactions in biochemical systems. 3. One-electron reduction of quinones by microsomal flavin enzymes. *Biochim Biophys Acta.* 1969. 172:370-81. doi: 10.1016/0005-2728(69)90133-9.

80. Iyanagi T, Yamazaki I. One-electron-transfer reactions in biochemical systems. V. Difference in the mechanism of quinone reduction by the NADH dehydrogenase and the NAD(P)H dehydrogenase (DT-diaphorase). *Biochim Biophys Acta.* 1970. 216:282-94. doi: 10.1016/0005-2728(70)90220-3.

81. Iyanagi T. On the mechanism of one-electron reduction of quinones by microsomal flavin enzymes: the kinetic analysis between cytochrome B5 and menadione. *Free Radic Res Commun.* 1990. 8:259-68. doi: 10.3109/10715769009053359.

82. Jacquot JP, Rivera-Madrid R, Marinho P, Kollarova M, Le Maréchal P, Miginiac-Maslow M, Meyer Y. *Arabidopsis thaliana* NAPHP thioredoxin reductase. cDNA characterization and expression of the recombinant protein in *Escherichia coli*. *J Mol Biol.* 1994. 235:1357-63. doi: 10.1006/jmbi.1994.1091.

83. Jameson M, Rischin D, Pegram M, Gutheil J, Patterson A, Denny W, Wilson W. A phase I trial of PR-104, a nitrogen mustard prodrug activated by both hypoxia and aldo-keto reductase 1C3, in patients with solid tumors. *Cancer Chemother Pharmacol.* 2010. 65:791-801. doi: 10.1007/s00280-009-1188-1.

84. Jarrom D, Jaberipour M, Guise CP, Daff S, White SA, Searle P, Hyde E. Steady-state and stopped-flow kinetic studies of three

Escherichia coli NfsB mutants with enhanced activity for the prodrug CB1954. *Biochemistry.* 2009. 48:7665-72. doi: 10.1021/bi900674m.

85. Jeon SJ, Ishikawa K. Characterization of novel hexadecameric thioredoxin peroxidase from *Aeropyrum pernix* K1. *J Biol Chem.* 2003. 278:24174-80. doi: 10.1074/jbc.M300618200.

86. Jiménez A, Pelto-Huikko M, Gustafsson JA, Miranda-Vizuete A. Characterization of human thioredoxin-like-1: potential involvement in the cellular response against glucose deprivation. *FEBS Lett.* 2006. 580:960-7. doi: 10.1016/j.febslet.2006.01.025.

87. Johansson E, Parkinson GN, Denny WA, Neidle S. Studies on the nitroreductase prodrug-activating system. Crystal structures of complexes with the inhibitor dicoumarol and dinitrobenzamide prodrugs and of the enzyme active form. *J Med Chem.* 2003. 46:4009-20. doi: 10.1021/jm030843b.

88. Kanzok SM, Schirmer RH, Turbachova I, Iozef R, Becker K. The thioredoxin system of the malaria parasite *Plasmodium falciparum.* Glutathione reduction revisited. *J Biol Chem.* 2000. 275:40180-6. doi: 10.1074/jbc.M007633200.

89. Kaplan N, Ciotti M. Chemistry and properties of the 3-acetylpyridine analogue of diphosphopyridine nucleotide. *J Biol Chem.* 1956. 221:823-32.

90. Karplus P, Pai EF, Schulz GE. A crystallographic study of the glutathione binding site of glutathione reductase at 0.3-nm resolution. *Eur J Biochem.* 1989. 178:693-703. doi: 10.1111/j.1432-1033.1989.tb14500.x.

91. Knox R, Burke P, Chen S, Kerr D. CB 1954: from the Walker tumor to NQO2 and VDEPT. *Curr Pharm Des.* 2003. 26:2091-104. doi: 10.2174/1381612033454108.

92. Knox R, Friedlos F, Sherwood R, Melton R, Anlezark G. The bioactivation of 5-(aziridin-1-yl)-2,4-dinitrobenzamide (CB1954)--II. A comparison of an *Escherichia coli* nitroreductase and Walker DT diaphorase. *Biochem Pharmacol.* 1992. 44:2297-301. doi: 10.1016/0006-2952(92)90672-6.

93. Kobori T, Sasaki H, Lee WC, Zenno S, Saigo K, Murphy M, Tanokura M. Structure and site-directed mutagenesis of a flavoprotein from *Escherichia coli* that reduces nitrocompounds: alteration of pyridine nucleotide binding by a single amino acid substitution. *J Biol Chem.* 2001. 276:2816-23. doi: 10.1074/jbc.M002617200.

94. Koder R, Haynes C, Rodgers M, Rodgers D, Miller AF. Flavin thermodynamics explain the oxygen insensitivity of enteric nitroreductases. *Biochemistry*. 2002. 48:14197-205. doi: 10.1021/bi025805t.

95. Koder R, Miller AF. Steady-state kinetic mechanism, stereospecificity, substrate and inhibitor specificity of *Enterobacter cloacae* nitroreductase. *Biochim Biophys Acta.* 1998.1387:395-405. doi: 10.1016/s0167-4838(98)00151-4.

96. Koike H, Sasaki H, Kobori T, Zenno S, Saigo K, Murphy ME, Adman ET, Tanokura M. 1.8 Å crystal structure of the major NAD(P)H:FMN oxidoreductase of a bioluminescent bacterium, *Vibrio fischeri*: overall structure, cofactor and substrate-analog binding, and comparison with related flavoproteins. *J Mol Biol.* 1998. 280:259-73. doi: 10.1006/jmbi.1998.1871.

97. Kovacic P, Kassel M, Feinberg B, Corbett M, McClelland R. Reduction potentials in relation to physiological activities of benzenoid and heterocyclic nitroso compounds: Comparison with the nitro precursors. *Bioorganic Chemistry*. 1990. 18: 265-275.

98. Krone F, Westphal G, Meyer HE, Schwenn J. PAPS-reductase of *Escherichia coli*. Correlating the N-terminal amino acid sequence with the DNA of gene *cys H*. *FEBS Lett.* 1990. 260:6-9. doi: 10.1016/0014-5793(90)80052-k.

99. Kumagai Y, Nakajima H, Midorikawa K, Homma-Takeda S, Shimojo N. Inhibition of nitric oxide formation by neuronal nitric oxide synthase by quinones: nitric oxide synthase as a quinone reductase. *Chem Res Toxicol.* 1998. 11:608-13. doi: 10.1021/tx970119u.

100. Kuriyan J, Kong X, Krishna T, Sweet R, Murgolo N, Field H, Cerami A, Henderson G. X-ray structure of trypanothione reductase from *Crithidia fasciculata* at 2.4-A resolution. *Proc Natl Acad Sci U S A.* 1991. 88:8764-8. doi: 10.1073/pnas.88.19.8764.

101. Ladenstein R, Ren B. Protein disulfides and protein disulfide oxidoreductases in hyperthermophiles. *FEBS J.* 2006. 273(18):4170-85. doi: 10.1111/j.1742-4658.2006.05421.x.

102. Ladenstein R, Ren B. Reconsideration of an early dogma, saying "there is no evidence for disulfide bonds in proteins from archaea". *Extremophiles.* 2008. 12:29-38. doi: 10.1007/s00792-007-0076-z.

103. Le Fourn C, Fardeau ML, Ollivier B, Lojou E, Dolla A. The hyperthermophilic anaerobe *Thermotoga maritim*a is able to cope with limited amount of oxygen: insights into its defence strategies. *Environ Microbiol.* 2008. 10:1877-87. doi: 10.1111/j.1462-2920.2008.01610.x.

104. Lei B, Liu M, Huang S, Tu SC. *Vibrio harveyi* NADPH-flavin oxidoreductase: cloning, sequencing and overexpression of the gene and purification and characterization of the cloned enzyme. *J Bacteriol.* 1994. 76:3552-8. doi: 10.1128/jb.176.12.3552-3558.1994.

105. Lei B, Wang H, Yu Y, Tu SC. Redox potential and equilibria in the reductive half-reaction of *Vibrio harveyi* NADPH-FMN oxidoreductase. *Biochemistry.* 2005. 44:261-7. doi: 10.1021/bi047952s.

106. Lennon BW, Williams CH Jr, Ludwig ML. Crystal structure of reduced thioredoxin reductase from *Escherichia coli:* structural flexibility in the isoalloxazine ring of the flavin adenine dinucleotide cofactor. *Protein Sci*. 1999. 8:2366-79. doi: 10.1110/ps.8.11.2366.

107. Lennon BW, Williams CH Jr. Enzyme-monitored turnover of *Escherichia coli* thioredoxin reductase: insights for catalysis. *Biochemistry.* 1996. 35:4704-12. doi: 10.1021/bi952521i.

108. Lennon BW, Williams CH Jr. Reductive half-reaction of thioredoxin reductase from *Escherichia coli.* Biochemistry. 1997. 36:9464-77. doi: 10.1021/bi970307j.

109. Leskovac V, Svircević J, Trivić S, Popović M, Radulović M. Reduction of aryl-nitroso compounds by pyridine and flavin coenzymes. *Int J Biochem.* 1989. 21:825-34. doi: 10.1016/0020-711x(89)90279-6.

110. Li R, Bianchet MA, Talalay P, Amzel LM. The three-dimensional structure of NAD(P)H:quinone reductase, a flavoprotein involved in cancer chemoprotection and chemotherapy: mechanism of the two-electron reduction. *Proc Natl Acad Sci U S A.* 1995. 92:8846-50. doi: 10.1073/pnas.92.19.8846.

111. Liang W, Fernandes AP, Holmgren A, Li X, Zhong L. Bacterial thioredoxin and thioredoxin reductase as mediators for epigallocatechin 3-gallate-induced antimicrobial action. *FEBS J*. 2016. 283:446-58. doi: 10.1111/febs.13587.

112. Lind C, Cadenas E, Hochstein P, Ernster L. DT-diaphorase: purification, properties, and function. *Methods Enzymol.* 1990. 186:287-301. doi: 10.1016/0076-6879(90)86122-c.

113. Lönn ME, Hudemann C, Berndt C, Cherkasov V, Capani F, Holmgren A, Lillig CH. Expression pattern of human glutaredoxin 2 isoforms: identification and characterization of two testis/cancer cell-specific isoforms. *Antioxid Redox Signal.* 2008. 10:547-57. doi: 10.1089/ars.2007.1821.

114. Lovering A, Hyde E, Searle P, White S. The structure of *Escherichia coli* nitroreductase complexed with nicotinic acid: three crystal forms at 1.7 Å, 1.8 Å and 2.4 Å resolution. *J Mol Biol.* 2001. 309:203-13. doi: 10.1006/jmbi.2001.4653.

115. Malik G, Nagy N, Ho YS, Maulik N, Das D. Role of glutaredoxin-1 in cardioprotection: an insight with Glrx1 transgenic and knockout animals. *J Mol Cell Cardiol.* 2008. 44:261-9. doi: 10.1016/j.yjmcc.2007.08.022.

116. Marcus R, Sutin, N. Electron transfers in chemistry and biology. *Biochim. Biophys. Acta.* 1985. 811:265-322.

117. Marozienė A, Kliukienė R, Šarlauskas J, Čėnas N. Methemoglobin formation in human erythrocytes by nitroaromatic explosives. *Z Naturforsch C J Biosci*. 2001. 56:1157-63.

118. Masullo M, Raimo G, Dello Russo A, Bocchini V, Bannister JV. Purification and characterization of NADH oxidase from the archaea *Sulfolobus acidocaldarius* and *Sulfolobus solfataricus*. *Biotechnol Appl Biochem.* 1996. 23:47-54.

119. Matsuda H, Kimura S, Iyanagi T. One-electron reduction of quinones by the neuronal nitric-oxide synthase reductase domain. *Biochim Biophys Acta.* 2000. 1459:106-16. doi: 10.1016/s0005-2728(00)00117-1.

120. Matthews R, Ballou DP, Williams CH Jr. Reactions of pig heart lipoamide dehydrogenase with pyridine nucleotides. Evidence for an

effector role for bound oxidized pyridine nucleotide. *J Biol Chem.* 1979. 254:4974-81.

121. Matthews R, Williams CH Jr. Measurement of the oxidation-reduction potentials for two-electron and four-electron reduction of lipoamide dehydrogenase from pig heart. *J Biol Chem.* 1976. 251:3956-64.

122. McKeown S, Cowen R, Williams K. Bioreductive drugs: from concept to clinic. *Clin Oncol (R Coll Radiol)*. 2007. 19:427-42. doi: 10.1016/j.clon.2007.03.006.

123. Meotner M, Neta P. Kinetics of Electron Transfer from Nitroaromatic Radical Anions in Aqueos Solutions. Effects of Temperature and Steric Configuration. *J. Phys. Chem.* 1986. 90:4648–4650.

124. Meyer Y, Buchanan BB, Vignols F, Reichheld JP. Thioredoxins and glutaredoxins: unifying elements in redox biology. *Annu Rev Genet.* 2009. 43:335-67. doi: 10.1146/annurev-genet-102108-134201

125. Misevičienė L, Anusevičius Ž, Šarlauskas J, Čėnas N. Reduction of nitroaromatic compounds by NAD(P)H:quinone oxidoreductase (NQO1): the role of electron-accepting potency and structural parameters in the substrate specificity. *Acta Biochim Pol.* 2006. 53:569-76.

126. Miškinienė V, Šarlauskas J, Jacquot JP, Čėnas N. Nitroreductase reactions of *Arabidopsis thaliana* thioredoxin reductase. *Biochim Biophys Acta*. 1998. 1366:275-83. doi: 10.1016/s0005-2728(98)00128-5.

127. Mowday A, Ashoorzadeh A, Williams E, Copp J, Silva S, Bull R, Abbattista M, Anderson R, Flanagan J, Guise C, Ackerley D, Smaill J, Patterson A. Rational design of an AKR1C3-resistant analog of PR-104 for enzyme-prodrug therapy. *Biochem Pharmacol*. 2016. 116:176-87. doi: 10.1016/j.bcp.2016.07.015.

128. Mulrooney S, Williams CH Jr. Evidence for two conformational states of thioredoxin reductase from *Escherichia coli:* use of intrinsic and extrinsic quenchers of flavin fluorescence as probes to observe domain rotation. *Protein Sci.* 1997. 6:2188-95. doi: 10.1002/pro.5560061013.

129. Nagy N, Malik G, Tosaki A, Ho YS, Maulik N, Das DK. Overexpression of glutaredoxin-
2 reduces myocardial cell death by preventing both apoptosis and necrosi
s. *J Mol Cell Cardiol.* 2008. 44:252-60. doi: 10.1016/j.yjmcc.2007.08.021.

130. Nauser T, Dockheer S, Kissner R, Koppenol WH. Catalysis of electron transfer by selenocysteine. *Biochemistry.* 2006. 45:6038-43. doi: 10.1021/bi0602260.

131. Nelson KE, Clayton RA, Gill SR, Gwinn ML, Dodson RJ, Haft DH, Hickey EK, Peterson JD, Nelson WC, Ketchum KA, McDonald L, Utterback TR, Malek JA, Linher KD, Garrett MM, Stewart AM, Cotton MD, Pratt MS, Phillips CA, Richardson D, Heidelberg J, Sutton GG, Fleischmann RD, Eisen JA, White O, Salzberg SL, Smith HO, Venter JC, Fraser CM. Evidence for lateral gene transfer between *Archaea* and bacteria from genome sequence of *Thermotoga maritima. Nature.* 1999. 399:323-9. doi: 10.1038/20601.

132. Nemeikaitė-Čėnienė A, Šarlauskas J, Anusevičius Ž, Nivinskas H, Čėnas N. Cytotoxicity of RH1 and related aziridinylbenzoquinones: involvement of activation by NAD(P)H:quinone oxidoreductase (NQO1) and oxidative stress. *Arch Biochem Biophys.* 2003. 416:110-8. doi: 10.1016/s0003-9861(03)00281-9.

133. Neta P, Simic M, Hoffman M. Pulse radiolysis and electron spin resonance studies of nitroaromatic radical anions . Optical absorption

spectra, kinetics and one-electron redox potentials. *The Journal of Physic Chem.* 1976. 80:2018-2023. doi: 10.1021/j100559a014

134. Nivinskas H, Jacquot JP, Čėnas N. Conformational change of *Arabidopsis thaliana* thioredoxin reductase after binding of pyridine nucleotide and thioredoxin. *Z Naturforsch C J Biosci.* 2001b. 56:188-92. doi: 10.1515/znc-2001-3-404.

135. Nivinskas H, Koder R, Anusevičius Ž, Šarlauskas J, Miller AF, Čėnas N. Quantitative structure-activity relationships in two-electron reduction of nitroaromatic compounds by *Enterobacter cloacae* NAD(P)H:nitroreductase. *Arch Biochem Biophys*. 2001a. 385:170-8. doi: 10.1006/abbi.2000.2127.

136. Nivinskas H, Staškevičienė S, Šarlauskas J, Koder RL, Miller AF, Čėnas N. Two-electron reduction of quinones by *Enterobacter cloacae* NAD(P)H:nitroreductase: quantitative structure-activity relationships. *Arch Biochem Biophys.* 2002. 403:249-58. doi: 10.1016/s0003-9861(02)00228-x.

137. Nivinskas H, Valiauga B, Šarlauskas J, Čėnas N. Reduction of aziridyl-substituted anticancer benzoquinones by lipoamide dehydrogenase. *Chemija.* 2014. 25:213–217.

138. Nonn L, Williams RR, Erickson RP, Powis G. The absence of mitochondrial thioredoxin 2 causes massive apoptosis, exencephaly, and early embryonic lethality in homozygous mice. *Mol Cell Biol.* 2003. 23:916-22. doi: 10.1128/mcb.23.3.916-922.2003.

139. Nordberg J, Arnér ES. Reactive oxygen species, antioxidants, and the mammalian thioredoxin system. *Free Radic Biol Med.* 2001. 31:1287-312. doi: 10.1016/s0891-5849(01)00724-9.

140. Nunoshiba T, Demple B. Potent intracellular oxidative stress exerted by the carcinogen 4-nitroquinoline-N-oxide. *Cancer Res.* 1993. 53:3250-2.

141. Oblong J, Gasdaska P, Sherrill K, Powis G. Purification of human thioredoxin reductase: properties and characterization by absorption and circular dichroism spectroscopy. *Biochemistry.* 1993. 32:7271-7. doi: 10.1021/bi00079a025.

142. O'Brien PJ. Molecular mechanisms of quinone cytotoxicity. *Chem Biol Interact.* 1991. 80:1-41. doi: 10.1016/0009-2797(91)90029-7.

143. O'Donnell ME, Williams CH Jr. Graphical analysis of interactions between oxidation-reduction sites in two site oxidation-reduction proteins. *Anal Biochem.* 1984. 136:235-46. doi: 10.1016/0003-2697(84)90330-0.

144. Olive P, Durand R. Fluorescent nitroheterocycles for identifying hypoxic cells. *Cancer Res.* 1983. 43:3276-80.

145. Orna M, Mason R. Correlation of kinetic parameters of nitroreductase enzymes with redox properties of nitroaromatic compounds. *J Biol Chem.* 1989. 264:12379-84.

146. Pai EF, Schulz GE. The catalytic mechanism of glutathione reductase as derived from x-ray diffraction analyses of reaction intermediates. *J Biol Chem.* 1983. 258:1752-7.

147. Parkinson G, Skelly J, Neidle S. Crystal structure of FMN-dependent nitroreductase from *Escherichia coli* B: a prodrug-activating enzyme. *J Med Chem.* 2000. 43:3624-31. doi: 10.1021/jm000159m.

148. Paterson E, Boucher S, Lambert I. Regulation of the nfsA Gene in *Escherichia coli* by SoxS. *J Bacteriol*. 2002. 184:51-8. doi: 10.1128/jb.184.1.51-58.2002.

149. Peterson F, Mason R, Hovsepian J, Holtzman J. Oxygen-sensitive and -insensitive nitroreduction by *Escherichia coli* and rat hepatic microsomes. *J Biol Chem*. 1979. 254:4009-14.

150. Pitsawong W, Haynes C, Koder R Jr, Rodgers D, Miller AF. Mechanism-Informed Refinement Reveals Altered Substrate-Binding Mode for Catalytically Competent Nitroreductase. *Structure*. 2017. 25:978-987. doi: 10.1016/j.str.2017.05.002.

151. Pitsawong W, Hoben JP, Miller AF. Understanding the broad substrate repertoire of nitroreductase based on its kinetic mechanism. *J Biol Chem.* 2014. 289:15203-14. doi: 10.1074/jbc.M113.547117.

152. Poole L. Bacterial defenses against oxidants: mechanistic features of cysteine-based peroxidases and their flavoprotein reductases. *Arch Biochem Biophys.* 2005. 433:240-54. doi: 10.1016/j.abb.2004.09.006.

153. Prosser G, Copp J, Syddall S, Williams E, Smaill J, Wilson W, Patterson A, Ackerley D. Discovery and evaluation of *Escherichia coli* nitroreductases that activate the anti-cancer prodrug CB1954. *Biochem Pharmacol*. 2010. 79:678-87. doi: 10.1016/j.bcp.2009.10.008.

154. Race P, Lovering A, Green R, Ossor A, White S, Searle P, Wrighton C, Hyde E. Structural and mechanistic studies of *Escherichia coli* nitroreductase with the antibiotic nitrofurazone. Reversed binding orientations in different redox states of the enzyme. *J Biol Chem.* 2005. 280:13256-64. doi: 10.1074/jbc.M409652200.

155. Race P, Lovering A, White S, Grove J, Searle P, Wrighton C, Hyde E. Kinetic and structural characterisation of *Escherichia coli* nitroreductase mutants showing improved efficacy for the prodrug substrate CB1954. *J Mol Biol.* 2007. 368:481-92. doi: 10.1016/j.jmb.2007.02.012.

156. Rakauskienė G, Čėnas N, Kulys J. A 'branched' mechanism of the reverse reaction of yeast glutathione reductase. An estimation of the enzyme standard potential values from the steady-state kinetics data. *FEBS Lett.* 1989. 243:33-6. doi: 10.1016/0014-5793(89)81212-8.

157. Riefler R, Smets B. Enzymatic Reduction of 2,4,6-Trinitrotoluene and Related Nitroarenes: Kinetics Linked to One-Electron Redox Potentials. *Environ. Sci. Technol*. 2000. 34:3900–3906

158. Roginsky V, Barsukova T, Stegmann H. Kinetics of redox interaction between substituted quinones and ascorbate under aerobic conditions. *Chem Biol Interact.* 1999. 121:177-97. doi: 10.1016/s0009-2797(99)00099-x.

159. Roldán M, Pérez-Reinado E, Castillo F, Moreno-Vivián C. Reduction of polynitroaromatic compounds: the bacterial nitroreductases. *FEMS Microbiol Rev.* 2008. 32:474-500. doi: 10.1111/j.1574-6976.2008.00107.x.

160. Ross D, Kepa J, Winski S, Beall H, Anwar A, Siegel D. NAD(P)H:quinone oxidoreductase 1 (NQO1): chemoprotection, bioactivation, gene regulation and genetic polymorphisms. *Chem. Biol. Interact.* 2000. 129:77–97. doi: 10.1016/S0009-2797(00)00199-X

161. Rudolph FB, Baugher BW, Beissner RS. Techniques in coupled enzyme assays. *Methods Enzymol.* 1979. 63:22-42. doi: 10.1016/0076-6879(79)63004-5.

162. Rudolph FB, Fromm HJ. Plotting methods for analyzing enzyme rate data. *Methods Enzymol.* 1979. 63:138-59. doi: 10.1016/0076-6879(79)63009-4.

163. Rudolph FB. Product inhibition and abortive complex formation. *Methods Enzymol.* 1979. 63:411-36. doi: 10.1016/0076-6879(79)63018-5.

164. Ruocco MR, Ruggiero A, Masullo L, Arcari P, Masullo M. A 35 kDa NAD(P)H oxidase previously isolated from the archaeon *Sulfolobus solfataricus* is instead a thioredoxin reductase. *Biochimie.* 2004. 86:883-92. doi: 10.1016/j.biochi.2004.10.008.

165. Russel M, Model P, Holmgren A. Thioredoxin or glutaredoxin in *Escherichia coli* is essential for sulfate reduction but not for deoxyribonucleotide synthesis. *J Bacteriol.* 1990. 172:1923-9. doi: 10.1128/jb.172.4.1923-1929.1990.

166. Šarlauskas J, Nemeikaitė-Čėnienė A, Anusevičius Ž, Misevičienė L, Julvez MM, Medina M, Gomez-Moreno C, Čėnas N. Flavoenzyme-catalyzed redox cycling of hydroxylamino- and amino metabolites of 2,4,6-trinitrotoluene: implications for their cytotoxicity. *Arch Biochem Biophys.* 2004. 425:184-92. doi: 10.1016/j.abb.2004.02.043.

167. Sarma G, Savvides S, Becker K, Schirmer M, Schirmer R, Karplus P. Glutathione reductase of the malarial parasite *Plasmodium falciparum*: crystal structure and inhibitor development. *J Mol Biol.* 2003. 328:893-907. doi: 10.1016/s0022-2836(03)00347-4.

168. Sayama M, Mori M, Nakada Y, Kagamimori S, Kozuka H. Metabolism of 2,4-dinitrotoluene by *Salmonella typhimurium* strains TA98, TA98NR and TA98/1,8-DNP6, and mutagenicity of the metabolites of 2,4-dinitrotoluene and related compounds to strains TA98 and TA100. *Mutat Res.* 1991. 264:147-53. doi: 10.1016/0165-7992(91)90132-n.

169. Scrutton NS, Berry A, Perham RN. Redesign of the coenzyme specificity of a dehydrogenase by protein engineering. *Nature*. 1990. 343:38-43. doi: 10.1038/343038a0.

170. Sengupta R, Holmgren A. Thioredoxin and glutaredoxin-mediated redox regulation of ribonucleotide reductase. *World J Biol Chem.* 2014. 5:68-74. doi: 10.4331/wjbc.v5.i1.68.

171. Skelly J, Sanderson M, Suter D, Baumann U, Read M, Gregory D, Bennett M, Hobbs S, Neidle S. Crystal structure of human DT-diaphorase: a model for interaction with the cytotoxic prodrug 5-(aziridin-1-yl)-2,4-dinitrobenzamide (CB1954). *J Med Chem.* 1999. 42:4325-30. doi: 10.1021/jm991060m.

172. Spain J. Biodegradation of nitroaromatic compounds. *Annu Rev Microbiol*. 1995. 49:523-55. doi: 10.1146/annurev.mi.49.100195.002515.

173. Sullivan F, Sobolov S, Bradley M, Walsh C. Mutational analysis of parasite trypanothione reductase: acquisition of glutathione reductase activity in a triple mutant. *Biochemistry.* 1991. 30:2761-7. doi: 10.1021/bi00225a004.

174. Sunters A, Baer J, Bagshawe KD. Cytotoxicity and activation of CB1954 in a human tumour cell line. *Biochem Pharmacol.* 1991. 41:1293-8. doi: 10.1016/0006-2952(91)90100-j.

175. Swallow AJ. Physical chemistry of semiquinones. In: *Function of Quinones in Energy Conserving Systems. (Ed. Trumpower) New York: Academic Press.* 1982. 59-72.

176. Tamura T, Stadtman T. A new selenoprotein from human lung adenocarcinoma cells: purification, properties, and thioredoxin reductase activity. *Proc Natl Acad Sci U S A.* 1996. 93:1006-11. doi: 10.1073/pnas.93.3.1006.

177. Taylor M, Kelly J, Chapman C, Fairlamb A, Miles M. The structure, organization, and expression of the *Leishmania donovani* gene encoding trypanothione reductase. *Mol Biochem Parasitol.* 1994. 64:293-301. doi: 10.1016/0166-6851(94)00034-4.

178. Tedeschi G, Chen S, Massey V. DT-diaphorase. Redox potential, steady-state, and rapid reaction studies. *J Biol Chem.* 1995. 270:1198-204. doi: 10.1074/jbc.270.3.1198.

179. Tyagi C, Bathke J, Goyal S, Fischer M, Dahse HM, Chacko S, Becker K, Grover A. Targeting the intersubunit cavity of *Plasmodium falciparum* glutathione reductase by a novel natural inhibitor: computational and experimental evidence. *Int J Biochem Cell Biol.* 2015. 61:72-80. doi: 10.1016/j.biocel.2015.01.014.

180. Uršič S, Vrčik V, Ljubas D, Vinkovič I. Interaction of L-ascorbate with substituted nitrosobenzenes. Role of the ascorbate 2-OH group in antioxidant reactions. *New J. Chem.* 1998. 22:221–223.

181. Veine D, Arscott L, Williams CH Jr. Redox potentials for yeast, *Escherichia coli* and human glutathione reductase relative to the NAD^+/NADH redox couple: enzyme forms active in catalysis. *Biochemistry.* 1998. 37:15575-82. doi: 10.1021/bi9811314.

182. Vermilion J, Ballou D, Massey V, Coon M. Separate roles for FMN and FAD in catalysis by liver microsomal NADPH-cytochrome P-450 reductase. *J Biol Chem.* 1981. 256:266-77.

183. Vienožinskis J, Butkus A, Čėnas N, Kulys J. The mechanism of the quinone reductase reaction of pig heart lipoamide dehydrogenase. *Biochem J.* 1990. 269:101-5. doi: 10.1042/bj2690101.

184. Vlamis-Gardikas A, Potamitou A, Zarivach R, Hochman A, Holmgren A. Characterization of *Escherichia coli* null mutants for glutaredoxin 2. *J Biol Chem.* 2002. 277:10861-8. doi: 10.1074/jbc.M111024200.

185. Waksman G, Krishna TS, Williams CH Jr, Kuriyan J. Crystal structure of *Escherichia coli* thioredoxin reductase refined at 2 Å

resolution. Implications for a large conformational change during catalysis. *J Mol Biol.* 1994. 236:800-16.

186. Wang P, Veine D, Ahn S, Williams CH Jr. A stable mixed disulfide between thioredoxin reductase and its substrate, thioredoxin: preparation and characterization. *Biochemistry.* 1996. 35:4812-9. doi: 10.1021/bi9526793.

187. Wang P, Marcinkevičienė J, Williams CH Jr, Blanchard JS. Thioredoxin reductase-thioredoxin fusion enzyme from *Mycobacterium leprae*: comparison with the separately expressed thioredoxin reductase. *Biochemistry.* 1998. 37:16378-89. doi: 10.1021/bi980754e.

188. Wardman P, Clarke ED. Oxygen inhibition of nitroreductase: electron transfer from nitro radical-anions to oxygen. *Biochem Biophys Res Commun.* 1976. 69:942-9. doi: 10.1016/0006-291x(76)90464-2.

189. Wardman P. Electron transfer and oxidative stress as key factors in the design of drugs selectively active in hypoxia. *Curr Med Chem.* 2001. 8:739-61. doi: 10.2174/0929867013372959.

190. Wardman P. Reduction Potentials of One-Electron Couples Involving Free Radicals in Aqueous Solutions. *Journal of Phys and Chem Ref Data.* 1989. 18:1637-1655. doi: 10.1063/1.555843

191. Watson WH, Pohl J, Montfort WR, Stuchlik O, Reed MS, Powis G, Jones DP. Redox potential of human thioredoxin 1 and identification of a second dithiol/disulfide motif. *J Biol Chem.* 2003. 278:33408-15. doi: 10.1074/jbc.M211107200.

192. Weber M, Kaplan N. Flavoprotein-catalyzed pyridine nucleotide transfer reactions. *J Biol Chem.* 1957. 225:909-20.

193. Williams CH Jr. Flavin-containing dehydrogenases. In *The Enzymes, Boyer, P. D. (Ed.), Academic Press, New York.* 1976. 13:89-172.

194. Williams CH Jr. Mechanism and structure of thioredoxin reductase from *Escherichia coli. FASEB J.* 1995. 9:1267-76. doi: 10.1096/fasebj.9.13.7557016.

195. Williams CH Jr. Lipoamide dehydrogenase, glutathione reductase. thioredoxin reductase. and mercuric ion reductase - a family of flavoenzyme transhydrogenases. In: *Chemistry and Biochemistry of Flavoenzymes (Miiller. F., Ed.). CRC Press. Boca Raton. FL.* 1992. 3:121-211

196. Williams E, Little R, Mowday A, Rich M, Chan-Hyams J, Copp J, Smaill J, Patterson A, Ackerley D. Nitroreductase gene-directed enzyme prodrug therapy: insights and advances toward clinical utility. *Biochem J.* 2015. 471:131-53. doi: 10.1042/BJ20150650.

197. Yamamoto K, Kimura S, Shiro Y, Iyanagi T. Interflavin one-electron transfer in the inducible nitric oxide synthase reductase domain and NADPH-cytochrome P450 reductase. *Arch Biochem Biophys.* 2005. 440:65-78. doi: 10.1016/j.abb.2005.05.027.

198. Yang J, Zhan J, Bai J, Liu P, Xue Y, Yang Q. Residue Phe42 is critical for the catalytic activity of *Escherichia coli* major nitroreductase NfsA. *Biotechnol Lett.* 2013. 35:1693-700. doi: 10.1007/s10529-013-1262-y.

199. Yang X, Ma K. Characterization of a thioredoxin-thioredoxin reductase system from the hyperthermophilic bacterium *Thermotoga maritima. J Bacteriol.* 2010. 192:1370-6. doi: 10.1128/JB.01035-09.

200. Zanetti G, Williams CH Jr, Massey V. Influence of photoirradiation on the oxidation-reduction state of thioredoxin reductase. *J Biol Chem.* 1968. 243:4013-9.

201. Zeldes B, Keller M, Loder A, Straub C, Adams M, Kelly R. Extremely thermophilic microorganisms as metabolic engineering

platforms for production of fuels and industrial chemicals. *Front Microbiol.* 2015. 6:1209. doi: 10.3389/fmicb.2015.01209.

202. Zenno S, Kobori T, Tanokura M, Saigo K. Conversion of NfsA, the major *Escherichia coli* nitroreductase, to a flavin reductase with an activity similar to that of Frp, a flavin reductase in *Vibrio harveyi*, by a single amino acid substitution. *J Bacteriol.* 1998. 180:422-5.

203. Zenno S, Koike H, Kumar AN, Jayaraman R, Tanokura M, Saigo K. Biochemical characterization of NfsA, the *Escherichia coli* major nitroreductase exhibiting a high amino acid sequence homology to Frp, a *Vibrio harveyi* flavin oxidoreductase. *J Bacteriol.* 1996b. 178:4508-14. doi: 10.1128/jb.178.15.4508-4514.1996.

204. Zenno S, Koike H, Tanokura M, Saigo K. Conversion of NfsB, a minor *Escherichia coli* nitroreductase, to a flavin reductase similar in biochemical properties to FRase I, the major flavin reductase in *Vibrio fischeri*, by a single amino acid substitution. *J Bacteriol.* 1996a. 178:4731-3. doi: 10.1128/jb.178.15.4731-4733

205. Zheng R, Čėnas N, Blanchard JS. Catalytic and potentiometric characterization of E201D and E201Q mutants of *Trypanosoma congolense* trypanothione reductase. *Biochemistry.* 1995. 34:12697-703. doi: 10.1021/bi00039a028.

206. Zhong L, Arnér ES, Holmgren A. Structure and mechanism of mammalian thioredoxin reductase: the active site is a redox-active selenolthiol/selenenylsulfide formed from the conserved cysteine-selenocysteine sequence. *Proc Natl Acad Sci U S A.* 2000. 97:5854-9. doi: 10.1073/pnas.100114897.

PUBLICATIONS

1. B. Valiauga, N. Rouhier, J.P. Jacquot, N. Čėnas. Quinone- and nitroreductase reactions of *Thermotoga maritima* thioredoxin reductase. *Acta Biochimica Polonica*. 2015. 62:303-309.

2. B. Valiauga, E. Williams, D. Ackerley, N. Čėnas. Reduction of quinones and nitroaromatic compounds by *Escherichia coli* nitroreductase A (NfsA): Characterization of kinetics and substrate specificity. *Archives of Biochemistry and Biophysics.* 2017. 614:14-22.

3. B. Valiauga, L. Misevičienė, M. Rich, D. Ackerley, J. Šarlauskas, N. Čėnas. Mechanism of Two-/Four-Electron Reduction of Nitroaromatics by Oxygen-Insensitive Nitroreductases: The Role of a Non-Enzymatic Reduction Step. *Molecules.* 2018. 23:1672.

4. B. Valiauga, N. Rouhier, J.P. Jacquot, N. Čėnas. Characterization of redox properties of FAD cofactor of *Thermotoga maritima* thioredoxin reductase. *Chemija.* 2020. 31:191-195.

CONFERENCES

POSTER PRESENTATIONS

1. B. Valiauga, E. Williams, D. Ackerley, N. Čėnas. Kinetic properties of nitroreductase A (NfsA) from *Escherichia coli*. 19th International Symposium on Flavins and Flavoproteins, July 2-6, 2017. Groningen, the Netherlands.

2. B. Valiauga, L. Misevičienė, M. Rich, D. Ackerley, J. Šarlauskas, N. Čėnas. Mechanism of Two-/Four-Electron Reduction of Nitroaromatics by Oxygen-Insensitive Nitroreductases: The Role of a

Non-Enzymatic Reduction Step, XV LBD conference, June 26-29, 2018. Dubingiai, Lithuania.

3. B. Valiauga, M. Rich, D. Ackerley, N. Čėnas. Potentiometric properties and substrate specificity of *E. coli* nitroreductase A, a candidate for gene-directed enzyme prodrug anticancer therapy. 26th SCT Young Research Fellows Meeting, February 20-22, 2019. Paris, France.

4. B. Valiauga, L. Misevičienė, A. Marozienė, J. Šarlauskas, Q. Cheng, E. S. J. Arnér, N. Čėnas. Tirapazamine derivatives as substrates of mammalian thioredoxin reductase. 27th SCT Young Research Fellows Meeting, January 29-31, 2020. Caen, France.

ACKNOWLEDGMENTS

I am extremely grateful to my PhD thesis supervisor Dr. Narimantas Čėnas, for opportunity to work at the Department of Xenobiotics Biochemistry, also for all the advice, help and patience which was needed along the way.

I would also like to extend my deepest gratitude to Prof. David F. Ackerley, Dr. Michelle Rich and Dr. Elsie Williams from Victoria University of Wellington for the purification of *Escherichia coli* NfsA.

I would like to extend my sincere thanks to Prof. Nicolas Rouhier and Prof. Jean-Pierre Jacquot from University of Lorraine for the purification of *Thermotoga maritima* thioredoxin reductase and related proteins.

I am also grateful to dr. Jonas Šarlauskas for the synthesis of various nitroaromatic compounds and quinones.

Many thanks to Prof. Saulius Klimašauskas for opportunity to use "stopped-flow" spectrophotometer in the Department of Biological DNA Modification.

And I also very much appreciate all the help from the people of Department of Xenobiotics Biochemistry, without whom this may not be possible.

Funding: We gratefully acknowledge the support of the European Social Fund (Measure No. 09.33-LMT-K-712, grant No. DOTSUT-34/09.3.3.-LMT-K712-01-0058/LSS-600000-58).

NOTES

NOTES

NOTES

NOTES

Vilnius University Press
9 Saulėtekio Ave., Building III, LT-10222 Vilnius
Email: info@leidykla.vu.lt, www.leidykla.vu.lt
Print run copies 12
168